| Title | Study on Interactive Behaviors of Dopamine with AB on Liposome Membrane under Oxidative Stress Condition |
|---|---|
| Author(s) | Vu, Thi Huong |
| Citation | 大阪大学, 2010, 博士論文 |
| Version Type | VoR |
| URL | https://hdl.handle.net/11094/903 |
| rights | |
| Note | |

# Study on Interactive Behaviors of Dopamine with Aβ

# on Liposome Membrane under Oxidative Stress Condition

**VU Huong Thi**

**March 2010**

# Study on Interactive Behaviors of Dopamine with Aβ

# on Liposome Membrane under Oxidative Stress Condition

A dissertation submitted to

THE GRAGUATION SCHOOL OF ENGINEERING SCIENCE

OSAKA UNIVERSITY

In partial fulfillment of the requirement for the degree of

DOCTOR OF PHILOSOPHY IN ENGINEERING SICENCE

BY

VU Huong Thi

March 2010

# Preface

This PhD dissertation work has been carried out under the supervision of Professor-Doctor Ryoichi Kuboi in the Division of Chemical Engineering, Graduate School of Engineering Science, Osaka University, Japan from 2006 to 2010.

The objective of this study is to clarify the interactive behaviors of the dopamine with $A\beta$ on the liposome membrane under the oxidative stress condition. Prior to the investigation, the author developed the analytical methods for the above behaviors, such as dopamine sensor and immobilized liposome QCM sensor. The interactive behaviors of (i) dopamine with liposome membrane and (ii) $A\beta$ with the membrane in the absence or presence of dopamine were analyzed by using the above sensors under the normal condition and oxidative stress conditions. The role of the dopamine on the membrane was shown to be elucidated through the regulation of (a) the dopamine oxidation via $A\beta$/Cu complex and (b) the solubilization of the formed $A\beta$ fibrils on the liposome surface, depending on the state of the liposome membrane. The author hopes that this research would contribute to the development of the new therapy of Alzheimer's disease and its diagnostics.

**VU Huong Thi**

Division of Chemical Engineering
Graduate School of Engineering Science
Osaka University
1-3 Machikaneyama-cho,
Toyonaka, Osaka 561-8531
JAPAN

# Contents

# Summary

Dopamine (DA) has been reported to play an important role as a neurotransmitter in neuronal system. The lack of DA in neuron is known to induce the dementia symptom although the existence of DA at extremely high level induces the oxidative stress, together with the formation of toxic DA-quinone (DAQ) through the "auto-oxidation" pathway. On the other hand, the deposition of amyloid β-peptides (Aβs) on the neuronal cell membrane has been reported to be related with the "oxidative stress". In a biological system, the cells could be protected from the oxidative stress by antioxidative enzymes, such as superoxide dismutase and catalase. However, in some cases, the antioxidative enzymes may lose their functions by the reactive oxygen species (ROS), leading to the loss of their protective function. It is necessary to study the mechanism on the prevention and removal of the toxic species including "oxidative stressors" to recover the cells.

In this thesis, systematic studies have been carried out, mainly focusing on: (i) the interactive behaviors of DA with Aβs in order to reduce the toxicity of both of them and (ii) the potential function of the membrane against the toxicity induced by DA and Aβs. Prior to the investigation on the mechanism of the above studies, the methodologies to characterize the DA and Aβs on the membrane were also developed.

**In chapter 1,** the DA sensor was developed by using the conducting polymer based on electrochemical method. The developed DA sensor was found to response in the DA concentration with high sensitivity in the range of $5 \times 10^{-7}$ to $2 \times 10^{-4}$M. The DA sensor was then utilized for the evaluation of the interaction of DA with the model cell membrane (liposome). The DA was found to show the propensity to partition onto the liposome membrane. The DA-oxidation was also found to be promoted in the presence of liposomes. Through its partitioning on the liposome membrane, the DA was found to induce the membrane damage, caused by auto-oxidation to form the DAQ together with the generation of superoxide ($O_2^-$).

**In chapter 2,** the liposome-based sensor was developed by the liposome immobilization onto the surface of the modified QCM electrode in order to evaluate the membrane-protein interaction, focusing on the amyloidogenic proteins (i.e. Aβs). By using the covalent binding methods, the liposomes were shown to be immobilized with "intact" shape and high density for long time. The immobilized liposomes were applied to evaluate: (i) the interaction between liposomes and Aβs in term of hydrogen bond stability of proteins ($\rho_{pr}$) and (ii) the DA-Aβ interaction on the liposome membrane. It was found that the liposome membrane could modulate its interaction with Aβs, depending on its surface characteristics under the stress conditions, and the DA could reduce the interaction of Aβ with liposome membrane.

**In chapter 3,** the Aβ/Cu complex on the liposome (Aβ/Cu LIPOzyme) was found to be utilized for the regulation of the DA-oxidation as an enzyme-like pathway, instead of the auto-oxidation pathway. The DA was oxidized by Aβ/Cu on the liposome, resulting in the formation of a DAQ together with the formation of less toxic ROS (hydrogen peroxide). It has been shown that the membrane could regulate both the DA concentration and the ROS generation by the control of the enzyme-like activity of Aβ/Cu complex.

**In chapter 4,** the effect of DA against amyloid β-peptide on the liposome membranes under stress condition was investigated, focusing on (i) the inhibition of fibril formation on the liposome membrane and (ii) the disaggregation of Aβ fibril on the oxidized liposome membrane. The DA showed the ability to reduce the toxicity from Aβ fibril both by the inhibition of fibril formation and the fibril disaggregation. Inversely, Aβ may have the effect to deactivate the toxic DAQ. Finally, the function of biomembrane to defend itself from toxicity under the oxidative stress were summarized and discussed. In brief, the membrane could modulate the DA concentration by regulating the enzyme-like activity of Aβ/Cu complex or by regulating the DA-Aβ interaction. The membrane also possesses the ability to regulate the Aβ fibril level either by promoting Aβ fibril formation or disaggregation of Aβ fibrils. When the membrane was exposed to the oxidative stress conditions, the oxidized membrane can make responses against the stress (a) by accelerating the formation of less toxic Aβ fibrils and (b) by promoting the disaggregation of Aβ fibrils to reduce the toxicity level of both of DAQ and aggregated Aβ.

The obtained results demonstrate that the potential function of membrane on the regulation of stress induced by neurotransmitter dopamine and Aβ in order to protect membrane from stress and recover itself.

# General Introduction

Neurotransmitters are endogenous chemicals, which can relay, amplify, and modulate signals between a neuron and another cell. Neurotransmitters are packaged into the synaptic vesicles that cluster beneath the membrane on the presynaptic side of a synapse, and are released into the synaptic cleft, where they bind to receptors in the membrane on the postsynaptic side of the synapse. The release of neurotransmitters usually follows the arrival of an action potential at the synapse, but may follow the graded electrical potentials. Major neurotransmitter systems include the noradrenaline (norepinephrine) system, the dopamine system, the serotonin system and the cholinergic system.

Catecholamines are sympathomimetic hormones that are released by the adrenal glands in response to stress. They play a partial role of the sympathetic nervous system. The most abundant catecholamines in human tissue are epinephrine (adrenaline), norepinephrine (noradrenaline) and dopamine, which can act as central neurotransmitters. Among three catecholamines, nor-epinephrine (NE) is released by peripheral sympathetic nerves onto blood vessels and both NE and epinephrine (EP) are hormones secreted by the adrenal medulla (Burke *et al.*, 2004). These catecholamines as neurotransmitters have widespread projections to the cortex, basal ganglia, limbic areas and spinal cord. They play an important role in regulation of brain functions of memory, mood, movement, behavior and autonomic functions, such as blood pressure regulation. These functions are lost in the brain of the patients of Alzheimer's disease (AD) and Parkinson's disease (PD) due to the loss of the catecholamine neurotransmitters, which can regulate these brain functions (Burke *et al.*, 2004). In neuronal system, catecholamines are synthesized in the neuronal system first by the hydroxylation of the L-tyrosine to L-DOPA via the tyrosine hydroxylase, and then by the decarboxylation of L-DOPA by dopa decarboxylase. After the synthesis of DA, it is packaged into vesicles, which are then released into the synapse in response to a presynaptic action potential (**Fig.1**).
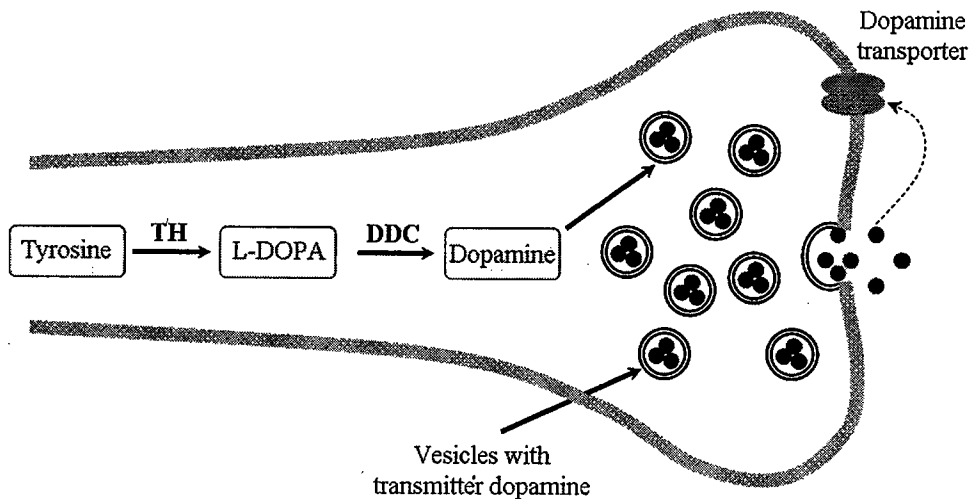
**Fig.1** Formation of chemical transmitter DA from the precursors tyrosine and L-DOPA, followed by being stored in vesicles in the nerve endings (Carlsson *et al.*, Nobel Prize on Medicine 2000).

In some neurons, the DA is further processed into norepinephrine by dopamine $\beta$-hydroxylase (D$\beta$H). The epinephrine is then synthesized via the methylation of the primary distal amine of norepinephrine by phenylethanolamine N-methyltransferase (PNMT) in the cytosol of adrenergic neurons and cells of the adrenal medulla (so-called chromaffin cells) **(Fig.2)**.

Among the catecholamines working as neurotransmitter, the dopamine (DA) has been reported to be one of the most important neurotransmitter in neuronal system. It plays an important role in neuronal system and is widely distributed throughout the brain. The lack of nigrostriatal dopaminergic neurons is known to induce the dementia symptom although the existence of DA at extremely high level has reported to be related with some serious diseases, such as Parkinson's disease, Alzheimer's disease and so on (Mo *et al.*, 2001). Normally, after its synthesis, DA is entrapped onto the synaptic vesicles immediately and is then released into the synapse in response to a presynaptic action potential. After the DA is inactivated by reuptake via the dopamine transporter, the enzymatic breakdown was achieved by catechol-O-methyl transferase (COMT) and monoamine oxidase (MAO). DA that is not broken down by
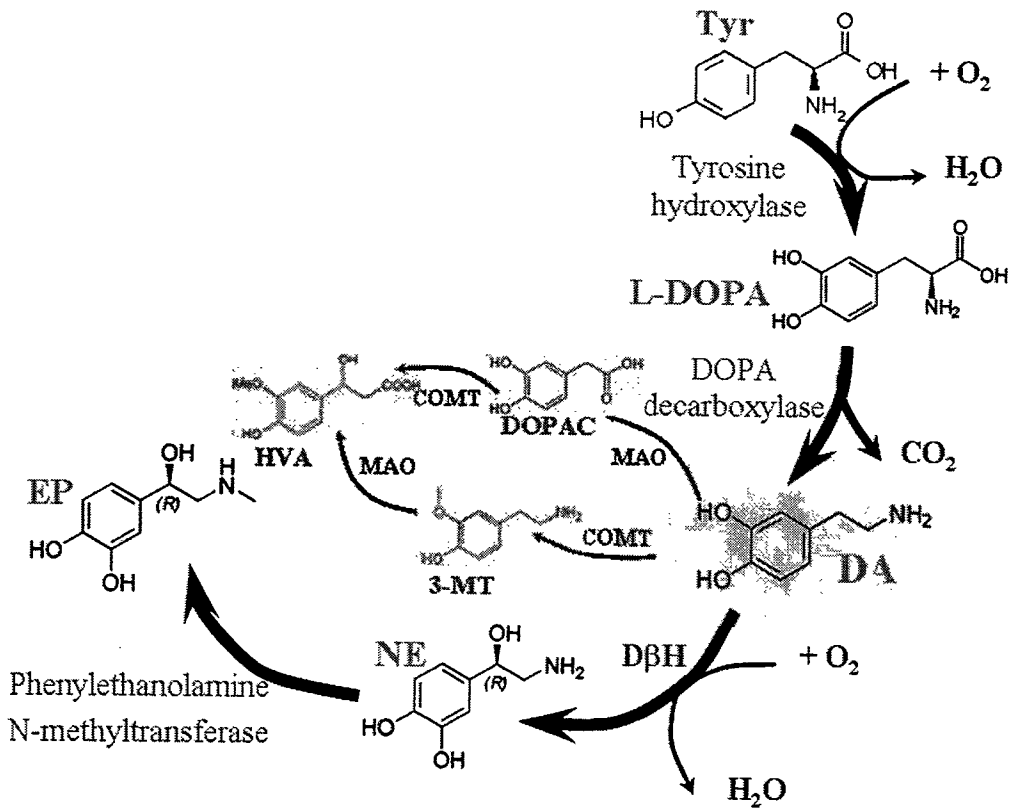
**Fig.2** Biosynthesis of catecholamine neurotransmitters focusing on DA metabolism pathway on neuronal system.

these enzymes can be repackaged into vesicles for its reuse. In general, the DA is stable inside the storage vesicles because of its acidic environment (Sulzer *et al.*, 2000), whereas they are easily "*oxidized*" outside the vesicles. The DA oxidation generates the dopamine semi-quinone free radical, dopamine quinone, dopaminochrome, as well as reactive oxygen species (Bors *et al.*, 1978; Pileblad *et al.*, 1988).

The treatment by L-DOPA, a precursor of DA, as a supplement can reduce the level of the DA concentration in the brain and has been widely used. However, long-term L-DOPA therapy often causes various adverse reactions. The adverse reactions are thought to be correlated, at least in part, with the neurotoxicity induced by "*auto-oxidation*" of the excess level of DA and L-DOPA. It has been reported that the spontaneous *auto-oxidation* of DA

3

produces "*ROS ($O_2^-$)*" and "*reactive quinone*" (Tse *et al.,* 1976). In the brain, the tyrosinase may enzymatically and rapidly convert the excess amount of DA and L-DOPA to catechol-quinone and $H_2O$, and may further convert it to neuro-melanin (Asanuma *et al.,* 2003). However, the tyrosinase could easily lose its function under oxidative stress condition (Andrwais *et al.,* 1985). Therefore, the *auto-oxidation* of DA will occur, resulting in the generation of the additional ROS. In normal condition, the generated ROS could be removed by antioxidative enzymes, such as superoxide dismutase (SOD) and catalase. However, under oxidative stress condition at the extremely-high level, the SOD could lose its function (Nagami *et al.,* 2005), resulting that the ROS could attack the membrane and could make the membrane damaged (**Fig.3**).

The functions of DA in neuronal system have been reported to play both neuroprotective and neurotoxic roles in neurodegenation disorders relating to some disease, such as Parkinson's, Schizophrenia's, and Alzheimer's diseases (Kostrzewa *et al.,* 2002; Spencer *et al.,* 1996; Burke *et al.,* 2004), which may be related with both of toxic DA-quinone and generated ROS (**Table 1**).
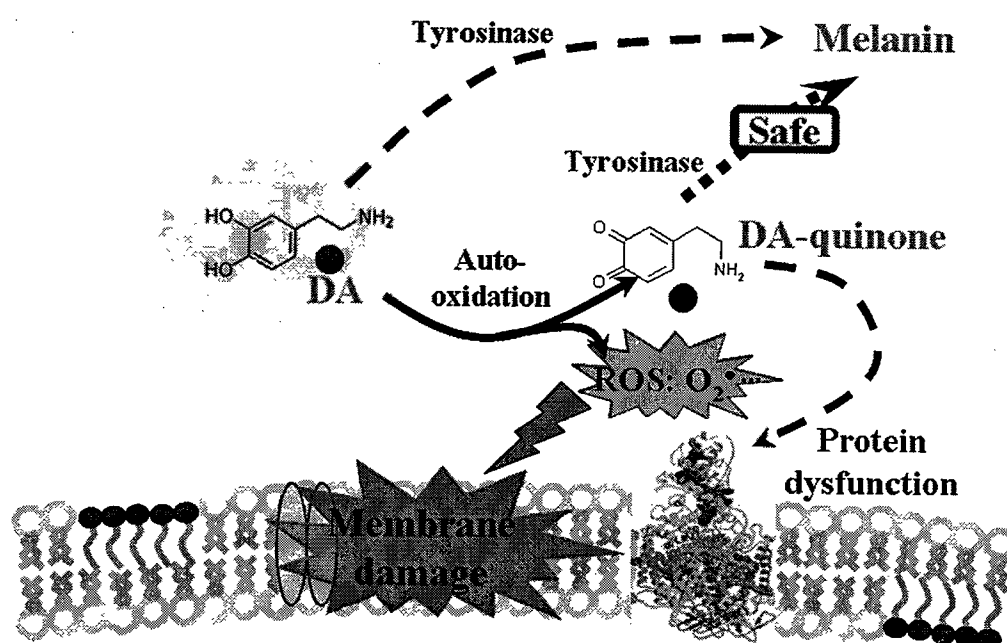


**Fig.3** Possible pathway of reactive oxygen species (ROS) generation by excess amount of free DA to induce the cell damage (Asanuma *et al.,* 2003).

**Table 1** Summary of catecholamines and their functions

| Compound | Effect | Function | System | References |
|---|---|---|---|---|
| DA, NE, EP | Negative | Catecholamines increase the vulnerability of cultured hippocampal neuronal cells to Aβ toxicity. Induce cell death at high concentration (100-200 μM) by generating oxidative stress. | Hippocampal neuronal cells | Fu et al., 1998 |
| DA, L-DOPA | Negative | Induced toxicity via quinone formation. Generate ROS by auto-oxidation. | | Asanuma et al., 2003 |
| DA, L-DOPA | Positive | Antioxidants: inhibit the peroxidation of lipids by react with superoxide radical ($O_2^{\bullet-}$). | Ox-brain phospholipid liposomes | Spencer et al., 1996 |
| | Negative | Pro-oxidant: generate free radicals, $H_2O_2$... by metabolism. | | |
| L-DOPA | Negative | Auto-oxidation to form high reactive quinone and reactive oxygen species. | | Kostrzewa et al., 2002 |
| | Positive | Act as antioxidant by becoming oxidized instead of other cellular elements. | | |
| DA, NE, EP, DOPAL | Negative | Metabolism of neurotransmitter catecholamines by monoamine oxidase generated ROS. | Neuron cells | Burke et al., 2004 |
| DA | Positive | Slow the progression of familial Parkinsonism. | | Gwinn-Hardy et al., 1999 |
| L-DOPA | Positive | Promote the recovery of striatal innervation in rats with partial lesions and slow the progression of familial Parkinsonism. | Female Wistar rats | Murer et al., 1998 |
| DA | Negative | Cytotoxic and genotoxic | | Stokes et al., 1999 |
| DA | Negative | Induce cells death | PC12 cells | Choi et al., 2000; Song et al., 2004. |
| DA, NE, EP | Negative | Toxic for cells | Neuronal cells and Glial cells | Rosenberg et al., 1988 |
| DA, NE, EP | Positive | Inhibit lipid peroxidation | | Andorn et al., 2001 |
| DA, NE | Positive | Inhibit iron-plus-ascorbate stimulated lipid peroxidation. | Rat-brain | Liu et al., 1993 |

As introduced above, the diseases relating to DA have reported to be caused by the level of DA concentration. The lack of neuron containing DA may often induce the

Parkinson's disease while the existence of DA at the extremely-high level can induce some diseases relating with neuronal degeneration. Therefore, in the human, the DA should be appropriately controlled at normal concentration for the prevention of the diseases. The estimation of the DA concentration is also helpful for the treatment of diseases, caused by the "abnormal" DA concentration. The determination of DA concentration has been attracted many researchers. The most commonly used methods for the determination of this biogenic amine are the fluorometric assay (Wang et al., 2002), radioenzymatic assay (Hard et al., 2001), HPLC analysis (Cannazza et al., 2005), and voltammetric assay (Zucolotto et al., 2006). However, for the convenience of the assay, the simple and fast measurement method is needed. Recently, there has been an increasing demand for more sensitive and simple analytical methods. Cyclic voltammetry (CV) and different pulse voltammetry (DPV) techniques are very useful and popular for the trace analysis because these techniques are compact, efficient, and sensitive (Zhang et al., 2006). Various voltammetric techniques have shown the low detection limit required for dopamine analysis, depending on the type of working electrode system. The sensitivity of voltammetric techniques mainly depends on the modification of surface of the working electrode, where the electrochemical responses can be obtained through the adsorption (Zheng et al., 2006) or the partition (Rocha et al., 2006) of the DA on the modified membrane surface.

Liposomes are the artificial biomembrane of spherical shape with the smaller size, which can be prepared from the natural phospholipids and other compounds (i.e. membrane proteins). In a biological system, the liposomes have been reported to contain some bio-molecules, such as enzymes, neurotransmitters, and so on. Recently, the activities of liposomes are very broad in application based on their sophisticated functions and properties. More widely, the liposomes have been often used as model membrane systems to reveal the basic nature of cell membranes and used for the deeper understanding of biological events in cell membranes, such as permeability, fluidity, protein anchoring, and fusion of membrane. For example, the liposome has a chaperone-like function to assist the refolding of protein,

where the denatured-proteins could interact with the liposome membrane to be refolded and returned to native form (Kuboi et al., 1997; Yoshimoto et al., 1998; Yoshimoto et al., 1999; Kuboi et al., 2000). Liposomes also show the "potential" function under "stress" condition, such as LIPOzyme (Tuan, 2008) and the regulation of gene expression by its recognition of the biomolecules relating to the gene expression (Bui, 2009) in a dependent manner on its surface properties (i.e. surface charge density, hydrophobicity, and hydrogen bonds stability) (Tuan, 2008; Bui, 2009; Ngo, 2009).

The biomembrane can be regarded as an important physical barrier to wrap-up the biofunctional molecules (i.e. proteins, nucleotides, etc.) and, also, as an active interface to make a response against the environmental change. The biological cell, which is a minimal unit of "life", could get into a death if the biomembrane could be destroyed or if its function as an active interface could be lost. From the viewpoint of the protection of the structure and function of the "membrane" under the stress conditions (i.e. ROS), it is rational to consider that the "membrane" could assist the potential functions of proteins or peptides, possibly induced under the stress condition. The experiments have previously been conducted to evaluate the oxidation of lipid by coper, focusing on the Alzheimer's disease as a target. The obtained result indicated that the unsaturated lipid bilayer was easy to be oxidized by copper. However, the addition of Aβ slightly decreased the amount of ROS generation and the lipid peroxidation. By recruiting Aβ, the membrane could inhibit the ROS generation by Aβ-Cu interaction to protect itself (Nagami, 2005). Under the oxidative stress condition with $H_2O_2$, the superoxide dismutase (SOD) lost its activity although its activity could be maintained in the presence of membrane (Nagami, 2005). Furthermore, the membrane could recruit the oxidized and fragmented SOD together with metal ion (Cu(II) and Zn(II)) to induce the SOD-like activity function of LIPOzyme (Tuan, 2008). From the above results, the interaction between the membrane and proteins/peptides on the membrane surface showed an ability to prevent of both membrane and proteins/peptides from further oxidation by ROS.

Monomers Oligomers Fibrils

Nucleation Elongation
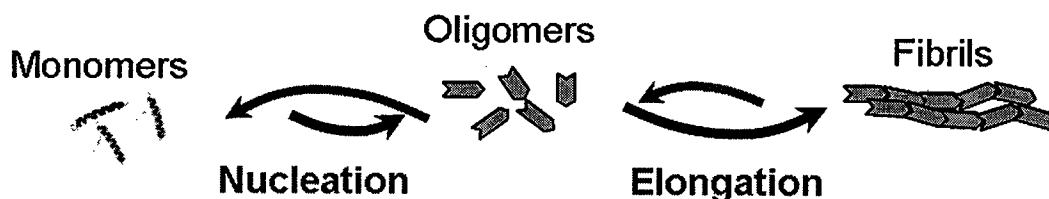
**Fig.4** Conventional pathway of Aβ fibril formation. Most researchers consider that the oligomers or fibrils of Aβ on the neural cell surface could be toxic in the Alzheimer's disease.

Amyloid β-peptide (Aβ), which is a normally water soluble 4.3 kDa peptide, is the main constituent of amyloid plaques in the brains of Alzheimer's disease (AD) patients (Scheumer *et al.,* 1996). Aβ is secreted from amyloid precursor protein (APP), an 87 kDa transmembrane proteins with apparent homology to a cell-surface receptor (Kang *et al.,* 1987). Various stress conditions are known to increase the Aβ production, such as oxidative stress (Frederikse *et al.,* 1996) and the increase of the cholesterol concentration (Michikawa *et al.,* 2003). Importantly, it has been reported that the Aβ was increasingly produced, especially under oxidative stress condition induced by different ways. Both hydrogen peroxide and UV irradiation have reported to elevate the Aβ peptides production on monkey lenses eyes (Frederikse *et al.,* 1996), and neuroblastoma cells (Olivieri *et al.,* 2001; Zhang *et al.,* 1997). Increased production of Aβ in the presence of hydrogen peroxide is not related with the increased synthesis of APP, but rather related with the increased generation of Aβ from APP (Misonou *et al.,* 2000). Many previous findings could thus imply the possible relation of oxidative stress with the Alzheimer's disease.

The deposition of aggregated Aβ on neuronal cell membrane has been reported to be associated with Alzheimer's disease. The progressive deposition of Aβ in Alzheimer's disease is generally considered to be fundamental in the development of neurodegenerative pathology (Mattson *et al.,* 2004). The aggregation of the soluble Aβ monomers into toxic oligomeric or fibrillar species is considered to be a crucial step in the pathology of the disease (Resende *et al.,* 2008). It has been reported that the most neurotoxic species are oligomers acting as

8

intermediates during formation of fibrils (Kayed *et al.*, 2003). The aggregated Aβ deposition was proposed as the formation of toxic oligomers and fibrils in bulk solution, and then deposit on the cell membranes as shown in **Fig.4.**

The mechanism of Aβ-mediated neurodegeneration in Alzheimer's disease was proposed to be involved by several pathways (Crouch *et al.*, 2008), such as mitochondrial dysfunction (Aleardi *et al.*, 2005; Takuma *et al.*, 2005), axonal trafficking (Matsuoka *et al.*, 2001), synaptic transmission (Mesulam *et al.*, 1999), membrane disruption (Ciccotosto *et al.*, 2004), formation of channel in membranes (Hirakura *et al.*, 1999), and especially relation with the oxidative stress (Clarke *et al.*, 1999; Varadarajan *et al.*, 2000). The Aβ peptides have shown to contribute to the oxidative stress that accompanies with Alzheimer's disease (Smith *et al.*, 1997; Bush *et al.*, 2003; Barnham *et al.*, 2004). The deposition of the aggregated Aβ has been reported to be associated with the metal ions, such as Cu(II), Zn(II), Fe(II) and Fe(III), at high concentration in amyloid plaque (Lovell *et al.*, 1998). It is considered that the deposition of Aβ could induce not only the negative effect but also the positive one.

From another point of view, the soluble monomeric Aβ is found to be non-toxic. Monomeric Aβ has been reported to inhibit the ROS generation from free metal ions (Nagami, 2005) and to reduce the toxicity of both Aβ and metal ions (Matsuzaki *et al.*, 2007b). Furthermore, monomeric Aβ has been reported to reduce the toxicity of Cu(II) by the formation of Aβ/Cu complex (Opazo *et al.*, 2002; Zou *et al.*, 2002) and plays as antioxidant (Curtain *et al.*, 2001; Murray *et al.*, 2005). From the view point of *"membrane"*, the above results lead to one hypothesis that, under stress condition, the membrane intends to make response against the oxidative stress although it could not do by itself. Therefore, the cofactors with "potential" activity could be recruited on the membrane surface and its potential functions could be induced there. In relation to Alzheimer's disease, the monomeric Aβ was secreted from APP to reduce the toxicity of metal ions. Otherwise, the formation of fibril on biomembrane (**Fig.5**) could also protect the membrane from the metal toxicity

9
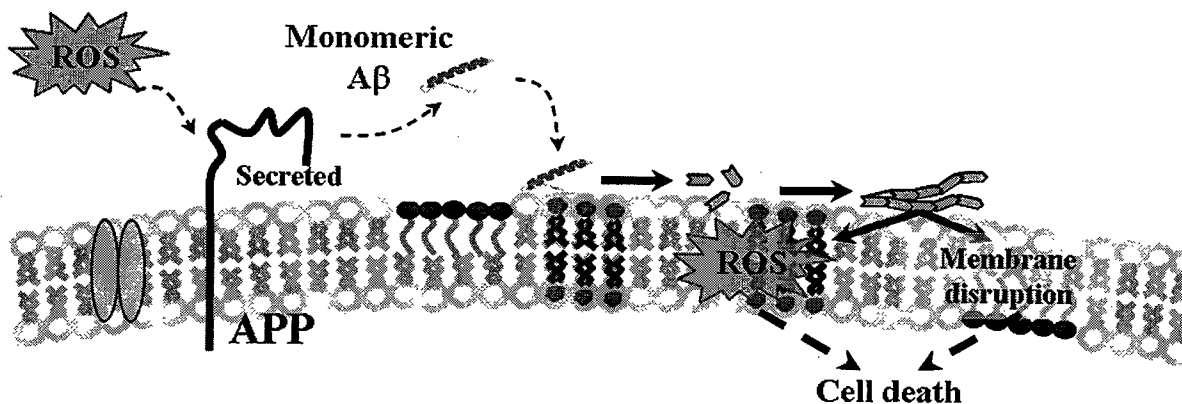
**Fig.5** Model for Aβ fibril formation on biomembrane and induction of cell death.

(Nagami, 2005). In terms of antioxidant, by combining with some cofactor, Aβ may expose its ability on the reduction of the ROS generation both by the inhibition of ROS generation or regulation of the reaction onto other pathways, which generate the less toxic species. In short, Aβ could act as an antioxidant molecule on the cell surface in the biological system. The extremely high amounts of aggregated Aβ deposition has been reported to induce the toxicity according to several reports (Dahlgren *et al.*, 2002; Yang *et al.*, 2005; Durairajan *et al.*, 2008). From view point of regeneration of the abnormal membrane, it has been reported that the microdomain of the oxidized fatty acids on the liposome membrane could cooperatively accelerate the amyloid fibrils formation of Aβ (Lee, 2005) and that the cholesterol domain could recruit the Aβ/Cu complex to oxidize the cholesterol molecules and to remove them from the membrane (Yoshimoto, 2005). It is needed to study the above potential functions of membrane under oxidative stress condition by considering the possible role of DA in neuronal system.

In this thesis, systematic studies have been achieved, mainly focusing on: (i) the interactive behaviors of DA with Aβ on liposome membrane in order to reduce the toxicity of both of them and (ii) the potential function of membrane against the toxicity induced by DA and Aβ. Prior to the investigation on the mechanism of above studies, the methodologies to characterize the DA and Aβ on the membrane were developed.

The neurotransmitter DA is known as both of neuroprotective and neurotoxic compound. In this study, the behavior of DA in a biological system was investigated from the view point of its toxicity, focusing on *(i)* ROS generation by auto-oxidation of DA, which could make the membrane damaged and *(ii)* toxic DA-quinone. In order to prevent the ROS generation, the membrane could recruit Aβ and Cu(II) as cofactor to regulate the DA oxidation as enzyme-like pathway instead of the auto-oxidation pathway. On the other hand, the oxidation of DA produces the DA-quinone, which induces toxicity to the cell by formation of Schiff-base with Cys on the active domain of protein, leading to the protein dysfunction (Miyazaki *et al.,* 2009). Under such stress condition, the membrane could utilize Aβs as cofactors to remove the toxic DA-quinone by direct interaction with both DA and DA-quinone. The level of fibrillar Aβ deposition on the liposome membrane could also be reduced by both the inhibition of the Aβ fibril formation and the enhancement of the disaggregation of Aβ fibrils.

The framework and flow chart of presence study are schematically shown in **Figs.6** and **7**, respectively, where the DA was considered as neurotoxic compound. Aβs were utilized as cofactors of membrane to prevent the ROS generation and remove toxic production of DA. Taken together, these processes also indicated the ability to reduce the negative effect of aggregated Aβ.

**In chapter 1,** the DA sensor was developed to monitor the DA concentration based on the electrochemical method by using the conducting polymer to monitor the DA concentration. The mechanism of the DA oxidation on the electrode was also investigated based on the electrochemical viewpoint. The developed DA sensor was then utilized for the monitoring of the DA concentration to evaluate the interaction of DA with the model cell membrane (liposome). The DA was found to show the propensity to partition onto the liposome membrane. Through its partitioning on the liposome membrane, the DA was found to induce the membrane damage, caused by auto-oxidation, together with the generation of superoxide
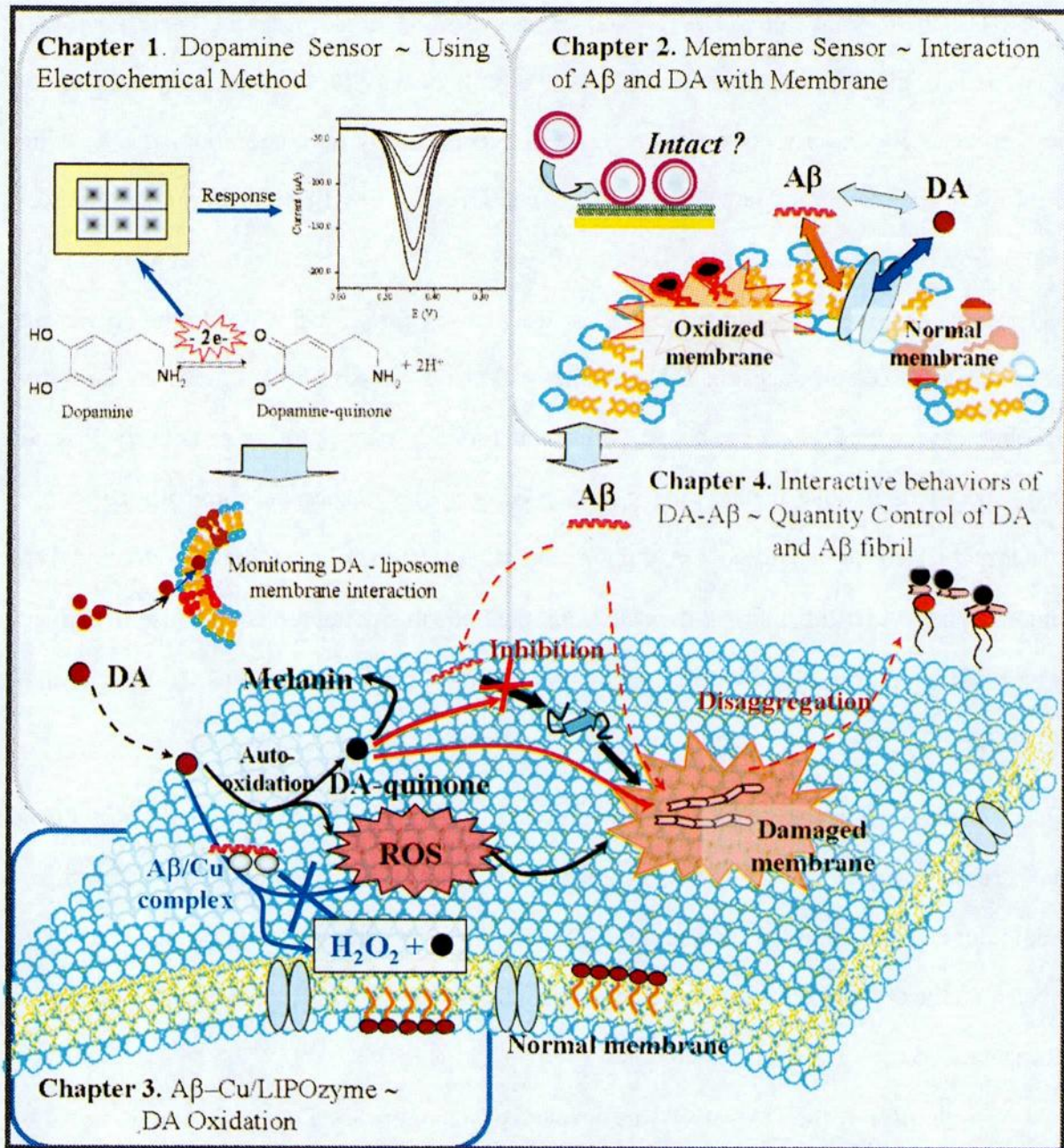
**Fig.6** Framework of present study.

**Chapter 1. Development of Electrochemical Sensor Based on Conducting Polymer for Detection of Dopamine Concentration – Monitoring of Dopamine - Liposome Membrane Interaction**

♣ Development of electrochemical sensor for measurement of DA concentration based on conducting polymer modified glassy carbon electrode.

♣ Response of DA at modified electrode.

♣ Characterization DA properties - possibility of DA partitioning on hydrophobic environment.

♣ Dopamine partitioning onto liposome membrane – Evaluation by dopamine sensor.

♣ Interactive effect of DA and liposome membrane.

**Chapter 2. Development of Membrane Sensor ~ Detection of Dopamine - Protein Interactions on Liposome Membrane ~**

♣ Development of membrane sensor based on immobilized liposome modified QCM (IL-QCM).

♣ Interaction of amyloidogenic proteins and liposome controlled by the extend of hydrogen bond stability.

♣ Behaviors of DA - Aβ on liposome membrane – evaluated by IL-QCM.

**Chapter 3. Regulation of Dopamine Oxidation by Aβ/Cu LIPOzyme**

♣ Metalloenzyme-like function of Aβ-Cu complex for DA oxidation.

♣ Membrane enhanced enzyme activity of Aβ/Cu complex for DA oxidation – effect of hydrated water on the membrane.

♣ Modulation of DA concentration and generated ROS by Aβ/Cu LIPOzyme

**Chapter 4. Interactive Behaviors of DA with Aβ on Liposome Membrane ~ Quantity Control of DA and Aβ fibrils ~**

♣ Liposome regulates Aβ fibril formation – Dopamine inhibits Aβ fibril formation on liposome membrane.

♣ Dopamine/dopamine-quinone disaggregate Aβ fibril on liposome membrane.

♣ Quantity Control of DA and Aβ fibrils by liposome membrane.

♣ The Role of Membrane on Preventing and Recovering Itself from Toxicity.

**Fig.7** Flow chart of the present study.

13

$(O_2^-)$. The addition of the liposomes was found to promote the DA-oxidation.

**In chapter 2,** the liposome-based sensor was designed and developed by the liposome immobilization onto the surface of modified QCM electrode in order to evaluate the membrane-protein interaction, focusing on the amyloidogenic proteins. By using the covalent binding methods, the liposomes were shown to be immobilized with intact shape and high density for long time. The immobilized liposomes were applied to evaluate: *(i)* the interaction between liposomes and proteins, specially Aβ proteins, controlled by both of hydrogen bond stability of proteins ($\rho_{pr}$) and hydrogen bond instability of liposome ($m_{lip}$), and *(ii)* the DA-Aβ interaction on liposome membrane, in order to clarify the mechanism of Aβ fibril formation and its interaction with DA.

**In chapter 3,** the Aβ-Cu-LIPOzyme was found to be utilized for the regulation of the DA-oxidation as an enzymatic-like pathway instead of the auto-oxidation pathway. It has been shown that the membrane could regulate both the DA concentration and the ROS generation through the control of enzyme-like activity of Aβ/Cu complex. The enzyme-like activity of Aβ/Cu was regulated by liposomes depending on the hydrogen bond instability of liposomes ($m_{lip}$). The non-oxidized membrane (low $m_{lip}$) could enhance the enzyme-like activity of Aβ/Cu, leading to the reduction of the ROS generation to protect the membrane from the damage induced by ROS.

**In chapter 4,** the effect of DA addition against the Aβ on the liposome membranes were investigated, focusing on *(i)* the inhibition of fibril formation on the liposome membrane and *(ii)* the disaggregation of Aβ fibril on the liposome membrane. The DA was found to reduce the toxic Aβ fibrils both by the inhibition of fibril formation at nucleation step and by the fibril disaggregation. Inversely, Aβ was also found to have the effect to deactivate the toxic DA/DA-quinone by reducing level of DA/DA-quinone through their interaction. The oxidatively damaged membrane was found to (i) recruit Aβ monomer on its surface to quickly form Aβ fibril with less toxicity, and to (ii) promote of the disaggregation of Aβ fibrils with

14

the assist of DA, which could reduce the level of both of DA-quinone and aggregated Aβ for the reduction of toxicity from both. The function of biomembrane was finally summarized and discussed in order to claify its ability to defend itself from toxicity under the oxidative stress. Through the removal of Aβ fibrils with the assist of DA/DA-quinone, the possibility to remove the oxidized lipids associating with Aβ fibrils in order to recover the membrane was finally hypothesised.

The results obtained from this work are summarized in the General Conclusions section. Suggestions for future work are described as extension of the present study.

# Chapter 1. Development of Electrochemical Sensor Based on Conducting Polymer for Detection of Dopamine Concentration – Monitoring of Dopamine - Liposome Membrane Interaction

## 1. Introduction

Dopamine (DA) plays a very important role in neuronal system as a neurotransmitter. The existence of DA at extremely high level has been reported to be related with some serious diseases, such as Parkinson's disease, Alzheimer's disease, and so on (Burke *et al.*, 2004). DA is, in the neuronal system, synthesized from L-tyrosine by two reaction steps: (i) a hydroxylation of the L-tyrosine to L-DOPA via tyrosine hydroxylase and (ii) a decarboxylation of L-DOPA by dopa decarboxylase. In some neurons, DA is further processed into norepinephrine by dopamine $\beta$-hydroxylase (D$\beta$H) and finally converts to epinephrine by phenylethanolamine N-methyltransferase (PNMT). In almost all neurons, after the synthesis of DA, the DA is entrapped immediately into the synaptic vesicles and is then released into the synapse in response to a presynaptic action potential. After the DA is inactivated by re-uptake via a dopamine transporter, an enzymatic breakdown was achieved by catechol-O-methyl transferase (COMT) and monoamine oxidase (MAO) to give a homovanillic acid (degraded form of DA). DA that is not broken down by the enzymes can be re-packaged into vesicles for its reuse. In general, the DA is stable inside storage vesicles because of low pH value (Sulzer *et al.*, 2000), whereas they are easily oxidized outside the organelles. The DA oxidation generates a dopamine semi-quinone free radical, dopamine quinone, dopaminochrome, as well as the reactive oxygen species (Bors *et al.*, 1978; Pileblad *et al.*, 1988). The treatment by L-DOPA, precursor of DA, as a supplement can reduce the level of DA in the brain and has been widely used. However, long-term L-DOPA therapy frequently causes various adverse reactions. The adverse reactions are thought to be correlated, at least in

part, with the neurotoxicity induced by auto-oxidation of excess level of the DA. It has been reported that the spontaneous auto-oxidation of DA produces ROS ($O_2^-$) and reactive quinone (Tse *et al.*, 1976). In the brain, the tyrosinase may enzymatically and rapidly convert the excess amount of DA to DA-quinone and $H_2O$, and then convert to neuro-melanin (Asanuma *et al.*, 2003). However, the tyrosinase could lose its function under the oxidative stress condition (Andrwais *et al.*, 1985). Therefore, the DA oxidation will occur by auto-oxidation pathway of DA to generate ROS, which could make membrane damaged. However, the relationship between DA and membrane has not been clarified yet.

Extremely abnormal levels of DA concentration have been reported to be symptoms of several diseases, such as Parkinsonism and schizophrenia (Mo *et al.*, 2001; Wightman *et al.*, 1988). Therefore, the detection of DA concentration is useful for the prevention of disease and for the monitoring of the disease treatment. Much research on the determination of DA concentration has been carried out. The most common methods for the determination of this biogenic amine are the fluorometric combined chromatography (Takahashi *et al.*, 1972; Peat *et al.*, 1983; Mori *et al.*, 1985), radio-enzymatic assay (Hard *et al.*, 2001), HPLC (Cannazza *et al.*, 2005), and voltammetric assays (Atta *et al.*, 1991; Zucolotto *et al.*, 2006). Although the chromatography system works very well with high sensitivity, it is an expensive system with complicated sample treatment. Therefore, the sensor systems need to be applied because those can provide the cheaper, more portable, easier sample preparation and faster measurement. The detection can be often achieved by the electrochemical methods utilizing an anodic oxidation because the DA is easily oxidized compound. Voltammetric assays were known as the simple method with high sensitivity and fast measurement. Recently, there has been an increasing demand for more sensitive and simple analytical methods. Cyclic voltammetry (CV) and different pulse voltammetry (DPV) techniques are very useful and popular for the trace analysis because these techniques are compact, efficient, and sensitive (Zhang *et al.*, 2006; Zhao *et al.*, 2001). Various voltammetric techniques have been shown to have the low detection limit required for DA analysis, depending on the type of working electrode system.

Among the various approaches used, the polymer-modified electrodes can offer several advantages in terms of the ease of preparing stable and adherent films and the possibility to manipulate the selectivity and sensitivity through the incorporation of functional groups. The polymer modified conventional electrodes, such as glassy carbon, platinum, gold, carbon paste, etc. (Erdoğdu et al., 1997; Zheng et al., 2006), have attracted great attention because of their good stability and reproducibility. Among the electronically conducting polymers, a poly(3-methylthiophene) (PMeT) has been widely investigated. It can be easily electrodeposited onto an electrode surface by the electro-oxidation of its monomer.

In this chapter, a glassy carbon electrode modified with a PMeT layer or a composition of Nafion and PMeT were prepared in order to develop the sensing method of DA. The Nafion film was first prepared on the surface of a GC electrode before the preparation of the PMeT film. Both of PMeT and Nafion/PMeT modified GC electrode showed high sensitivity in the DA detection. Second, for the deeper understanding of the behavior of DA on the biomembrane and the effect of biomembrane on DA and its oxidation, a series of experiments were performed in order to clarify: *(i)* how the DA partitions onto lipid membrane? *(ii)* how the DA make the membrane damaged, and *(iii)* how the membrane affects the stability of DA. Some kinds of liposomes were prepared to mimic both normal membrane and damaged membrane under the oxidative stress condition (oxidized membrane). The experiments were achieved by monitoring the DA concentration measured by DA sensor.

## 2. Materials and Methods

### 2.1. Materials

Dopamine hydrochloride (DA), L-tyrosine (Tyr), catechol (Cat), 3,4-dihydroxy-L-phenylalanine (L-DOPA), norepinephrine (NE) and epinephrine (EP) were purchased from Sigma-Aldrich (St. Louis, MO, USA). 3-Methylthiophene (MeT), and Nafion® 117 were purchased from Fluka (Switzerland) and used without further purification. Dopamine

hydrochloride (DA) and tetrabutylammonium tetrafluoroborate (TBATFB) were purchased from Sigma-Aldrich. 1-(4-Trimethylammo-niumphenyl)-6-phenyl-1,3,5-hexatriene (TMA-DPH), 1,6-diphenyl-1,3,5-hexatriene (DPH) from Molecular Probes (Eugene, OR). 1,2-dioleoyl-3-trimethylammonium-propane (chloride salt) (DOTAP), 1-palmitoyl-2-oreloyl-*sn*-glycero-3-phosphocholine (POPC), 1,2-ditetradecanoyl-*sn*-glycero-3-phospho-(1'-*rac*-glycerol) (sodium salt) (DMPG), 1-octadecanoyl-2-arachidonyl-*sn*-glycero-3-phosphocholine (SAPC) were obtained from Avanti Polar Lipids (Alabaster, AL, USA). Cholesterol (Ch) was obtained from Wako Pure Chemical (Osaka, Japan). Stearic acid (SA) was purchased from Sigma Aldrich. The chemical structure of lipids used here was listed in **Table 1-1**. Other reagents used were purchased form Sigma Aldrich and Wako Pure Chemical (Osaka, Japan). All of the aqueous solutions were prepared with twice-distilled water.

**Table 1-1** Chemical structure of lipids used in this chapter

| Lipids | M.W. | Chemical aspect | Chemical structure |
|--------|------|-----------------|--------------------|
| DMPC | 677.93 | | |
| POPC | 760.06 | One C=C in acyl chain. | |
| SAPC | 810.135 | Four C=C advantageous for its oxidation | |
| DMPG | 688.845 | Negatively charge | |
| DOTAP | 698.54 | Positively charge | |
| Cholesterol | 386.64 | Decrease in membrane fluidity | |
| SA(stearic acid) | 284.48 | Negatively charge | |

## 2.2. Apparatus

Electropolymerization was carried out with a 750A Electrochemical analyzer (Tokyo, Japan) in a three electrode cell (Bioanalytical Systems, USA) consisting of a Ag/AgCl (3M NaCl) reference electrode (Bioanalytical Systems, USA), a platinum coil auxiliary electrode (Bioanalytical Systems, USA), and a glassy carbon (GC) disk electrode (2 mm $i.d.$, Metrohm, Switzerland) used as the working electrode. All of the electrochemical measurements were performed in a standard cell (Tokyo, Japan).

## 2.3. Fabrication of Modified Glassy Carbon Electrode

Three kinds of electrodes were used in this study (**Table 1-2**). The GC electrodes were pretreated by using the following process. First, the surface of a GC electrode was polished with alumina slurry (0.05 μm), washed with distilled water, and placed in a water-filled ultrasonic bath for 30 s. Each GC electrode was subsequently subjected to cyclic voltammetry in 1.0 M sulfuric acid between -0.1 and +1.6 V with a scan rate of 100 mV/s for 5 cycles, washed, and allowed to dry at room temperature in a desiccator. Electrochemical polymerization was carried out in a one compartment cell containing a nitrogen-purged solution of 100 mM TBATFB and 150 mM MeT in acetonitrile. The PMeT film was grown for 20 s at a constant potential of 1.8 V vs. Ag/AgCl. After electropolymerization, the polymer film was kept at the reduction potential (−0.2 V) for 5 min. The preparation of a GC/Nafion/PMeT electrode required an additional step prior to the polymerization of the PMeT film on the electrode. A 0.5% Nafion solution in ethanol was prepared from a 5% Nafion® 117 solution. 5 μl of the 0.5% Nafion solution was carefully deposited on the electrode surface using a 25-μl syringe (SGE, Australia). The electrode was then left in a desiccator for 5 min to evaporate the solvent to create a thin film. The average thickness of the Nafion film was estimated using a recast density of 1.98 g cm$^{-3}$ (Rocha $et\ al.,$ 2006).

**Table 1-2** Conditions for preparation of modified electrode

| No | Electrode | Contents |
|---|---|---|
| 1 | GC[1] | Bare |
| 2 | GC/PMeT[2] | PMeT was electrochemically deposited on GC |
| 3 | GC/Nafion/PMeT | PMeT was polymerized on surface of Nafion-coated GC |

[1] GC: glassy carbon, [2] PMeT: poly(3-methyl thiophene)

## 2.4. Scanning Electron Microscopy

To obtain SEM images, the Nafion film and Nafion/PMeT film were prepared on indium tin oxide (ITO)-coated glass substrates (BAS Inc., Tokyo, Japan), instead of GC electrodes. All the films were prepared on the ITO electrodes using the same conditions as the GC electrodes. These films were sputtered with Pt and observed with a scanning electron microscope (S-3500, Hitachi Co. Ltd.).

## 2.5. Electrochemical Measurement

Electrochemical experiments were performed in a 0.1 M $H_2SO_4$ solution containing the catecholamine with specific concentrations and deoxygenated by purging with high-purity nitrogen. All the CVs and DPVs were recorded in a suitable potential range. All the experiments were performed at room temperature and under an air atmosphere in a standard cell.

## 2.6. Liposome Preparation

Liposomes were prepared by the following method as previously reported (Yoshimoto *et al.*, 2006). The lipid mixture was dissolved in chloroform and then dried onto the wall of a round-bottom flask in vacuum and was then left overnight to ensure the removal of all of the

solvent. The dried thin lipid film was hydrated with adequate buffer solution to form multilamellar vesicles (MLVs). Large unilamellar vesicles (LUVs) were formed from the MLVs with five cycles of freeze-thaw treatment. The liposomes were made in a diameter of 100 nm. For the preparation of oxidized lipid, the $SAPC_{ox}$ was prepared by mixing SAPC vesicles with $CuSO_4/H_2O_2$ (1 mM) solution over night at 25 °C. After that, the lipid was extracted into chloroform/MeOH phase by Folch's method (Folch *et al.*, 1957). The oxidized liposomes were prepared by mixing $SAPC_{ox}$ with DMPC or DMPG lipid in a molar ratio 4:6.

## 2.7. Membrane Fluidity Measurement

Membrane fluidity of liposomes was analyzed by measuring the fluorescence polarization (P) of TMA-DPH/DPH incorporated in lipid membranes according to the previous report (Yoshimoto *et al.*, 2006). The method is simply described here as follows. A solution of TMA-DPH or DPH (in ethanol) was added to the liposome solution to maintain the lipid/probe molar ratio 250 ([TMA-DPH/DPH] $_{final}$ = 1 μM, water/ethanol volume ratio ≥ 100). The mixture was incubated at 37 °C at least 1 h with gentle stirring. The fluorescence polarization of samples was measured with a spectrofluorimeter (FP-777 JASCO Co. Ltd., Tokyo). The sample was excited with vertically polarized light (360 nm), and emission intensities (430 nm) both parallel ($I_{//}$) and perpendicular ($I_{\perp}$) to the excited light were recorded. Then, polarization of TMA-DPH was calculated using the following equation:

$$P = \frac{I_{//} - I_{\perp}}{I_{//} + I_{\perp}}$$   (1-1)

The term "fluidity" is inversely proportional to the degree of fluorescence polarization of the probe; that is, "membrane fluidity" of the surface of membrane was defined by (*1/P*) of TMA-DPH/ DPH.

# 3. Results and Discussion

## 3.1. Development of Sensor Based on Conducting Polymer

### 3.1.1. Electrochemical Polymerization

The polymer film was deposited on the GC electrode by electrochemical method. The polymerization was carried out in a one compartment cell containing a nitrogen-purged solution of 100 mM TBATFB and 150 mM MeT in acetonitrile. The PMeT film was grown for 20 s at a constant potential of 1.8 V vs. Ag/AgCl. The condition for preparation of electrodes was shown in **Table 1-2**.
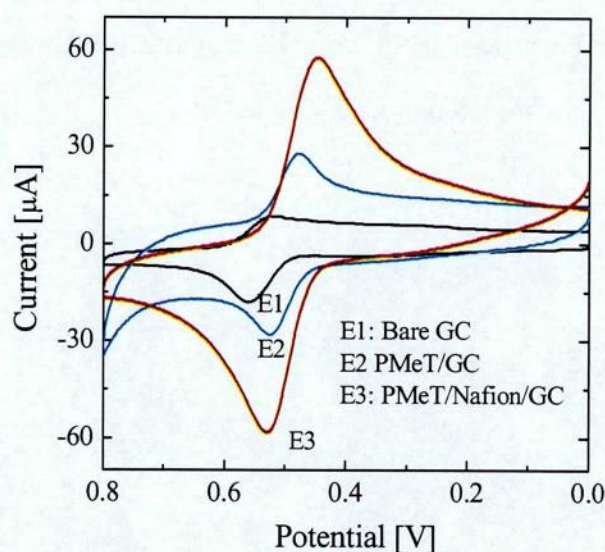


**Fig.1-1** Cyclic voltammograms of 1 mM DA solution at different electrodes: (E1) Bare GC, (E2) GC/PMeT, and (E3) GC/Nafion/PMeT. Electrolyte $H_2SO_4$ 0.1M, scan rate: 50 mV s$^{-1}$, measurement temperature: 25 °C.

A comparison was made in the cyclic voltammetric behavior of DA at three kinds of modified electrodes (**Table 1-2**). The CVs of solutions containing 1 mM DA in 0.1 M $H_2SO_4$ at three different electrodes are shown in **Fig.1-2**. At the bare GC electrode (curve E1), the response was very poor. The response of DA increased at PMeT modified GC electrode (curve E2). The reason for the higher peak current may originate from the larger surface area of the PMeT film as compared with that of the bare GC electrode, along with the electronic

conductivity of the PMeT. The Nafion and PMeT composite was designed to modify the electrode based on the above results, showing the more improvement on the DA response (curve E3). The reason on the above results may originate form the negatively-charged property of Nafion film to enhance the partitioning of DA at cationic form. It is expected that the polymerization of the PMeT after the Nafion modification of the GC electrode would improve the response of DA in both the Nafion and PMeT.

### 3.1.2. Observation of Hybrid Film Using SEM

The surface properties of the electrode are the key for the selective detection of DA. The surface structures of electrodes modified with polymer films were observed. PMeT and Nafion were used for the modification of an ITO glass electrode. **Figures.1-2a, 1-2b,** and **1-2c**
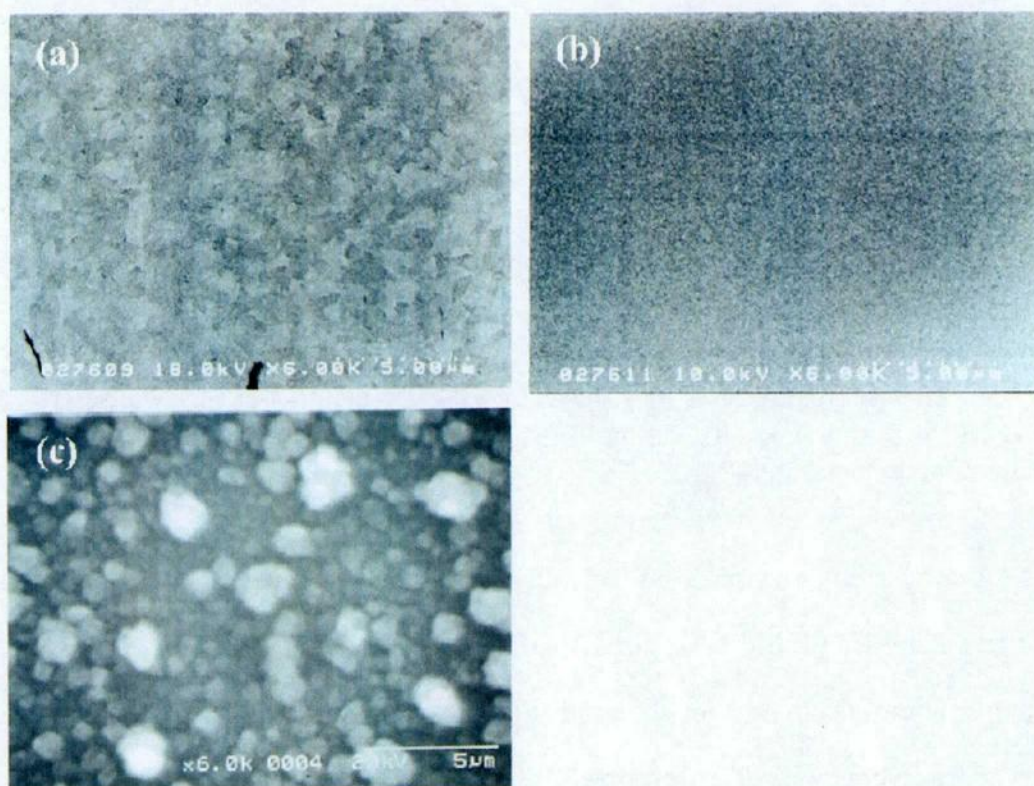


**Fig.1-2** SEM images of (a) bare ITO electrode, (b) Nafion modified ITO electrode, and (c) Nafion/PMeT modified ITO electrode.

show the SEM images of a bare ITO electrode, an ITO/Nafion electrode mimicking the GC/Nafion electrode, and an ITO/Nafion/PMeT electrode mimicking the GC/Nafion/PMeT electrode, respectively. The surface of a bare ITO electrode was found to have a slight roughness (**Fig.1-2(a)**). However, it became smoother when the surface of the electrode was coated with Nafion film (**Fig.1-2(b)**). The results indicated that there was Nafion film on the surface of the ITO electrode. In the case of the Nafion/PMeT film, a compact spherical grain of polymer was observed on the surface of the electrode (**Fig.1-2(c)**), resulting in an increase on the surface area of the electrode to increase the peak current.

### *3.1.3. Effect of Scan Rate on the Peak Currents for Dopamine at the GC/Nafion/PMeT Electrode*

The effect of the scan rate on the peak current for DA was investigated in a 0.1 M $H_2SO_4$ solution containing 1 mM DA. As shown in **Fig.1-3(a)**, both the cathodic and anodic peak currents increased with an increase in the scan rate from 10 to 200 mV s$^{-1}$, and the peak potential shifted slightly. The anodic or cathodic peak currents were proportional to the scan rates from 10 to 200 mV s$^{-1}$ and the curves were linear (**Fig.1-3(b)**), suggesting that the
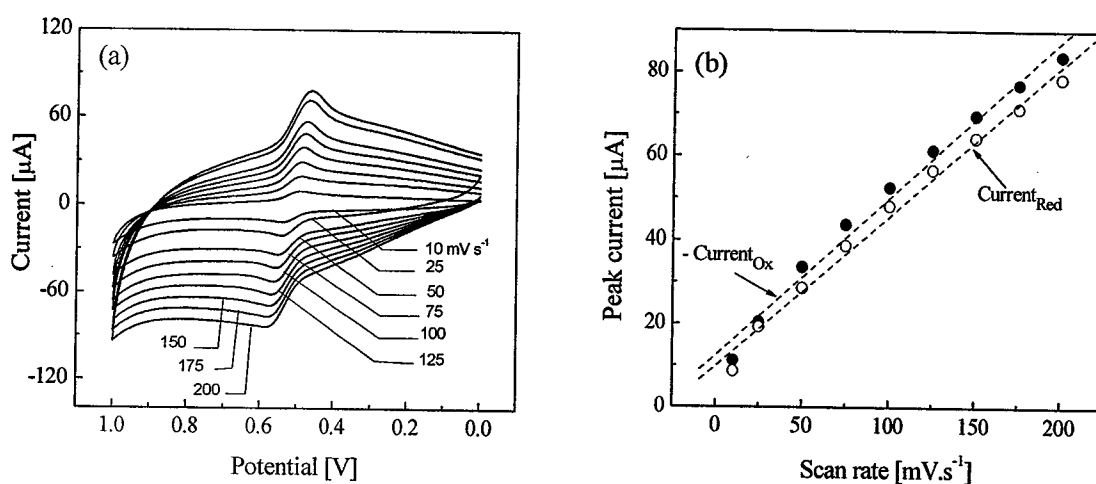
**Fig.1-3** (a) Electrochemical response of 1 mM DA in 0.1 M $H_2SO_4$ solution at Nafion/PMeT modified GC electrode with different scan rates, from 10 to 200 mV• s$^{-1}$ and (b) the plot of the peak current against the scan rate. Measurement temperature: 25 °C.

electrode reaction of DA at the Nafion/PMéT modified GC electrode was a typical adsorption-controlled process.

### 3.1.4. Effect of Nafion Film

At pH values below 7.0, DA (p$K_a$ = 8.93) (Tuckerman et al., 1959) exists predominantly in the cationic form. Because of this, the DA signal can be enhanced by improving the cation exchange capacity of the conducting polymer layer. The proton exchange polymer Nafion was used. The addition of Nafion to the GC electrode was shown to improve the DA signal since Nafion has a negatively charged ion-exchange group ($SO_3^-$), which could enhance the adsorption of DA on the surface of the electrode via the following equation (Rocha et al., 2006):

$$Nafion(\sim SO_3^-)(H^+)^{film} + (DA^+)^{solu} \rightleftharpoons Nafion(\sim SO_3^-)(DA^+)^{film} + (H^+)^{solu} \qquad (1\text{-}2)$$
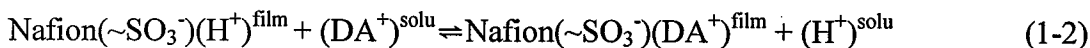
At a condition of [$H^+$] $\gg$ [$DA^+$], the partitioning behavior of DA, described above, can be simply described by $(DA^+)^{solu} \rightleftharpoons (DA^+)^{film}$ and the partition coefficient of DA has been
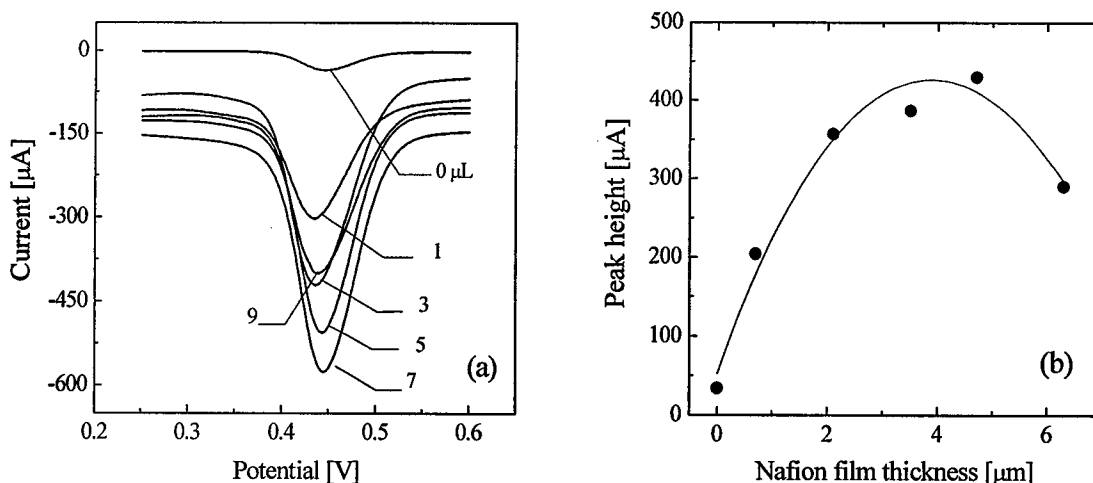


**Fig.1-4** Effect of the amount of Nafion on measurement of DA. (a) DPV voltammograms of DA on electrodes were prepared from different volumes of Nafion (0 to 9 μl). (b) Effect of the average Nafion film thickness on the oxidation peak height of DA. Measurement temperature: 25 °C.

reported to be given by $K = C_{DA}^{film} / C_{DA}^{solu} = 401$ in the range of $C_{DA}^{solu} < 0.1$ mM (Rocha *et al.*, 2006). In the above condition tested here, the DA was considered to preferably partition into the Nafion film.

The degree of improvement was also dependent on the amount of Nafion. In order to estimate the effect of the amount of Nafion (corresponding to the number of ion-exchange sites), five kinds of GC/Nafion/PMeT electrodes were prepared with the different volumes of Nafion coated on the surfaces of GC electrodes. Other than the Nafion content, all of the PMeT films were prepared under the same conditions.

As shown in **Fig.1-4**, the peak height was shown to be increased as the average thickness of the Nafion film increased to 4.9 μm. The peak current decreased when the average thickness of the Nafion film became higher than 4.9 μm. Nafion has the ability both to attract the DA due to its high affinity to cations (partition coefficient = 401 (Rocha *et al.*, 2006) and to reduce the mass transfer rate of both DA and electrons (Wang *et al.*, 2006). Therefore, the addition of Nafion with a little amount forms a thin film, resulting in poor sensitivity to DA, while a larger amount of Nafion forms a relatively thick film decreasing the mass transfer rate of DA and the transfer rate of electrons within the Nafion film. Therefore, in this study, an average Nafion film thickness of 3.5 μm (corresponding to 5 μl of the 0.5% Nafion solution) was chosen for the modification of an electrode in all further experiments.

## 3.2. Response of Dopamine at Modified Electrodes

### 3.2.1. Sensitivity of Modified Electrode for Dopamine

The detection by electrochemical methods is possible based on the anodic oxidation considering the fact that DA is easily-oxidized compound. The oxidation of DA was simply described in **Fig.1-5**.

27
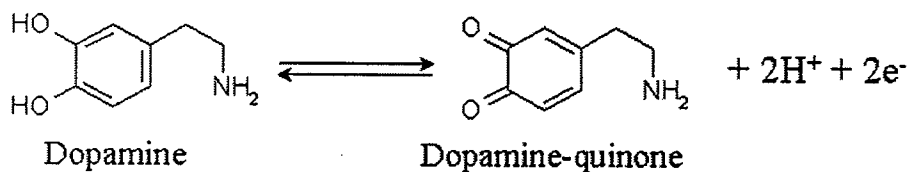
Fig.1-5 Reaction for oxidation of DA to form DA-quinone.

The detection limit of sensor for DA was also shown in **Fig.1-6**. In a 0.1 M $H_2SO_4$ solution, the voltammetric response of DA on the GC/PMeT electrode shows linearity range as follows: 1 to 1000 μM. The linear regression equation was $I(\mu A) = 0.739 + 0.038 \times C_{DA}$ (μM) with a correlation coefficient of 0.999 (**Fig.1-6(a)**). In the case of the GC/Nafion/PMeT electrode, the linear regression equation was $I(\mu A) = 7.23 + 0.845 \times C_{DA}$ (μM) with a correlation coefficient of 0.999 in the range of 0.5 - 200 μM. In the case of the GC/Nafion/PMeT electrode, the linear regression equation was $I(\mu A) = 7.23 + 0.845 \times C_{DA}$ (μM) with a correlation coefficient of 0.999 in the range of 0.5 - 200 μM (**Fig.1-6(b)**). The slopes representing the sensitivities of two electrodes were 1.21 and 26.7 μA μM$^{-1}$ cm$^{-2}$, respectively.
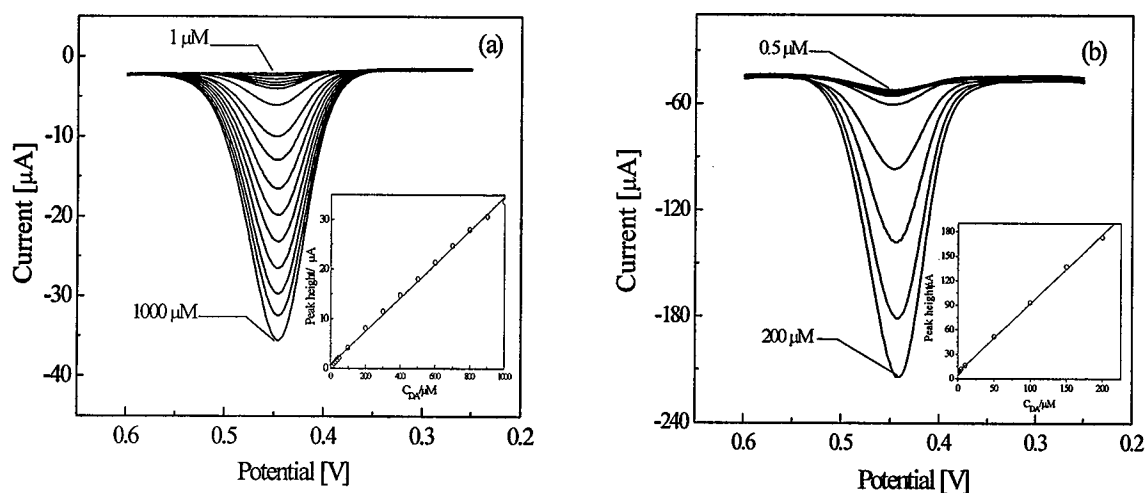


Fig.1-6 DPV voltammograms for various DA concentrations in a 0.1 M $H_2SO_4$ solution. (a) DA concentration: 1 - 1000 μM at GC/PMeT electrode and (b) DA concentration: 0.5 - 200 μM at GC/Nafion/PMeT electrode. Inset figures show the relationship between the height of the peak current and the concentration of DA. Measurement temperature: 25 °C.

*3.2.2. Analytical Application*

In order to check the reproducibility of DA response at conducting polymer modified GC electrode. The response of DA solution was performed at both of PMeT/GC and PMeT/Nafion/GC electrode. The recovery concentration of DA calculated by this method was shown in **Table 1-2**. The response of 50 μM DA solution on PMeT/GC and 10 μM DA at PMeT/Nafion/GC was performed with 10 times for reproducibility.

**Table 1-2** Response of 50 μM DA solution at PMeT modified GC electrode and 10 μM DA solution at Nafion/PMeT modified GC electrode

| PMeT/GC electrode | | PMeT/Nafion/GC electrode | |
|---|---|---|---|
| DA conc. [μM] | Recovery [%] | DA conc. [μM] | Recovery [%] |
| 50 | 94.57 ± 2.17 (n=10) | 10 | 97.05 ± 6.35 (n=10) |

## 3.3. Dopamine-Liposome Membrane Interaction ~ Application of DA Sensor

*3.3.1. Conventional Pathway of DA Oxidation and Possible Lipid Peroxidation*

From the numerous researches relating to the neurotransmitters, their metabolic pathway has been clarified to some extent. **Figure 1-7** shows the pathway of dopamine-relating metabolism, together with the relating enzymes. In its scheme, the DA-oxidation is achieved by an auto-oxidation associated with the production of the $O_2^-$ with strong toxicity or by an enzymatic oxidation associated with $H_2O$ production. In the auto-oxidation process, the generated $O_2^-$ can give the damages to (membrane) proteins or genes although the damage of biomembranes has not been mentioned in the conventional research. Considering the downstream of DA metabolism to produce the epinephrine, its hydroxylation process from dopamine to norepinephrine is catalyzed by a dopamine β-hydroxylase (DβH). It has been reported that the DβH has the membranous form (the conformational state to bind to the membrane) (Grouselle *et al.*, 1982), strongly suggesting that DA is likely to partition into

lipid membrane phase. However, there is a little information on the partitioning behavior of these neurotransmitters. Therefore, two problematic issues could be elucidated as below:

(1) The relationship between the DA-relating metabolites and the biomembrane.

(2) The oxidative stress of DA to biomembrane.

In order to discuss the above two points, the partitioning behavior for these compounds was quantitatively studied in the following section based on the analytical data using an immobilized-liposome chromatography (ILC). The DA sensor was also applied for the detection of DA concentration in this series of experiment. The experimental condition was selected to investigate the DA-lipid membrane interaction in order to clarify *(i)* how DA behaves on liposome membrane and *(ii)* how the liposome membrane affects on DA
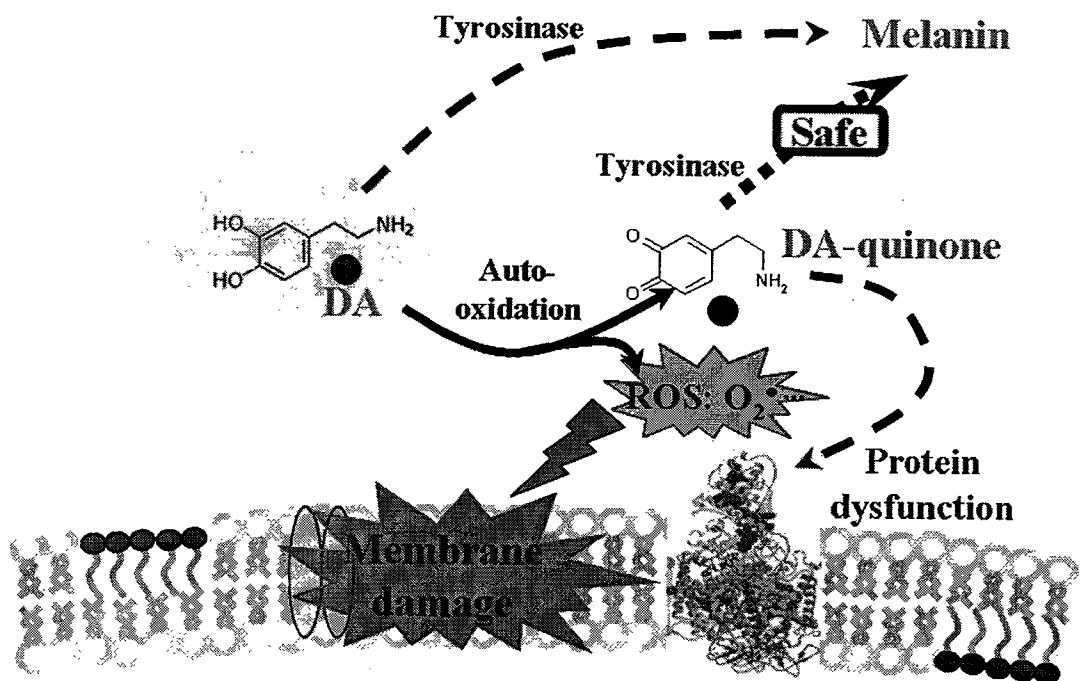


**Fig.1-7** Possible pathway of reactive oxygen species (ROS) generation by excess amount of free DA and induces cell damage (Asanuma *et al.*, 2003).

*3.3.2. Partitioning of Dopamine onto Liposome Membrane*

It has been previously reported that the ILC is a useful tool to evaluate the affinity of target material to (model) biomembrane (Yang *et al.*, 1994, Yoshimoto *et al.*, 2006). In terms

of the quantitative structure toxicity relationships (QSTR) study, there are many reports that the partitioning behavior of target compounds can be explained by their hydrophobicity. Among the evaluation method of hydrophobicity of substrates, such as drugs or amino acids, the partition coefficient of target between water and octanol (LogP) has been well-known (Abraham *et al.*, 1987). A linear correlation of $k_s$ value for various compounds with their LogP value was also obtained:
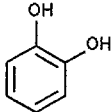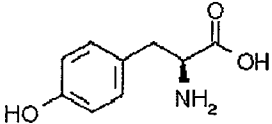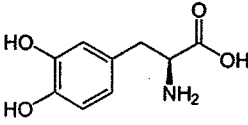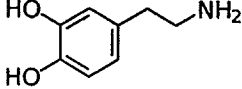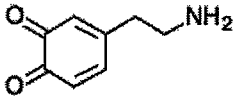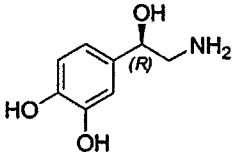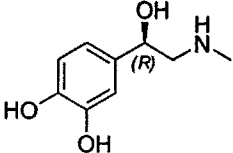
$$k_s = 1.199 + 0.4485 \log P \ (R^2 = 0.9297) \tag{1-3}$$

This equation is consistent with the previous findings in relation to the assessment of toxicity of drug molecules with ILC (Yang *et al.*, 2001) or other methods (Moridani *et al.*, 2003). There is a calculation rule to get the $\log P$ value for target. For examples, a "fragmentation rule" is a typical method to calculate the $\log P$ value by a fragmentation of chemical structure of target into the elemental structure with defined LogP value (Abraham *et al.*, 1987). Therefore, the chemical structure can give the rough estimate for its membrane affinity.

The $\log P$ value and the $k_s$ value for catechol and its derivatives were calculated by using the equations (1-3) and the fragmentation rule (**Table 1-3**). As a whole, the trend of the partition behavior of catechol derivatives could roughly be expressed with the equation based on the amino acids although there are some deviations of calculated $k_s$ value from the measured value exist. Among the above catecholamines, the DA was found to show the largest $k_s$ value ($k_s = 4.7$), indicating that the DA could strongly partition to the liposome membrane. On the other hand, L-DOPA was found to show the negative $k_s$ value ($k_s = -0.54$), indicating that L-DOPA disfavors the partitioning on membrane and exists in bulk aqueous solution. This finding also suggests that the decarboxylation of L-DOPA might occur for the enhancement of its partitioning characteristics on membrane.

In order to compare the DA partitioning in different liposome membranes with different hydrophobic nature, a series of liposomes were prepared as for both normal liposome membranes and oxidized liposome membranes. The 2 ml mixed solution containing0.5 mM DA and 1 mM liposome was incubated for 30 min for the partitioning of

**Table 1-3** Hydrophobicity of some neurotransmitter catecholamines

| Compounds | Structure | LogP* [-] | $k_s$ [ml/mmol] |
|---|---|---|---|
| Catechol | | 0.29[a] | 1.33(calc.)[g] |
| L-Tyrosine | | -2.05[a] | 0.279(calc.) 0.189(obs.)[h] |
| L-DOPA | | -1.22[b] | 0.652(calc.) -0.541(obs.) |
| Dopamine (DA) | | 0.12[c] | 1.25(calc.) 4.71(obs.) |
| Dopamine-quinone | | -0.34[d] | 1.05(calc.) |
| Nor epinephrine (NE) | | -1.75[e] | 0.41(calc.) 2.15(obs.) |
| Epinephrine (EP) | | 1.87[f] | 2.04(calc.) 2.80(obs.) |

*Water-to-octanol partitioning coefficient. According to the fragmentation rule, LogP value was calculated. LogP = $\Sigma$ f(R). Here, f(R) is the fragment constant of the elemental group R. [a] Moriani et al., 2003, [b] f(L-DOPA) = f(DA)-f($CH_2$)+f(CH)+f($COO^-$) = 0.12-0.66+0.43+(-1.11) = -1.22. [c] Liu et al., 2004, [d] f(DA-quinone) = f(DA)-f($C_6H_5O_2$)+f($C_6H_3O_2$) = 0.12-0.575+0.115 = -0.34. Here, f($C_6H_5O_2$) = 3f($CH_{aromatic}$)+3f($C_{aromatic}$)+2f($OH_{aromatic}$) = 3(0.355)+3(0.13)+2(-0.44) = 0.575 and f($C_6H_3O_2$) = 3f($CH_{aromatic}$)+3f($C_{aromatic}$)+2f($OH_{aromatic}$)-2f(H) = 3(0.355)+3(0.13)+2(-0.44)-2(-0.23) = 0.115. [e] f(NE) = f(DA)-f($CH_2$)+f(CH)+f(OH) = 0.12-0.66+0.43+(-1.64) = -1.75. [f] f(EP) = f(NE)-f($NH_2$)+f(NH)+f($CH_3$) = -1.75-(-3.40)+(-0.67)+0.89 = 1.87. [g] $k_s$ values was calculated from LogP value with equation (1-3). [h] $k_s$ was experimentally determined.

DA onto lipid bilayer, and then the non-partitioned (unbound) DA was separated form solution by ultra-filtration with the membrane filter to cut off 3 kDa molecules (The operation was schematically shown in **Fig.1-8(a)**).
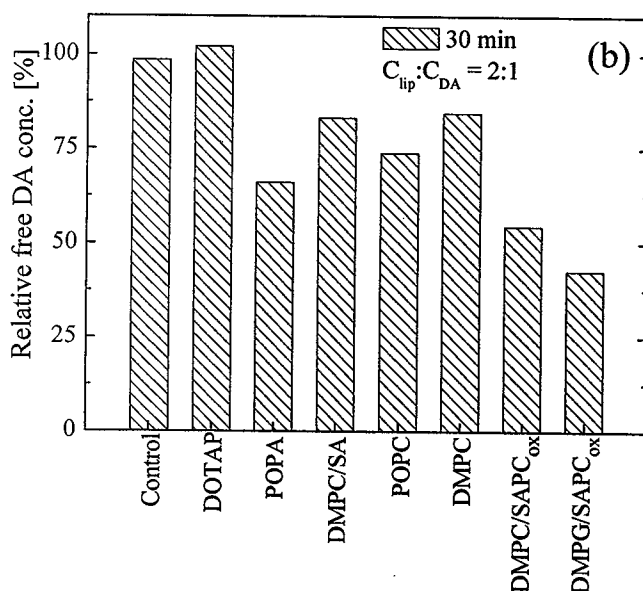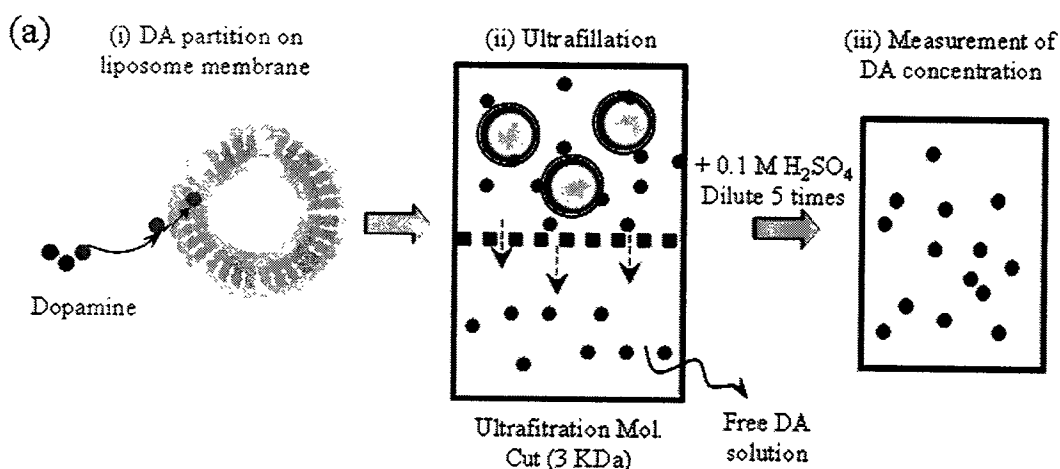
**Fig.1-8** (a) Conceptual illustration for ultra-filtration for separation of free DA from liposome solution. (b) Free remained DA concentration after 30 min incubated with liposome at 37 °C.

As shown in **Fig.1-8(a)**, the DA concentration was remained at 100% in the case of control sample, indicating the non-oxidation of DA within 30 min. However, the DA concentration deceased in the presence of liposomes, indicating that the DA could partitions (adsorbs) onto the liposome membrane, except for the cationic DOTAP liposome. The DA concentration with the cationic DOTAP liposome was similar as that of control sample. This is caused by the electrostatic repulsion between the liposomes and DA. On the contrary, the anionic liposomes (POPA and DMPG/SAPC$_{ox}$ liposomes) show more effective partitioning

into the liposome membrane. These results also indicate that the partitioning (adsorption) of the DA on the liposome membrane may be contributed by both of the hydrophobic interaction and electrostatic interaction, caused by the cationic group of DA which has a positive charge at physiological pH value ($pK_a$= 8.93).

The partition coefficient for water-lipid was calculated for different liposomes by using the following equation:

$$K_{LD} = C_{DA}^{lip}/C_{DA}^{water}$$

where $C_{DA}^{water}$ is DA concentration on water phase and $C_{DA}^{lip}$ was the DA concentration on lipid phase. The $C_{DA}^{water}$ value was estimated by unbound DA concentration measurement (**Fig.1-8(b)**).

The DA concentration on lipid phase was calculated based on the mole of DA partitioning onto lipid membrane and total volume of lipid. In order to estimate the volume of

**Table 1-5** Partition coefficient of DA onto different liposome membrane

| Liposome | $V_{lip}$* $10^{-3}$ [ml] | $K_{LD}$ [-] | $\Delta(1/P)$** TMA-DPH | $\Delta(1/P)$ DPH | $m_{lip}$# [-] | $LH_{lip}$# [-] |
|---|---|---|---|---|---|---|
| POPC | 3.164 | 224.13 | 0.031 | 0.105 | 0.0240 | 0.81 |
| DMPC | 3.164 | 116.8 | 0.042 | -0.004 | 0.0038 | 0.95 |
| DMPC/SA (10:4) | 3.164 | 126.73 | -0.200 | 0.145 | 0.0710 | 0.24 |
| DMPC/SAPC$_{ox}$ (6:4) | 3.164 | 529.86 | 0.001 | -0.157 | 0.0620 | 0.23 |
| DMPG/SAPC$_{ox}$ (6:4) | 3.164 | 853.46 | 0.025 | -0.080 | 0.0510 | 0.21 |
| DOTAP | 3.164 | n.d | -0.016 | -0.095 | n.d. | n.d |
| POPA | 3.164 | 325.27 | 0.027 | -0.070 | 0.0021 | 0.21 |

** $V_{lip}$, volume of liposome on 2 ml solution of 1 mM lipid concentration, was calculated as method described above, herewith be assumed that lipid bilayer thickness of 3.7 nm (Tahara el al., 1994), lipid molecule head group of area of 0.72 nm$^2$ (Tazan et. al., 1996); thickness of other compounds incorporated POPC or DMPC bilayer membrane is similar to POPC, DMPC bilayer membrane. ** $\Delta(1/P) = (1/P)_{DA} - (1/P)_0$  # The $m_{lip}$ value and $LH_{lip}$ value were measured at 25 °C.

34

lipid, it is assumed that all liposomes solution contains the same volume of lipid at the same concentration of lipid and volume of liposome concentration. $V_{lip}$ could be calculated in the following by selecting POPC liposome as an example: $V_{lipid}/1$ liposome $= (4/3)\pi(R_{out}^3-R_{in}^3) = (4/3)\pi (50^3 - 46.3^3) = 107.8 \times 10^3$ $(nm^3) = 107.8\times10^3\times10^{-21} = 107.8\times10^{-18}$ $(cm^3) = 107.8\times10^{-18}$ (ml). The number of liposomes on 2 ml of solution with 1 mM lipid concentration is:

$$N_{liposome} = 2\times10^{-3}\times1\times10^{-3}\times6.023\times10^{23}/40503 = 2.934\times10^{13} \text{ (liposomes)}$$

The number 40503 is number of lipid molecules per 1 liposome, herewith be assumed that liposome is a 100 nm in diameter spherical shape, a PC head group of area of 0.72 $nm^2$ (Tazan et al., 1996), a POPC lipid bilayer thickness of 3.7 nm (Tahara et al., 1994). Therefore, the calculated volume of lipid on 2 ml lipid solution with 1 mM lipid concentration is: $V_{lip} = 107.8\times10^{-18}\times2.934\times10^{13} = 3.164\times10^{-3}$ (ml). The value of $K_{LD}$ was summarized in **Table 1-5**. The partitioning(adsorption) of DA into liposome membrane can lead to the change in the membrane fluidity. The membrane fluidity, $(1/P)_{TMA-DPH}$ and $(1/P)_{DPH}$, for both of surface and inner membrane fluidity, respectively, were measured. The variation in surface membrane fluidity $\Delta(1/P)_{TMA-DPH}$ is considered to be induced by the adsorption of DA on surface of liposome. Otherwise, the $\Delta(1/P)_{DPH}$ value is considered to be induced by the partitioning of DA into hydrophobic region of lipid bilayer. The experiments were performed by incubating DA with liposome for 30 min. The data were shown is **Table 1-5**. Not a significant variation of membrane fluidity was observed in all the liposome. In the following, the effect of an auto-oxidation of DA on membrane property of liposome was investigated by measuring of the membrane fluidity after 24-h incubation of liposome with DA.

### 3.3.3. Toxicity of Dopamine in Biological System

As shown in the previous reports, under normal condition, the DA exists inside the vesicles, which keep it stable because of low pH value of inner vesicle solution (Sulzer et al., 2000). Outside of the vesicle, it is easy for DA to be oxidized by auto-oxidation pathways

which produce ROS ($O_2^-$, OH•) (Asanuma *et at.,* 2003). According to the above result, the DA was found to adsorb on the surface of membrane and to partition onto hydrophobic region of lipid bilayer. On the surface of liposome membrane, the DA may be coverted into DA-quinone and therefore produces ROS. ROS is easily attached on the lipid membrane.

In order to confirm the effect of DA in term of the membrane damage by ROS generation, the effect of DA on the liposome membrane was estimated by the membrane fluidity $(1/P)_{DPH}$ for inner membrane fluidity. The membrane fluidity $(1/P)$ using DPH measurement was performed after incubating 100 µM DA with 250 µM liposome for 24 h at 37 °C and the obtained result was compared to that without DA. The variation of membrane fluidity is shown in **Fig.1-9** to compare the oxidable liposome (POPC) and non-oxidable liposome (others) in term of double bond. As expected, the membrane fluidity of POPC liposome, containing 1 double bond on each lipid molecule, decreased significantly in comparison with other liposomes, which have no unsaturated fatty acid. Form these results, although the more clear evident is needed, it could be concluded that that the DA induced the peroxidation of unsaturated lipid on the liposome surface by ROS generation during its
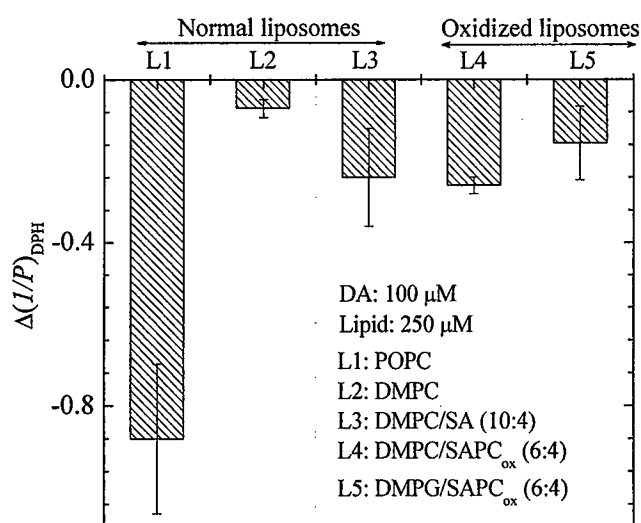


**Fig.1-9** Variation of membrane fluidity, $\Delta(1/P)_{DPH}$, by lipid oxidation of liposomes composed of various lipid composition induced by DA after incubated with DA at 37 °C for 24 h.

auto-oxidation and that a possible lipid-DA adduct might be generated at high extent enough to raise the packing density of lipid membrane structure. This result is helpful to clarify the mechanism of the toxicity of DA and other neurotransmitter induced in the case of their extremely high concentration.

### 3.3.4. Oxidation of Dopamine Promoted by Lipid Membrane

Inversely, by entrapping DA on the membrane, the liposome may have the effect to the DA, especially on an auto-oxidation of DA. In order to make this point clearly, the experiments were performed. The effect of liposome on the DA oxidation was evaluated by monitoring the free DA concentration remaining in the bulk solution after incubated for 24 h at 37 °C for its auto-oxidization in the absence and presence of liposomes. The free DA was also separated from the solution treated by an ultra-filtration membrane to cut off 3 kDa molecules as schematically shown in **Fig.1-8(a)**. The DA was oxidized by auto-oxidation
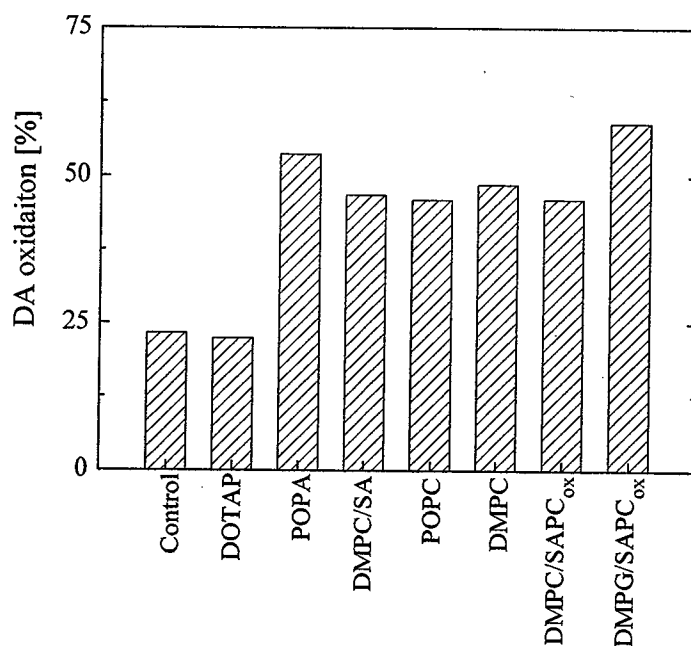


**Fig.1-10** Oxidation of DA with and without liposomes, DA was incubated with and without DA for 24 h incubated at 37 °C.

pathway in the presence and the absecence of liposomes was calculated based on remained free DA and DA partitioning (adsorption) onto liposomes. The results were shown in **Fig.1-10.** After the incubation for 24 h, the concentration of free remained DA decreased significantly as compared with that of DA after 30 min-incubation (**Fig.1-8(b)**), indicating that the auto-oxidation of DA occurred. In the presence of liposomes, the percentage of DA oxidized was much higher than that of without liposomes. This result indicates that liposome could accelerate the DA oxidation.

### 3.4. Principle of Dopamine Oxidation

As introduced above, the DA is very instable compound and is easily auto-oxidized to form DA-quinone. To be oxidized, a DA molecule will donate two electrons to the acceptor molecule, such as oxygen molecule (**Fig.1-11(a)**). The transferring electron occurs directly to the acceptor during contact between DA molecule and oxygen. Similarly, by electrochemical method, at anodic electrode of system under electrical potential, DA molecule donates 2 electrons and electrode plays as the mediator to transfer electrons to the acceptor which make process occur faster. In order to improve the sensitivity of method, the surface of electrode was modified by the conductive polymer membrane, where the DA could partition (adsorb) in the polymer film to enhance the DA concentration on surface of electrode (**Fig.1-11(b)**). In this chapter, by comparing with the bare GC electrode, the DA concentration was enhanced on the electrode surface not only on the anionic membrane prepared by anionic Nafion film and PMeT composite but also on the PMeT which is hydrophobic layer (Kim *et al.*, 2001). It may suggest that the enhanced partitioning of DA could improve the electrostatic force in derivative group and hydrophobic on aromatic ring. It could lead to the hypothesis that, on the oxidation of DA to form DA-quinone by enzymatic pathway, the enhanced partitioning of DA into the active center or neighboring environment may help to enhance the activity of enzyme. It has been reported that the DA could be oxidized in enzymatic (enzyme-like catalytic) pathway by $A\beta$/Cu complex (Opazo *et al.*, 2002). In this case, the DA also donates two
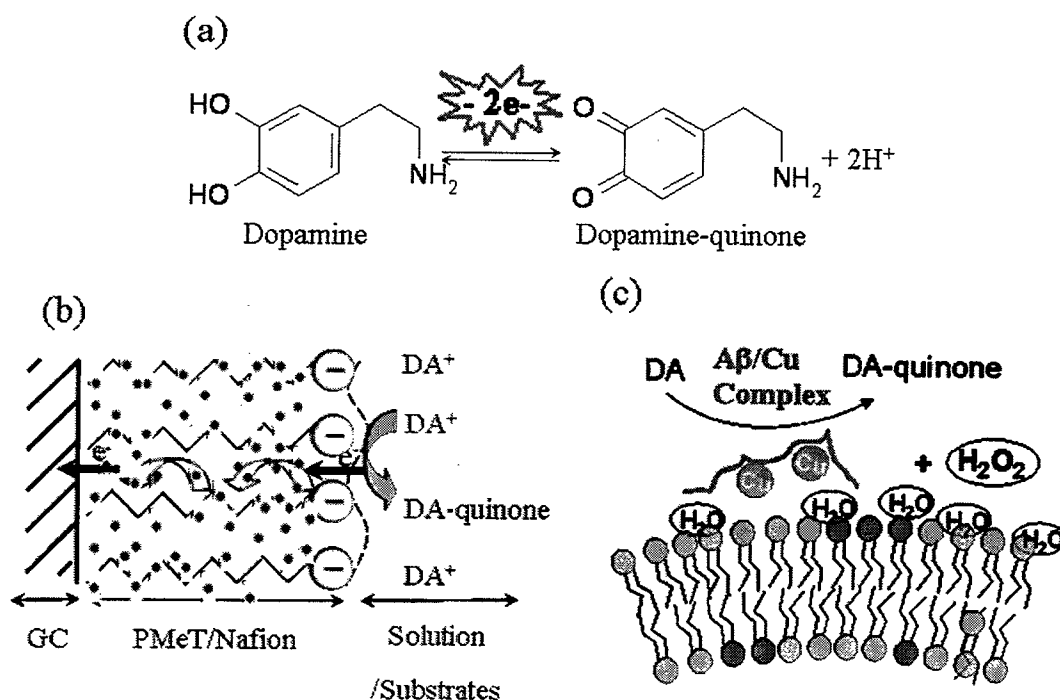
**Fig.1-11** Comparison of DA oxidation pathways. (a) Oxidation of DA to form DA-quinone (b) Electrical oxidation - electrode is mediator to transfer electron ~ Enhancement of DA concentration on "*hard*" film modified surface GC electrode (c) Model of enzymatical-like oxidation by $A\beta$/Cu complex, $A\beta$/Cu act the role as the mediator to transfer electron ~ Enhancement of DA concentration on "*soft*" layer (liposome membrane).

electrons to acceptor, where the $A\beta$/Cu complex plays an important role as a transporter of the electrons (**Fig.1-11(c)**). Furthermore, the enzyme-like activity of $A\beta$/Cu for the oxidation of cholesterol has been reported to be modulated by the liposome membrane (Yoshimoto *et al.*, 2005). It is therefore considered that the liposome membrane, in which the DA could be easily partitioned, will enhance the enzyme-like activity of $A\beta$/Cu complex for the oxidation of DA. In order to clarify this possibility, a systematic experiment was performed and introduced more in detail in chapter 3.

In short summary, the partition coefficient of DA in liposome, $K_{LD}$, was plotted against the corresponding $m_{lip}$ value of various liposomes as shown in **Fig.1-12**. A linear relationship was observed in almost all liposomes, except for DMPC/SA liposome (10:4 molar ratio). The liposome with high $m_{lip}$ value has the instable hydrogen bond between the headgroups of lipids because of the fully hydration on the membrane surface, suggesting that
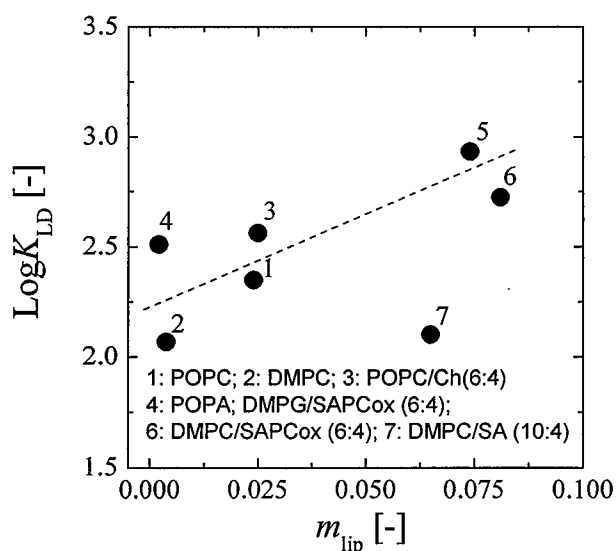
**Fig.1-12** Relationship between the DA partition to liposomes and their $m_{lip}$ values. DA partition coefficient $K_{LD}$ wad defined in **Table 1-5**.

the hydrophobic region of acyl chain could easily be exposed to the bulk aqueous phase. The above results show that the liposome with higher $m_{lip}$ value favors the partitioning of DA into the liposome membrane phase. It was thus found that the DA partitioning could be modulated by the hydrogen bond instability of the membrane itself.

It is suggesting that the membrane with higher $m_{lip}$ value could be oxidatively damaged in the presence of DA because of the higher DA accumulation considering the membrane-enhanced auto-oxidation of DA. At this condition, the membrane has no strategy to protect itself from the DA-induced stress, except for the auto-formation of melanin (Miyazaki *et al.*, 2009) or the release of DA-quinone because of oxidation (**Table 1-3**). It is considered that other kinds of reponse could be induced, depending on the state of liposome membrane. These possible responses will be described in the following chapters.

## 4. Summary

In this chapter, the electrochemical sensors were developed based on the conducting

polymer film (PMeT) and the composite of Nafion and conducting polymer film (PMeT/Nafion) modified GC electrode. The behavior of DA at both of GC/PMeT and GC/Nafion/PMeT electrode were examined at different concentration, resulting in a good relationship between DA concentration and signal amplitude. Both of electrodes show ability for detection DA at wide range of DA concentration, as $0.5 - 200$ μM μM and $1 - 1000$ μM for PMeT/Nafion/GC and PMeT/GC electrode, respectively. By using the electrochemical sensor, the DA concentration was easily measured with simply sample preparation and fast measurement. These sensors were applied for monitoring the DA concentration to evaluate the DA-liposome membrane behaviors. The interactive behavior of DA and liposome membrane was characterized. The DA was found to show the propensity to partition (adsorb) into liposome membranes, depending on the hydrogen-bond stability of the liposome. Through its partitioning on the liposome membrane, the DA was found to induce the membrane damage, caused by an auto-oxidation of DA together with the generation of ROS (OH$^{\bullet}$, O$_2^-$). At the same time, the addition of the liposomes was found to promote the DA-oxidation. These results are very helpful for the deeper understanding of the interactive behavior of DA with proteins on liposome membrane, which will be shown and discussed in chapter 3.

# Chapter 2. Development of Immobilized Liposome Sensor for Detection of Protein-Membrane Interaction

## 1. Introduction

Lipid membrane is one of the most important elements in biological systems. This is because they are essential constituents of all the biological membranes which are not only physical boundary against the environment but also the functional units that sense the environmental conditions and/or recognize other molecules. The immobilization of the liposome membrane on sensing devices is useful for studies involving the detection / evaluation / analysis of the protein-liposome interaction (Jung *et al.*, 2003; Morita *et al.*, 2006; Yoshimoto *et al.*, 2006) or the membrane-membrane interaction (Felix *et al.*, 2002). This is because the immobilization of liposome can minimize the effect of membrane-membrane interaction, such as the aggregation of liposomes and their membrane fusion. Since the most membrane-bound molecules are likely to have different structures and binding affinities in solution, it is desirable to immobilize them onto the analytical devices together with the reconstituted membrane systems for the investigation of the biomolecular interactions. Although supported planar lipid bilayer onto the solid surfaces yields stable membrane systems and reproducibility (Granél *et al.*, 2003; Navratilova *et al.*, 2006), these films could have less fluidity and could not perfectly mimic the plasma environments of the biological cells. In order to utilize the functions of the phospholipids membrane itself, it is important to maintain the fluidity or mobility of the membrane, which is deeply related to the expression of its functions, after their immobilizations onto sensor electrodes. Therefore, the immobilization of intact liposomes on the sensor surface has attracted much attention.

Since an immobilization technique has been developed, the immobilized liposomes have been utilized as the model of cell membranes in various techniques such as immobilized

42

liposome chromatography (ILC) (Lundahl *et al.*, 1991; Yoshimoto *et al.*, 1998; Yoshimoto *et al.*, 2006), a quartz crystal microbalance analysis (QCM) (Morita *et al.*, 2006), and immobilized liposome sensor (ILS) (Jung *et al.*, 2003). The kinetics of vesicles adsorption can be monitored by a variety of different techniques, such as ellipsometry, surface plasmon resonance spectroscopy, and most prominently the quartz crystal microbalance (QCM) (Keller *et al.*, 1998; Lüthgens *et al.*, 2003; Reimhult *et al.*, 2003). The QCM technique allows us to distinguish intact and ruptured liposomes. Normally, the immobilized liposomes are likely to (i) keep intact structure, (ii) form bilayer, and (iii) form monolayer, depending on the type of solid materials, the properties of modified solid surface, the immobilization methods and the liposomes properties (Keller *et al.*, 1998).

Recently, several studies have been performed to investigate the adsorption of liposomes on the solid surface. By using physical adsorption on the extremely hydrophobic surface, such as alkyl thiol, the adsorption of liposomes displays the simple exponential behavior of adsorption of monolayer (Keller *et al.*, 1998; Reimhult *et al.*, 2003). On other substrates such as $SiO_2$ and $Si_3N_4$, the adsorption of liposomes displays the formation of bilayer through two steps; firstly liposomes adsorb on the solid surface with own intact structure and then rupture for bilayer formation (Keller *et al.*, 1998; Reimhult *et al.*, 2002; Reimhult *et al.*, 2003; Richter *et al.*, 2003; Seantier *et al.*, 2005). Other studies reported that the intact liposomes were adsorbed onto extremely hydrophilic surface such as oxidized Au (Keller *et al.*, 1998; Reimhult *et al.*, 2003), oxidized Pt (Reimhult *et al.*, 2003), and $TiO_2$ (Reimhult *et al.*, 2002; Reimhult *et al.*, 2003). However, the densities of the adsorbed liposomes on the solid surface were small according to the small measured frequency shifts. For its applications in biotechnology, the community has developed a number of specific tethering methods based on chemical and biological ligation, *e. g.* the well studies receptor-ligand pair of biotin/streptavidin (Bäumle *et al.*, 2004), chemical binding (Morita *et al.*, 2006), avidin-biotin binding (Liebau *et al.*, 1998; Pignataro *et al.*, 2000; Reiss *et al.*, 2003), DNA complementary strand (Städler *et al.*, 2006). Almost all the studies have been mainly focused

on the binding method, selection of substrates, and applications of surface-based vesicle systems as functional nano-container by entrapped solutes inside vesicles (Vladimir *et al.,* 2005; Christensen *et al.,* 2007). There are a few reports describing the design of liposomes in term of membrane composition (Liebau *et al.,* 1998; Lüthgens *et al.,* 2003; Reiss *et al.,* 2003). However, there is no report which described the relationship between the shape of immobilized liposome and its properties and, furthermore, the stability of immobilized liposomes.

Recent study on amyloidgenic protein such as amyloid $\beta$-protein relating with Alzheimer's disease (AD) indicates that its accumulation on the lipid membrane is a key for its amyloid fibril formation (Axellsen *et al.,* 2007; Matsuzaki *et al.,* 2007a). The detection system of QCM combining with the liposome immobilization has the potential to get the direct evidence on the A$\beta$-accumulation on lipid membrane. In chapter 1, the DA favors its

**Table 2-1** The application of immobilized lipid membrane for biosensor

| Lipid | Determinant | Measuring method | Reference |
|---|---|---|---|
| POPC liposome | Denatured CAB protein based on hydrophobic interaction | Liposome immobilized on QCM | Morita *et al.,* 2006 |
| DLPC lipid bilayer | Amyloidogenic proteins based on hydrogen bond stability of proteins | Optical detection | Fernandez *et al.,* 2002 |
| POPC liposome | Amyloidogenic proteins based on hydrogen bond stability of proteins | Immobilized chromatography | Yoshimoto *et al.,* 2006 |
| POPC, POPG Liposome | Monomeric and aggregated A$\beta$(1-40) | Surface plasmon resonance | Kremer *et al.,* 2003 |
| DMPC/SA liposome | Amyloidogenic proteins based on hydrogen bond stability of proteins | Liposome immobilized QCM | This study |
| POPC; POPC/Ch; DMPC/SA; DMPC/SAPC$_{ox}$ liposome | Monomeric A$\beta$(1-40) protein | Liposome immobilized QCM | This study |

partitioning into lipid membrane phase because of its hydrophobicity, resulting in the oxidation of liposome membrane by an auto-oxidation of DA. Previous reports have described that the oxidized lipid membrane strongly interact with Aβ (Axellsen *et al.*, 2007). Taking into the consideration of the result in chapter 1, there is a possibility that the DA-induced oxidation of lipid membrane might promote the accumulation of Aβ and the subsequent nucleation / elongation of amyloid fibrils on lipid membrane.

The major purpose of this chapter is to design and develop the membrane sensor by immobilizing liposomes with high densities and long stability. Furthermore, the immobilized liposome sensor was applied for the dynamic analysis (and static analysis) of the interaction of the proteins with biomimetic membrane (liposomes). To utilize the immobilized liposome as sensor material for the investigation of the membrane-protein interaction, a systematic study of liposome immobilization on the solid surface was first performed, focusing on (i) the effect of immobilization methods, (ii) membrane compositions, and (iii) membrane properties on the liposome immobilization. The density of immobilized liposomes and their stability were also estimated. The relation of the protein-membrane interaction with the stability of hydrogen bond of proteins was then analyzed by using immobilized liposome quartz crystal microbalance (IL-QCM). The hydrogen bond wrapping ($\rho_{pr}$ value) (Fernandez *et al.*, 2003) was used as a standard parameter to establish the calibration which showed the relationship between number of adsorbed molecules per area unit of liposome against hydrogen bond wrapping. Furthermore, the hydrogen bond stability of unknown protein was estimated based on the number of adsorbed molecules. Finally, the IL-QCM was applied for evaluation of response of Aβ protein on liposome membranes with and without DA.

## 2. Materials and Methods

### 2.1. Materials

The phospholipids used were 1-palmitoyl-2-oleoyl-*sn*-glycero-3-phosphocholine

45

(POPC), 1-palmitoyl-2-oleoyl-*sn*-glycero-3-phosphoethanolamine (POPE), 1,2- dimyristoyl-*sn*-glycero-3–phosphocholine (DMPC), 1,2-dimyristoyl --*sn*-glycero-3-phosphoethanolamine (DMPE), *L*-α-phosphatidylethanolamine (Egg- PE), 1,2-dioleoyl-3-trimethylammonium-

**Table 2-2** Chemical structure of lipids used in this chapter

| Lipids | M.W. | Chemical aspect | Chemical structure |
|---|---|---|---|
| DMPC | 677.93 | |  |
| POPC | 760.06 | |  |
| SAPC | 810.135 | Easily oxidized because of for double bonds |  |
| DMPE | 635.85 | Indispensable reagent for amino-coupling method |  |
| POPE | 717.99 | Indispensable reagent for amino-coupling method |  |
| POPG | 770.99 | Negatively charge |  |
| DOTAP | 698.54 | Positively charge |  |
| Cholesterol | 386.64 | Decrease in membrane fluidity |  |
| SA(stearic acid) | 284.48 | Negatively charge |  |

propane (Chloride Salt) (DOTAP) (cationic lipid), and 1-palmitoyl-2-oleoyl-*sn*-glycero-3-[phospho-*rac*-(1-glycerol)] (Sodium Salt) (POPG) (anionic lipid), were purchased from Avanti Polar Lipids (Alabaster, AL). Stearic acid (SA) was purchased from Sigma (St. Louis MO, USA), 11-mercaptoundecanoic acid (MUA) from Sigma-Aldrich, 11-amino undecanthiol (AUT) from Dojindo (Kumamoto, Japan). *N*-(3-Dimethyl aminopropyl)-*N'*-ethylcarbodiimide hydrochloride (EDC) was purchased from Sigma-Aldrich, N-Hydroxysuccinimide (NHS) from Wako (Osaka, Japan). *N,N,N*-Trimethyl-4-(6-phenyl-1,3,5-hexatrien-1-yl) phenyl ammonium p-toluenesulfonate (TMA-DPH) were obtained from Molecular Probes (Eugene, OR), and 4-(4,6-dimethoxy-1,3,5-triazin-2-yl)-4-methyl morpholinium chloride (DMTMM) was from SYNTH (Kyoto, Japan). Solvents and other chemicals for preparation of buffers were purchased form CICA Reagent.

## 2.2. Preparation of Functionalized Quartz Crystal and Liposome Immobilization

Thiol SAM was formed on the gold surface by immersing the QCM electrode on the ethanol solution of 1 mM thiol for at least 12 h. After that, the electrode was rinsed with ethanol, then with distilled water and finally dried by air flow. In the case of carboxylic thiol-SAM, SAM was activated according to previous report (Morita *et al.*, 2006) and was briefly described here as follows: after the preparation of SAM, the QCM electrode was immersed in dioxane-distilled water solution (90:10 in volume ratio) solution contained 17 mM NHS and 17 mM EDC for 3~4 h. In the presence of EDC, the N-hydroxyl group of NHS interacts with bound carboxyl groups to form reactive sites (Kotarek *et al.*, 2008). NHS-activated SAM was rinsed and incubated with amino group doping liposomes for 1 h to allow a primary amine group within liposomes to displace a succinimide group. NHS residues were deactivated in 1M 2-aminoethanol solution for 30 min. The stearic acid (SA) containing DMPC liposomes were immobilized amino group layer by using DMTMM as catalysis according to the

previous report (Morita *et al.,* 2007).

## 2.3. Preparation of Liposomes

Liposomes were prepared by the following process described in previous report (Morita *et al.,* 2006). Briefly, the lipid mixture was dissolved in chloroform and then dried onto the wall of a round-bottom flask in vacuum and then left overnight to ensure the removal of all of the solvent. The dried thin lipid film was hydrated overnight with adequate buffer solution to obtain a total lipid concentration of 10 mM. Large unilamellar vesicles (LUVs) were formed with five cycles of freeze-thaw treatment. Alternatively, mono-dispersed LUVs were prepared by using an extruder (LiposoFast, Avestin Inc., Ottawa, Canada) equipped with polycarbonate filters possessing pore sizes of 50, 100, 200, and 400 nm (namely $LUVET_{50}$, $LUVET_{100}$, $LUVET_{200}$, and $LUVET_{400}$, respectively). Liposomes with 26 nm in diameter (SUVs) were prepared by a probe sonication of a MLV suspension in a 10-ml plastic tube on an ice-bath at 40 W for 20 min with 1 min intervals for each 1 min (Yoshimoto *et al.,* 1998). Just before the experiment, the liposomes solutions were diluted by adequate buffer to a final lipid concentration of 2 mM.

## 2.4. Membrane Fluidity Measurement

Membrane fluidity of liposomes was estimated by measuring the fluorescence polarization (P) of 1-(4-trimethylammo-niumphenyl)-6-phenyl-1,3,5-hexatriene (TMA-DPH) incorporated in lipid membranes according to the previous method (Yoshimoto *et al.,* 2006). The method is simply described here in the following. A solution of TMA-DPH (in ethanol) was added to the liposome solution to maintain the lipid/probe molar ratio 250 ([TMA-DPH] $_{final}$ = 2 μM, water/ethanol volume ratio > 100). The mixture was incubated at 25 °C for at least 1h at room temperature with gentle stirring. The fluorescence polarization of samples

48

was measured with a spectrofluorimeter (FP-777 JASCO Co. Ltd., Tokyo). The sample was excited with vertically polarized light (360 nm), and emission intensities (430nm) both parallel ($I_{//}$) and perpendicular ($I_{\perp}$) to the excited light were recorded. Then, the polarization of TMA-DPH was calculated by using the following equation:

$$P = \frac{I_{//} - I_{\perp}}{I_{//} + I_{\perp}} \tag{2-1}$$

The term "fluidity" is inversely proportional to the degree of fluorescence polarization of the probe; that is, "membrane fluidity" of the surface of membrane was defined by ($1/P$) of TMA-DPH.

## 2.5. QCM Measurement

AT-cut quartz crystal with diameter 5.1 mm gold electrode, which resonated at 8 MHz, (BAS Inc., Tokyo, Japan) was used in this study. The quartz crystal is connected to ALS/CHI electrochemical quartz crystal microbalance equipment (400, BAS Inc.).

According to Sauerbrey's equation (Sauerbrey et al., 1959), there is linear relationship between the frequency decrease (-$\Delta f$) and mass increase per unit area ($\Delta m/$A).

$$\Delta f = -\frac{2 f_0}{\sqrt{\mu_q \rho_q}} \frac{\Delta m}{A} \tag{2-2}$$

where $f_0$ is the basic frequency of the crystal, $\mu_q$ is its shear module and $\rho_q$ is its density. Equation (2-2) can be applied with precision only to the adsorption of a rigid thin layer on an electrode. Another theory of the resonant frequency of quartz crystal in liquid is proposed by Gordon and Kanazawa (Kanazawa et al., 1985).

$$\Delta f = -2 f_0^{3/2} \sqrt{\frac{\eta_1 \rho_1}{\pi \mu_q \rho_q}} \tag{2-3}$$

where $\eta_l$ and $\rho_l$ are the viscosity and density of liquid, respectively.

The frequency shifts corresponded simply to mass change by equation (2-2). In this study, the mass sensitivity of the crystal used in this study is $6.84 \times 10^{-2}$ ng/mm$^2$ per Hz of frequency shift.

## 2.6. Calculation of Number of Protein Molecules per Unit Area

The liposome coverage was temporarily calculated base on measured frequency shift ($\Delta f_{meas}^{lip}$) and maximum frequency shift ($\Delta f_0^{lip}$), which was calculated based on the adsorbed mass of liposome for 100% of liposome cover with an assumption all immobilized liposome keep intact shape.

$$\text{Coverage [\%]} = \Delta f_{meas}^{lip} * 100 / \Delta f_0^{lip} \qquad (2\text{-}4)$$

The number of immobilized liposomes also was calculated base on $\Delta f_{meas}$ with an assumption that all the immobilized liposomes keep their intact shape. The surface area of immobilized liposome was then calculated. On the other hand, from adsorbed mass of proteins calculated base on $\Delta f_{meas}^{pro}$, the number of adsorbed proteins was calculated for each protein. All calculation was performed by using equation (2-2) based on the relationship between adsorbed mass and frequency shift.

The number of protein molecules per one area unit can be estimated as follows:

Ads.mol [mol•$\mu$M$^{-1}$] = Number of adsorbed protein molecules/unit area

# 3. Results and Discussion

## 3.1. Development of QCM Combining with the Immobilization of Liposomes (IL-QCM)

### 3.1.1. Immobilization of Liposomes onto SAMs

The liposome immobilization on the solid support is important for its utilization as sensor material in order to monitor the interaction between membrane and other biomaterials. A systematic study of the liposome immobilization was performed to investigate the conditions for the liposome immobilization with high density and to keep its intact structure and high stability. Some possible methods of liposome immobilizations were schematically shown in **Fig.2-1.** Model (I) indicates the immobilization of liposomes modified with fatty acid on amino-thiol SAM (AUT-SAM) by covalent binding. Model (II) presented the immobilized liposomes modified with phosphoethanolamine lipids on the activated carboxylic thiol SAM (MUA-SAM) by the covalent binding. The immobilization of liposomes using above methods were monitored by quartz crystal microbalance.

A typical tendency of frequency shifts in the QCM analysis was studied when the surface of QCM sensor was modified with liposomes. As shown in **Fig.2-2**, the value of frequency shifts reached about 430 Hz when POPC/POPE (98:2)-LUVET$_{100}$ were immobilized on the activated MUA-SAM membrane (line (a)), where the value was not affected when the electrode was rinsed by buffer. The kinetic adsorption of liposomes described above was similar to that of previous report (Morita *et al.*, 2006). By using QCM sensor, a distinct decrease of the frequency during the adsorption of vesicles was observed for the several decade minutes while the frequency decrease rapidly stopped in a few minutes in the case of vesicle fusion (Reimhult *et al.*, 2002; Reimhult *et al.*, 2003). First, the frequency shift corresponding to a mass increase of 28 ng/mm$^2$ was extremely larger than the formation of a lipid bilayer of 3.06 ng/mm$^2$ (Calculated by equation (2-2) assuming bilayer formation with the surface area per lipid molecule was 0.72 nm$^2$ (Victoria *et al.*, 1996)). It has previously been reported that there was no cumulating of bilayers once the first bilayer
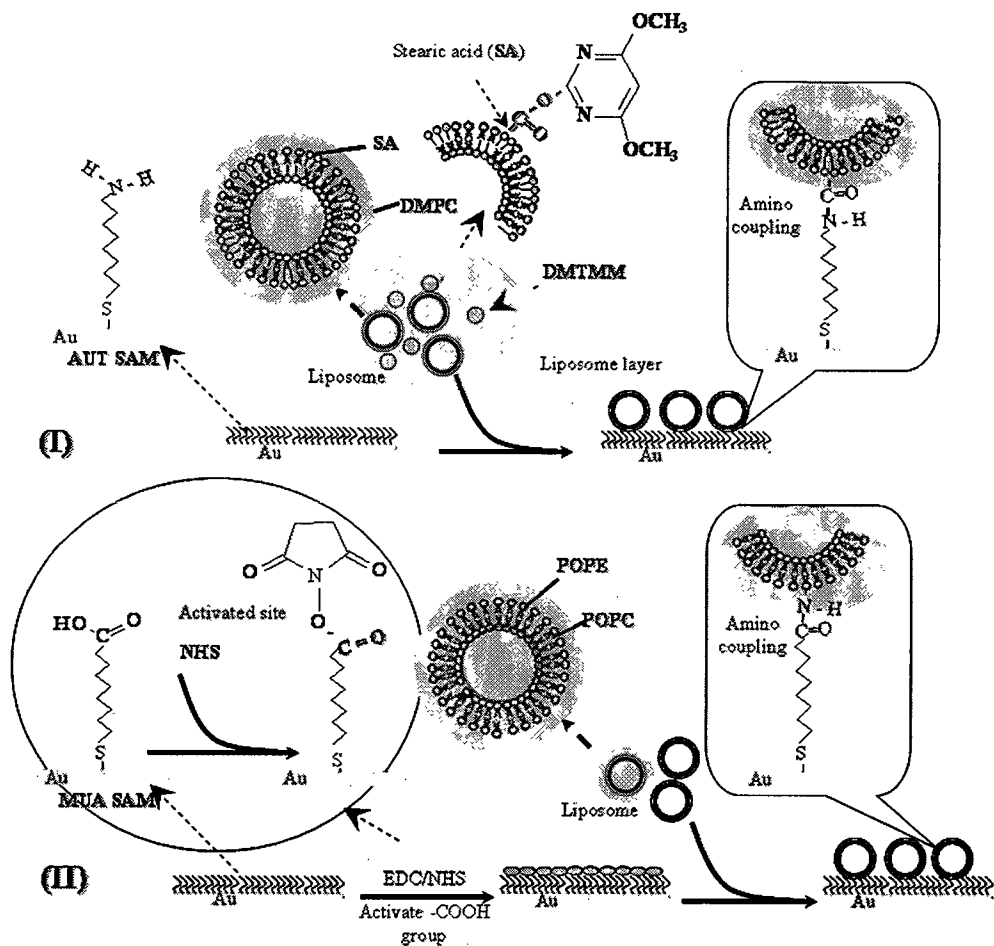
**Fig.2-1** Scheme, not to scale, of the surface immobilized lipid membrane modified QCM sensor: (I) Stearic acid containing liposomes immobilized on amino-thiol SAM, (II) phosphoethanolamine lipids containing liposomes immobilized on activated carboxylic thiol SAM.

formation by vesicle fusion was completed (Keller *et al.*, 1998). It is thought that a multilayer of the phospholipids on the QCM surface could not be formed under the conditions tested here since a rapid, single-step frequency shift was observed. Second, a large and rapid increase in the frequency was observed when the QCM electrode was treated with nonionic surfactant Triton X-100. The frequency increased and reached to the saturated value at 60 Hz, which is corresponding adsorbed mass 4.1 ng/mm$^2$ and is equal to the formation of POPC lipid bilayer (3.06 ng/mm$^2$). This result suggests that the adsorbed liposomes on the QCM surface were disrupted to release the entrapped water and form the lipid bilayer. Furthermore, to confirm the necessity of activation step of carboxylic group of MUA-SAM on the liposome
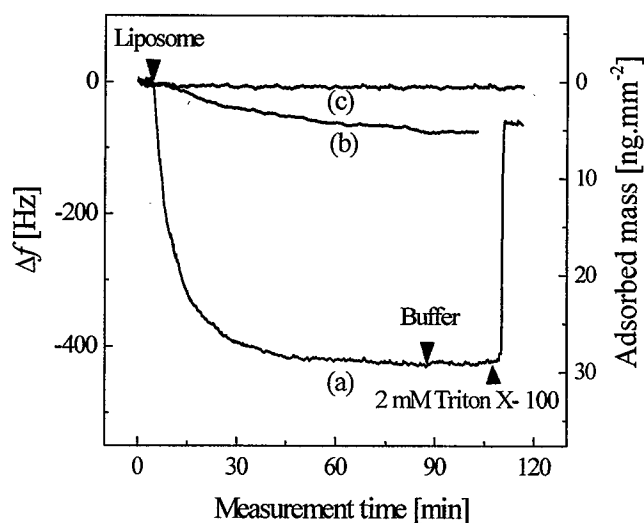
**Fig.2-2** Time-course of frequency shift of QCM sensors when POPC/POPE (98:2) liposomes immobilized on activated MUA-SAM (a), and on MUA-SAM without activation (b), only buffer was injected on activated MUA-SAM (c). Liposomes diameter: 100 nm.

immobilization, the frequency shift of QCM sensor was analyzed when POPC/POPE (98:2)-LUVET$_{100}$ was immobilized on the carboxylic thiol SAM without activation step (**Fig.2-2**, curve (b)). The results showed that, without activation step, the amount of liposomes immobilized onto SAMs was small as compared with that of activated SAM ($\Delta f = 80$ Hz). This result demonstrated that the activation of carboxylic group was necessary for the immobilization of liposomes.

### 3.1.2. Effect of Immobilization Methods

The effect of immobilization method was investigated based on the models shown in **Fig.2-1** in order to immobilize the liposomes as a layer on a solid planar surface with high density of liposome. The shift of the frequency change in the QCM analysis was 608 ± 126 Hz and with DMPC/SA-(10:4)-LUVET100 on AUT-SAM was 734 ± 89 Hz when surface of QCM sensor was modified with POPC/POPE-(70:30)-LUVET100 on carboxylic thiol SAM. The data showed that the amount of DMPC/SA-(10:4)-LUVET100 immobilized on AUT-

SAM was slightly higher than that of POPC/POPE (70:30)-LUVET100 on carboxylic thiol SAM and both of these cases showed the large change in frequency, showing the high amount of immobilized liposomes. Therefore, both of POPC/POPE-LUVET100 immobilized on carboxylic thiol-SAM and DMPC/SA-LUVET100 immobilized on amino thiol-SAM were selected for further investigation. Method I could be used for the immobilization of switterionic liposome or weakly negative charge liposomes onto positive charge surface of AUT-SAM, and the model of method II can be used for the immobilization of switterionic liposome or weakly positively-charged liposomes onto the negative charge surface of MUA-SAM. The selection of adequate method could eliminate the effect of electrostatic repulsion, which prevented the immobilization of liposome or the induction of the liposome rupture (Christensen *et al.,* 2007).

### *3.1.3. Stability of Immobilized Liposomes*

In order to apply the immobilized liposomes for detection of interaction between membrane and other biomaterial as model of material, there is an important requirement that the immobilized liposomes must be stable for long time. The stability of the immobilized liposomes was investigated by measuring the kinetics of the frequency shift, which is equivalent to the change in the immobilized amounts. Time courses of change in frequency of immobilized liposomes on modified QCM in buffer solutions were measured for 10 h at room temperature. The solutions used in these experiments are similar to buffer solutions used for the immobilization of liposomes. The results were shown in **Table 2-3**. After rinse by buffer for 10 h, the frequency was slightly changed (less than 5%). The control experiments were performed on bare crystal and MUA-SAM modified crystal by injection of buffer to contact with surface of QCM electrode for 10 h. An 11 Hz frequency shift and 18 Hz frequency were observed in the case of bare crystal in the case of MUA-SAM modified QCM electrode, respectively. These data were similar to the frequency shift in the case of converted from **Table 2-3**.

**Table 2-3** Frequency shifts of immobilized liposomes after their immobilization for 10 h

| Liposome | Molar ratio | Lip. diameter [nm] | Freq. shift [%] |
|----------|-------------|--------------------|-----------------|
| POPC/POPE | 98:2 | 26 | 2.8 |
| POPC/POPE | 98:2 | 100 | 2.7 |
| POPC/POPE | 98:2 | 400 | 2.0 |
| POPC/POPE | 70:30 | 100 | 4.8 |
| DMPC/SA | 72:28 | 100 | 4.6 |

The frequency shift of the immobilized liposomes modified QCM sensor may, therefore, not only be induced by liposome rupture but also be caused by the instability of quartz crystal itself. The frequency shift of immobilized POPC/POPE (70:30)-LUVET$_{100}$ and DMPC/SA (10:4)-LUVET$_{100}$ after keeping for 10 h are much more than that of POPC/PE (98:2)-LUVET$_{100}$. It can be explained that the increase of amount of PE or SA induces the increase of the number of reaction groups. As a result, for a long time, the reaction groups on other sites of liposomes can interact with the SAM membrane inducing the increase adhesive force between liposomes and surface of electrode. When the adhesion forces to the surface exceed the interactions forces between the individual lipids, the liposomes eventually ruptures partly and releases entrapped water, which lead to frequency increases.

In order to use the immobilized liposomes sensor for the evaluation of the membrane-protein interaction, the membrane properties should be stable. Since the result shown in **Table 2-3** suggested, at least, the 10-h stability of the immobilized liposomes, the stable detection of the protein-liposome during 10 h was examined. The POPC/PE (70:30) liposome showed the largest frequency shift among the liposomes tested here, suggesting that the most unstable liposomes in terms of their immobilization on QCM. Then, the POPC/PE (70:30) liposome was used as a test case. The IL-QCM using POPC/PE (70:30) was first prepared and 10 µM
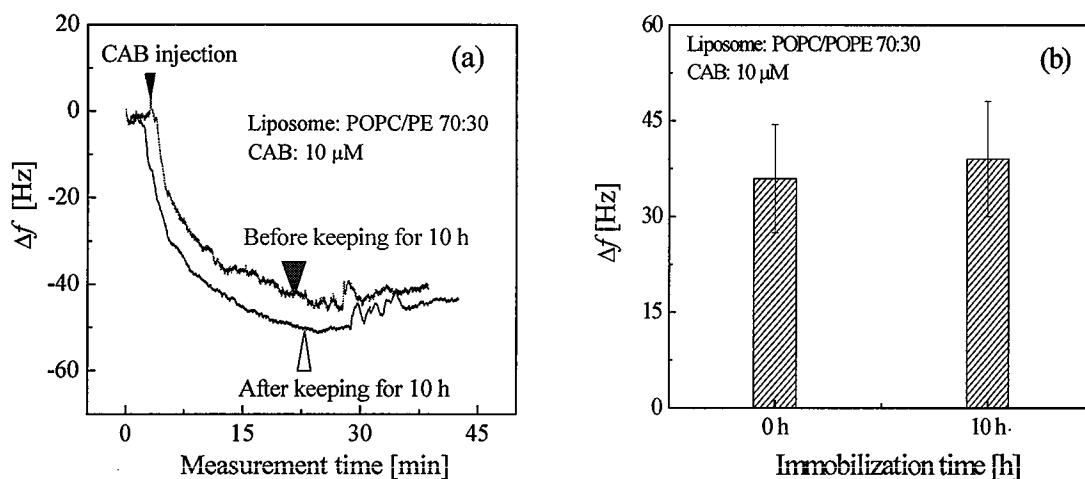
**Fig.2-3** (a) Time-course of frequency of IL-QCM by adding 10 μM CAB to the immobilized POPC/POPE (70:30) liposome with and without the 10-h incubation. (b) Frequency change of immobilized liposome for addition of 10 μM CAB.

of carbonic anhydrase from bovine (CAB) was then injected. The resulting frequency shift was 40 Hz or so (**Fig.2-3(a)**). By using the IL-QCM (10-h incubation of immobilized liposomes), 10 μM of CAB was also injected. A similar adsorption kinetics could be monitored (**Fig.2-3(a)**). Since the adsorption kinetics is, in general, dominated by the membrane property, this result suggests no significant variation in the membrane fluidity during a 10-h incubation of the immobilized liposome. The adsorbed mass of CAB was also statistically compared with both cases. No significant difference was observed (**Fig.2-3(b)**).

From these experiments, it is considered that the immobilized liposome has the high stability enough to detect the protein with high accuracy and stability during at least the first 10 h from the preparation of IL-QCM.

## 3.2. Detection of Protein-Liposome Interaction

### 3.2.1. Hydrogen Bonds Stability of Protein

Hydrogen-bond (HB) seems to be stable only when surrounded by a hydrophobic environment, where water is excluded or highly structured. It is informative to determine their

56

average extent of desolvation over many protein structures. This parameter can then be averaged over a statistical ensemble of protein structures to determine the typical environment of a HB.

This average environment, in turn, enables us to define and identify UWHB, which are highly relevant to our present study. A HB environment is operationally defined (with our coarser method) by the number of hydrophobic residues (third bodies) contained within the 7-Å-radius spheres centered at the carbons of the residues paired by the HB. Thus, the number of three-body hydrophobe-HB residue pair correlation characterizes an HB environment: a hydrophobic side chain whose center of mass is contained within the desolvation sphere of a HB is counted as a correlation.

To determine the extent of HB wrapping (desolvation), the desolvation spheres of radius R for a backbone HB by fixing R at 7.0 Å was defined and centering the spheres at the α-carbons of the residues paired by the HB was also defined. The interferences made are robust to moderate changes in the desolvation radius, holding within the range R = 7.0 ± 0.3 Å. An amide–carbonyl HB is defined by an N–O distances within the range 2.6-3.4 Å (typical extreme bond lengths) and a 45° latitude in the N–H–O angle. To calculate the extent of wrapping of an HB, one should count up the number of hydrophobic residues (third bodies) whose side-chain center of mass lies within the wrapping spheres. The counting includes residues paired by the HB themselves if they happen to be hydrophobic. Thus, the HB wrapping is determined by three-body (hydrophobe-HB pair) correlations. Residues Ala, Leu, Ile, Val, Phe, Met, Trp, and Tyr are regarded as hydrophobic in accordance with solvent-partitioning scales and the center of mass for each residue is computed by averaging over all side- chain rotamers using the native structures from the database described below. The average extent of HB wrapping, $\rho_{pr}$ is derived from two quantities: $C_3$, the total number of three-body correlations, and Q, the total number of backbone HB.

**Table 2-4** Physicochemical properties of various proteins (Fernandez *el al.,* 2003)

| Proteins | $M_W$ [kDa] | $\rho_{pr}$ [-] |
|---|---|---|
| Apolipoprotein A-1 | 23.3 | 3.9 |
| Insuline | 5.7 | 4.21 |
| Cystatine C | 13.3 | 4.4 |
| Cystatine (Chicken egg white) | 12.2 | 4.4 |
| Ubiquitin | 8.5 | 5.6 |
| Lysozyme | 14.3 | 6.1 |
| Human Carbonic Anhydrase II | 29.1 | 6.6 |
| Carbonic Anhydrase from Bovine | 29.2 | 6.6 |
| Myoglobin | 17.0 | 6.7 |
| β-Lactoglobin | 18.3 | 6.87 |

The average extend of H-bond wrapping for a protein is calculated as

$$\rho_{pr} = C_3/Q \qquad (2\text{-}5)$$

The $\rho_{pr}$ values for various proteins were summarized in **Table 2-4.**

### 3.2.2. Interaction of Amyloidogenic Proteins and Liposome Controlled by the Extend of Hydrogen Bond Stability

In order to get the relationship between the $\rho_{pr}$ value for various proteins and their adsorbed mass to liposomes, the interaction between the immobilized liposomes and target proteins were monitored with an IL-QCM. First, the adsorption behavior of protein was examined by using carbonic anhydrase from bovine (CAB). The injection of CAB with different concentration (from 0.1 to 5 µM) was consecutively performed (**Fig.2-4(a)**). The plateau value of $\Delta f$ was obtained above 5 µM (**Fig.2-4(b)**), suggesting that the adsorbed mass measured by an injection of 10 µM CAB is considered to reach the adsorption equilibrium state. Therefore, the frequency shift for four standard proteins (10 µM-each) was measured
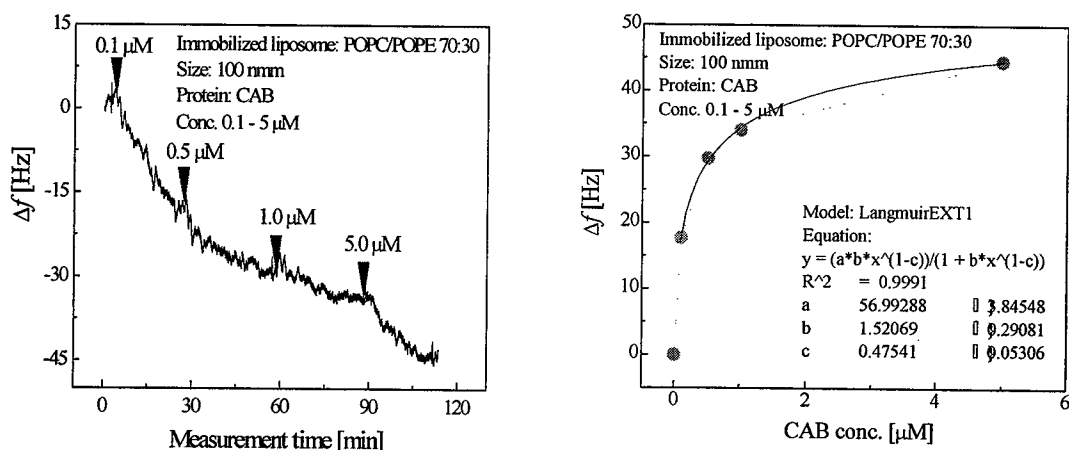
**Fig.2-4** Adsorption of CAB on immobilized POPC/PE 70:30 liposome membrane. (a) Injection of CAB with different concentrations (0.1 to 5 μM) and (b) concentration dependency of CAB against its adsorbed mass to the immobilized POPC/PE. Liposomes diameter: 100 nm.

and converted to the adsorbed mass. Subsequently those data were plotted against the corresponding $\rho_{pr}$ value (**Fig.2-5**). A liner relationship was obtained in consistent with the previous finding using DLPC planner membrane (Fernandez *et al.*, 2003), strongly suggesting the possibility of the evaluation of the $\rho_{pr}$ value for protein with unknown hydrogen bonding stability.
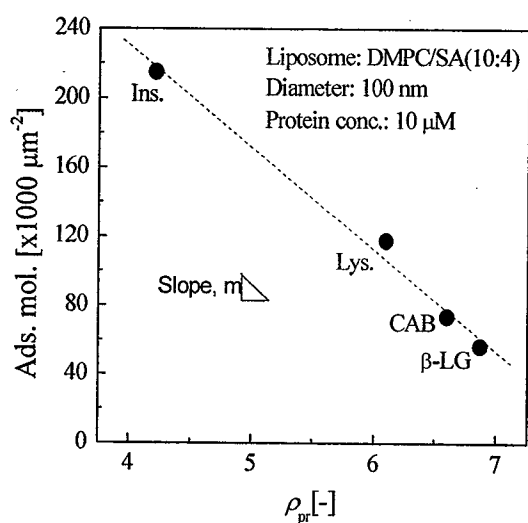


**Fig.2-5** Correlation between the number of adsorbed molecules per μm² at DMPC/SA liposomes of four proteins and their hydrogen bond wrapping, $\rho_{pr}$, value [-].

59

*3.2.3. Evaluation of Hydrogen Bond Stability of Aβ with IL-QCM*

The theoretical evaluation of $\rho_{pr}$ value needs the well-defined crystallographic data. Since the detailed information on X-ray crystallography for Aβ has not been reported, there is no information of hydrogen bonding stability for Aβ. Then, the experimental determination of $\rho_{pr}$ value for Aβ was tried with the relationship obtained in **Fig.2-5**. The resulting data for $\rho_{pr}$ value for Aβ(1-40) and Aβ(1-42) were shown to be 4.5 and 3.5, respectively (**Table 2-5**). According to the previous report (Fernandez and Berry, 2003), the condition of $\rho_{pr} = 6.2$ is the critical amyloidgenicity, implying that the proteins with lower $\rho_{pr}$ value than 6.2 is likely to spontaneously form the amyloid fibrils. It is, therefore, considered that both Aβ(1-40) and Aβ(1-42) posses the strong amyloidgenic propensity.

The association of the protein with the lower $\rho_{pr}$ value, such as a myoglobin ($\rho_{pr} = 6.7$) and β$_2$-microglobulin ($\rho_{pr} = 5.1$), could stabilize themselves by forming the complex or associate structures as can be seen in the case of hemoglobin ($\rho_{pr} = 7.2$) and MHCI ($\rho_{pr} = 6.21$). The Aβ(1-40) and Aβ(1-42) could therefore stabilize themselves by their association similarly in the case of above proteins. According to equation (2-5), the acquirement of hydrophobic environment neighboring to the hydrogen bonds is a advantageous way to stabilize the structure of Aβs. For examples, the protofibrils of Aβ(1-40) fibrils showed the lowest $\rho_{pr}$ value ($\rho_{pr} = 2.1$), whereas the Aβ(1-40) fibrils showed $\rho_{pr} = 7.2$. The above results indicate that the fibrillation process is the stabilization process of intramolecular hydrogen bonds of Aβ(1-40). The liposome can provide the lipid bilayer structure with hydrophobic environment of acyl chains, implying that the liposome-protein interaction could stabilize the hydrogen bonds of Aβs.

In the following, the Aβ-liposome interaction was examined with an IL-QCM in order to discuss the reinforcement of instable hydrogen bond of Aβs.

**Table 2-5** Evaluated stability of intramolecular hydrogen-bond for Aβ proteins and ladder of · $\rho_{pr}$ value

| Protein | Conditions | $\rho_{pr}$ [-] |
|---|---|---|
| Monomeric Aβ(1-40) | 4.3 kDa | 4.5 |
| Monomeric Aβ(1-42) | 4.5 kDa | 3.5 |
| Protofibrils of Aβ(1-40) fibrils | The protofibrils has the 200 − 600 nm in length from the observation with a total internal reflection fluorescence microscopy. | 2.1* |
| Aβ(1-40) fibrils | The fibrils have 8 μm in mean length and 4 kDa/nm in molecular weight per length. | 7.2* |
| Aβ(1-40)/DA | 10 μM Aβ(1-40) and 100 μM DA were mixed for 24 h. | n.d. |
| Aβ(1-42)/Cu | Aβ(1-42)/Cu was prepared with 1:2 stoichiometric ration. | n.d. |

*The $\rho_{pr}$ values were measured with IL-QCM using the DLPC-LB membrane.

### 3.2.4. Evaluation of Aβ -Liposome Interaction with IL-QCM

The Aβ-liposome interaction was examined by using several liposomes with different propensity (**Fig.2-6**). In the case of POPC as a normal liposome, the adsorption was observed as the frequency shift at most 10 Hz. In order to mimic the biomembrane, the liposome with domain structure on the lipid membrane was prepared. POPC/Ch (2/1) and DMPC/SA (10/4) liposomes are good models for the liposome with domain structure. The adsorption of Aβ was in the range of 12 to 35 Hz. In order to discuss the electric charge of the membrane surface, the adsorption of Aβ to positively charged POPC/DOTAP was compared with that to negatively charged DMPC/SA. In the case of POPC/DOTAP liposome, the most frequency shift with 22 Hz was observed, suggesting no significant influence of electrostatic contribution to Aβ-liposome interaction. In the case of an oxidized liposome using DMPC/SAPC$_{ox}$ (6:4), the largest adsorption of Aβ was observed among five liposomes. Therefore, the oxidation of liposome membrane is a key factor for the Aβ-liposome interaction.

From these results, Aβ is considered to stabilize itself by utilizing the hydrophobic
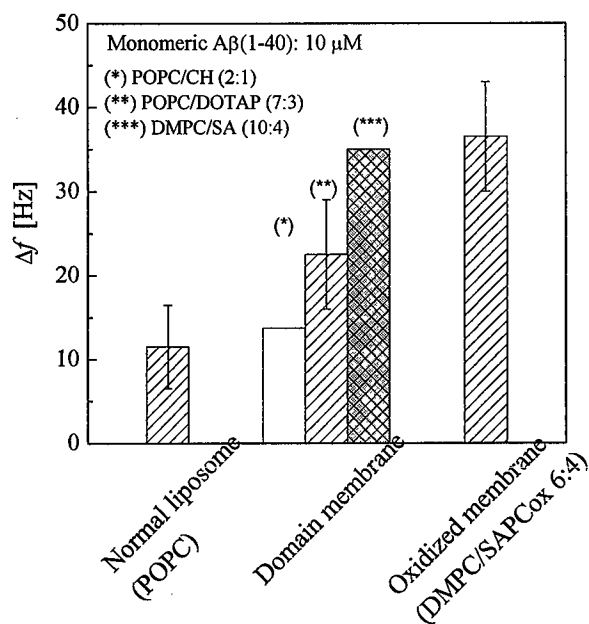
**Fig.2-6** Accumulation of Aβ(1-40) on liposomes. POPC liposome as a normal liposome, POPC/Ch (2:1), POPC/DOTAP (7:3), and DMPC/SA (10:4) liposome were used as domain liposome. DMPC/SAPC$_{ox}$ (6:4) was used as an oxidized liposome. These liposomes were LUVET$_{100}$.

environment of the liposome membranes. In the previous reports (Yoshimoto, 2005; Matsuzaki *et al.*, 2007a), it has been reported that the process of the Aβ-liposome interaction contributes to the nucleation of Aβ fibril on the surface of the liposome membrane. Here, the nucleation process is the first step of the fibril formation of Aβ. **Figure 2-6** indicated that the nucleation process of Aβs on the liposomes could be controlled by the membrane property. The relationship between the nucleation of Aβ on the liposome membranes and the accumulation behavior of Aβ on the liposomes will be investigated in chapter 4.

*3.2.5. Behaviors of Dopamine and Aβ on Immobilized Liposomes Membrane*

The interactive behavior of DA with Aβ on the liposome membrane was investigated, focusing on the surface of the oxidized DMPC/SAPC$_{ox}$ liposome immobilized on the QCM electrode. The solution containing 500 μM DA or 10 μM Aβ was independently injected onto

the immobilized liposomes on QCM electrode. A small decrease in frequency was observed for the injection of DA. The large decrease in frequency was observed for an injection of 10 $\mu$M monomeric A$\beta$(1-40) solution. However, the injection of the mixture of 500 $\mu$M DA and 10 $\mu$M A$\beta$(1-40) induced a small decrease in frequency (**Fig.2-7**). This result suggests that the DA may interact with monomeric A$\beta$, which could induce a change in property of A$\beta$, especially on the propensity for its binding to the lipid membrane. A certain stabilization effect of A$\beta$ by DA is also expected. Although further investigation on the DA-A$\beta$ interaction on the surface of the liposome membrane will be carried out in chapter 4, A$\beta$(1-40)-DA complex might show the lower amyloidgenecity in comparison with A$\beta$(1-40). The oxidized liposome membrane promoted the accumulation of A$\beta$ on membranes. In chapter 1, the DA easily partitions into the lipid membrane phase of non-oxidized liposomes. For the fibrillation of A$\beta$ on the biomembranes, the DA-induced membrane damage should be inhibited. For this purpose, the A$\beta$/Cu complex on the liposome membranes is a promising option for membranes (Yoshimoto *et al.*, 2005) because the toxic ROS is not generated by the catalytic oxidation of DA by A$\beta$/Cu complex (Opazo *et al.*, 2002). The behavior of A$\beta$/Cu complex on the liposome membranes would be introduced in chapter 3.



Liposome: DMPC/SAPC$_{ox}$ (6:4)
A$\beta$(1-40): 10 $\mu$M
DA: 500 $\mu$M
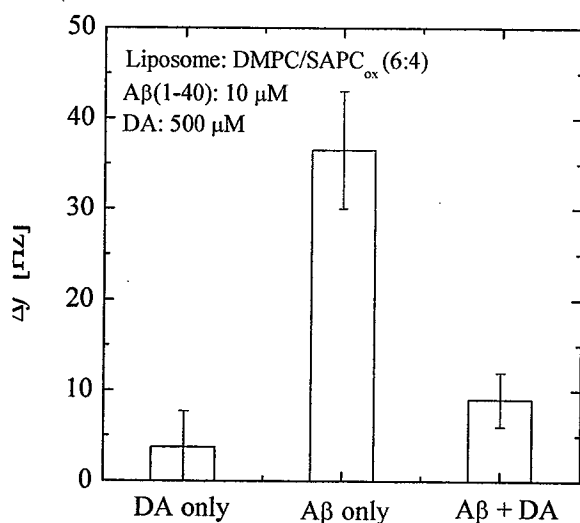
**Fig.2-7** Behaviors of DA and A$\beta$ on membrane of DMPC/SAPC$_{ox}$ (6:4) immobilized liposomes on QCM.

*3.2.6. Stability of Hydrogen Bonds within Liposome Membranes*

**Figure 2-5** shows the linear relationship between the $\rho_{pr}$ for various proteins and the protein-lipsome interaction, strongly suggesting that the slope involves the physical meaning of the hydrogen bonding stability of liposome membrane, from the rate theorem. According to the previous finding (Yoshimoto, 2005; Shimanouchi, 2005), the parameter of the protein-liposome interaction analyzed by the dielectric dispersion analysis and the immobilizd-liposome chromatography could give the similar index because they both employ a same approach to ultilize liposome as a sensor element. In those studies, the solpe has been defined as $m_{lip}$. Considering the experimental value for the protein-liposome interaction being F, the following equation can be difined.

$$F = a + m_{lip} \times \rho_{pr} \qquad (2\text{-}5)$$

where $a$ is an intercept and a conversion factor between methods. If F can be properly defined, $a$ can be excluded, so that the $m_{lip}$ value can become same nevertheless to the method for the measurement of F value.

The $m_{lip}$ value for representative liposomes used in this thesis was summarized in **Table 2-6**. The liposome with single lipid component is likely to show the small $m_{lip}$ value, such as DPPC ($m_{lip} = 0$), DMPC ($m_{lip} = 0.0024$), and POPC ($m_{lip} = 0.024$). Alternatively, the liposomes with binary lipid phase system showed the larger $m_{lip}$ value in contrast to those for liposomes with single lipid component. From another point of view, the hydration of liposome membrane was evaluated by using an FT-IR analysis since the bound water is generally advantageous to unstabilize the hydrogen bond. The adsorption observed at around 1230 cm$^{-1}$ is derived from the anti symmetric stretching bond for PO$_2^-$ of head group in phospholipid molecule. The representative $\nu_{max}$ was also summarized in **Table 2-6**.

A linear relationship can be obtained between the $m_{lip}$ value for various liposomes and their $\nu_{max}$ although some deviations (such as no.3 and 9) from the desired line were observed

**Table 2-6** Relationship between the $m_{lip}$ value of various liposomes and their phase state (Shimanouchi, 2005; Yoshimoto, 2005)

| No | Liposome | State at 25 °C | $v_{max}$ [cm$^{-1}$] | $m_{lip}$ [-] |
|----|----------|----------------|-----------------------|---------------|
| 1 | DMPC | $l_d + l_o$ | 1238 | 0.0024 |
| 2 | DMPC/SA (9:1) | $l_d + l_o$ | 1234 | 0.003 |
| 3 | DMPC/SA (2:1) | $l_d + l_o$ | 1229 | 0.085 |
| 4 | DMPC/LA (2:1) | $l_d$ | 1239 | 0.013 |
| 5 | DPPC | $s_o$ | 1239 | 0 |
| 6 | DOPC | $l_d$ | 1236 | 0.038 |
| 7 | DOPC/SM (1:1) | $l_d + s_o$ | 1243 | 0.042 |
| 8 | POPC/SM (1:1) | $l_d + s_o$ | 1241 | 0.030 |
| 9 | DMPC/SAPC$_{ox}$ (6:4) | $l_d + l_o$ is expected | 1231 | 0.081 |

(**Fig.2-8**). In the case of liposome with single lipid composition (no.1, 5, 6), the linear correlation between both was observed because the stability of hydrogen bond within liposome membranes is dominated by the interaction between headgroups. This head-head interaction can be simply weakend by the hydration around the PO$_2^-$ group in headgroup. In the binary lipid system, the domain formation is generally induced at a specific lipid composition (Almeida et al., 2003).

The modification by fatty acids such as stearic acid or linoreic acid (no.2, 3, 4), did not show the significant deviation effect in the desired line of $m_{lip}$ as a function of $v_{max}$. Since the fatty acid with single acyl chain cannot form the bilayer membrane structure, fatty acid-rich domain on DMPC liposome should be affected by the membrane property of DMPC. Then, a hydration around PO$_2^-$ of DMPC is anticipated to be influenced by an induction of fatty acids in dependent manner on their concentration.

In the case of other binary lipid system, such as DOPC/SM (no.7) and POPC/SM

(no.8), a significant deviation from the desired line was observed. The phase transition temperature of DOPC, POPC and SM are herewith -20, -3, and 32 °C. Therefore, the mixiture of DOPC/SM and POPC/SM cannot result in a considerable solubilization within liposome membranes. The boundary region between DOPC and SM or POPC and SM is expected to be the place to occurr the mismatch of hydrogen bonds between both lipids. Because of this, a binary lipid system with lower hydration around $PO_2^-$ could result in the relatively higher $m_{lip}$ value.

In the case of oxidized lipsome such as $DMPC/SAPC_{ox}$ (no.9), the phase transition temperarute of DMPC and SAPC are below the room temperature and the significant mismatch is unlikely to be induced relative to the case of DOPC/SM and POPC/SM. The oxidants including aldehyde and carboxylic PC also show the similar phase transition temperature, implying the similar effect to SAPC. The other oxidant derivatives, including 4 hexianonenal (4-HNE), have a single fatty acid and, therefore, the similar effect could be observed in the use the stearic and linoreic acid. The agreement of liposome (no.9) with the
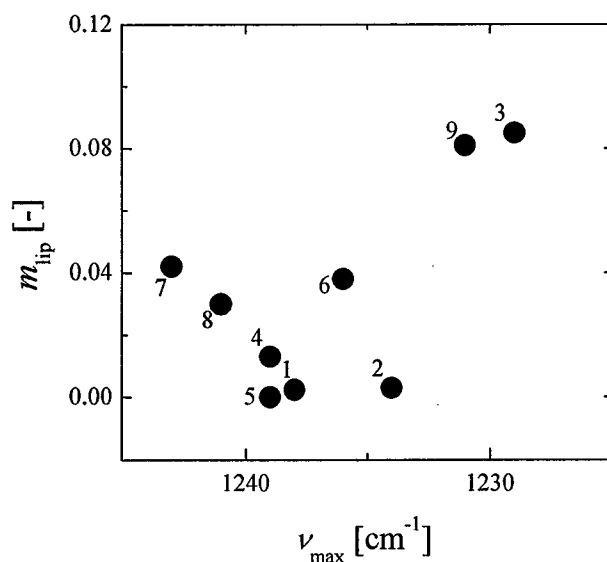


**Fig.2-8** Relationship between the $m_{lip}$ value for various liposomes and their hydration propensity. 1: DMPC, 2. DMPC/SA (9:1), 3: DMPC/SA (2:1); 4: DMPC/LA (2:1), 5: DPPC, 6: DOPC, 7: DOPC/SM (65:35), 8: POPC/SM (1:1), 9: $DMPC/SAPC_{ox}$ (6:4).

desired line is considered to be plausible.

In the following, the Aβ accumulation on the liposome membrane was investigated by using an IL-QCM. First, the accumation of Aβ on various liposomes were measured and the resulting $\Delta f$ for various liposomes was plotted against their $m_{lip}$ value for the liposomes (**Fig.2-9**). A linear relationship was observed, being consistent with the definition expressed as equation (2-5). Furthermore, the adsorbed amount of Aβ(1-40) treated with DA was measured and the resulting $\Delta f$ value was plotted in **Fig.2-9**. The co-existence of DA and Aβ reduced its accumulation on the liposome membrane. The formation of Aβ-DA adduct is expected to reduce its affinity to liposome membrane due to the variation of secondary structure. Alternatively, the slope of the **Fig.2-9** is corresponding to the $\rho_{pr}$ according to the equation (2-5). It is considered that the DA-Aβ adduct shows the greater $\rho_{pr}$ value ($\rho_{pr} > 4.5$) than that of Aβ(1-40). This suggests that the reaction of DA with Aβ(1-40) could lead to the conformational change to stabilize hydrogen bond in Aβ(1-40). It is considered that the



**Fig.2-9** The accumulation of Aβ(1-40) on various liposome membranes in the absence and the presence of DA. The absoubed amount of Aβ(1-40) was measured with an IL-QCM. DA concentration was 100 μM and the initial Aβ(1-40) concentration was 10 μM.

interaction between DA and Aβ could be modulated on the liposome surface in dependent manner on its state in order to protect the membrane itself from the toxicity of both DA (Chapter 1) and Aβ 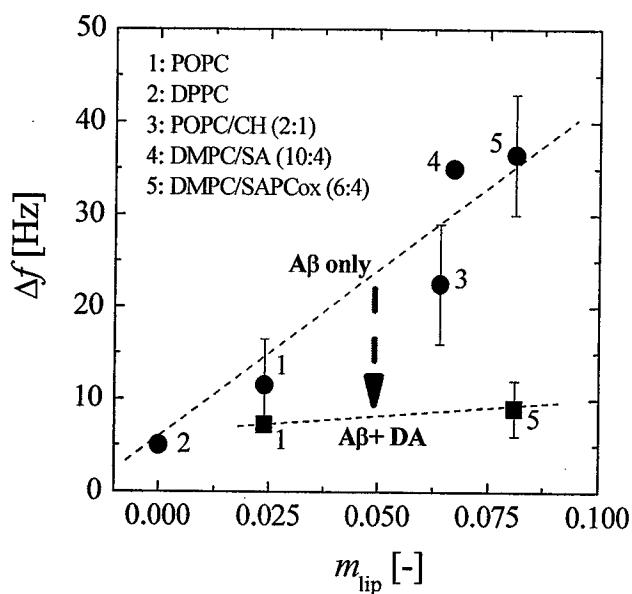(Chapter 2). The influence of the interactive behaviors of DA with Aβ on the liposome membrane would be introduced in chapter 4 in detail.

## 4. Summary

In this chapter, the "membrane sensor" was developed to evaluate the protein-membrane interaction. The method for immobilization of liposome on the SAM-modified Au electrode was investigated by modifying both of surface electrode and membrane components. All experiments were performed by using QCM electrode. It has been shown that the QCM is an effective tool to investigate immobilization of liposomes. Intact liposomes were found to be stably immobilized onto the planar surface of QCM electrode by covalent binding method. The large decrease in the resonance frequency of quartz crystals observed was dependent on the liposome diameter, showing that the small liposomes are proper for their immobilization. The electrostatic interaction could enhance the amount of immobilized liposomes by attractive force or to prevent the immobilization by repulse. By using the amino coupling method, the intact liposomes could be immobilized on the solid surface and immobilized liposomes could stably exist for 10 h with frequency changes less than 5%.

For the evaluation of membrane-protein interaction, "Membrane-sensor" was applied for the detection of unspecific interaction between the membrane and amyloidogenic proteins. The membrane-protein interactions were evaluated based on the adsorbed mass of proteins on immobilized liposome membrane. The hydrogen bond stability of several proteins ($\rho_{pr}$) was well correlated with their adsorbed amount, resulting in a successful evaluation of $\rho_{pr}$ for Aβ(1-40) and Aβ(1-42). Both proteins showed the strong amyloidgenic propensity, so that both could induce those fibrillations. As expected from the theoretical evaluation of complex formation to the stabilization of hydrogen bonds in proteins, the fibrils showed the largest $\rho_{pr}$

68

**(a) Protein**     **(b) Liposome**     **(c) Their Interaction**
(IL-QCM)

$\rho_{pr}$ [-]     $m_{lip}$ [-]     $\Delta f$ [Hz]

Aβ(1-40) Protofibrils — 2
Human Prion Fragment
Aβ(1-42)
Apolipoprotein A-1
Insulin — 4
Aβ(1-40)
β2-microglobullin
Lysozyme — 6
Myoglobin
β-LG
Aβ(1-40) Fibrils — 8

DOPC/DPPC/Ch (5mol%)
DLPC/DSPC(1/1)
DOPC/DAG (18.3 mol%)
0.10
DMPC/SA (30mol%)
DOPC/DAG(5 mol%)
DMPC/SA (20mol%)
0.05
DOPC
DMPC DPPC/Ch (60mol%)
0 DPPC

Aβ(1-40) vs DMPC/SAPC$_{ox}$ (6:4)
30
20
Aβ(1-40) vs POPC/Ch (2:1)
10

Correlation of $\rho_{pr}$ and the protein-liposome interaction could give the $m_{lip}$ as a slope

**Fig.2-10** Ladder of $\rho_{pr}$ value for various proteins.and $m_{lip}$ values for various liposomes and their nomograms.

of samples (**Fig.2-10**). The complex formation of Aβ(1-42) with copper and of Aβ(1-40) with DA also resulted in the stabilization of intramolecular hydrogen bonds of ordinal Aβs.

Furthermore, the Aβ-liposome interaction was examined to discuss the effect of membrane surface state. As shown in **Fig.2-10**, the interaction of certain liposome with the target protein given $\rho_{pr}$ value can be estimated (see red and blue colored lines in **Fig.2-10**). The oxidation of liposome membrane raises its $m_{lip}$ value, followed by the increase in interaction between protein and liposome. For example, the increase in interaction of Aβ with oxidized surface was observed in comparison with non-oxidized liposomes (POPC/Ch) and oxidized liposomes (DMPC/SAPC$_{ox}$). Finally, the behaviors of DA with Aβ on the immobilized liposomes were investigated. The DA was found to act as a modulator to reduce the membrane adsorption affinity of Aβ monomer.

# Chapter 3. Regulation of Dopamine Oxidation by Aβ/Cu LIPOzyme

## 1. Introduction

Oxidative stress has been reported to induce the cell death and to be involved in many diseases, such as Alzheimer's disease, atherosclerosis, Parkinson's disease, Heart Failure, etc. In a biological system, there are many reasons to induce the oxidative stress via the generation of the reactive oxygen species (ROS), such as the leakage of activated oxygen from mitochondria during oxidative phosphorylation, the metabolism of biological compounds, and so on. The dopamine (DA) plays a very important role in neuronal system as a neurotransmitter in a human brain. The loss of neuron containing DA induces the dementia symptom (Mo *et al.*, 2001). However, the existence of DA at extremely high level induces the oxidative stress, such as superoxide ($O_2^-$) and toxic DA-quinone by auto-oxidation pathway (Tse *et al.*, 1976; Asanuma *et al.*, 2003).



$$\text{DA} \qquad\qquad \text{DA-quinone}$$
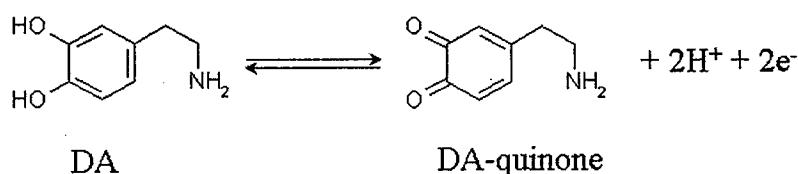
From another point of view, amyloid-β (Aβ) has been shown to contribute to the oxidative stress that accompanies with Alzheimer's disease (AD) (Bush *et al.*, 2003; Barnham *et al.*, 2004). Otherwise, a monomeric Aβ has been reported to serve as an antioxidant molecule against a metal-induced oxidative damage (Zou *et al.*, 2002). It has been reported that the Aβ/Cu complex can oxidize some reducing reagents, such as vitamin, cholesterol and catecholamines in the aqueous solution and, at the same time, can generate the $H_2O_2$ (Opazo *et al.*, 2002). For understanding of Aβ relating to both of toxic and protective functions, the

function of Aβ has been investigated (Opazo *et al.*, 2002; Murray *et al.*, 2005; Nagami, 2005; Yoshimoto *et al.*, 2005). In relation to the neurotoxic function, it has been reported that the Aβ/Cu could oxidize the cholesterol incorporated within a liposome membrane although it could not effectively oxidize the insoluble cholesterol in the aqueous solution (Yoshimoto *et al.*, 2005; Yoshimoto, 2005). Furthermore, the Aβ/Cu-catalyzed oxidation of cholesterol on the liposome membrane could result in a morphological change of liposome (Yoshimoto, 2005). This result implies the significance of the *"interactive behavior"* of cholesterol (within a membrane) and Aβ/Cu complex on the liposome membranes. Alternatively, a possible antioxidative function of Aβ has been proposed, where the toxicity of Cu ion in terms of ROS generation could be reduced by the formation of Aβ/Cu on liposome membranes via the entrapment of free Cu ion within a membrane by Aβ (Nagami, 2005).

In chapter 1, it is suggested that the DA partitions into the liposome membranes and can give the oxidative stress to the membranes via its auto-oxidation. The severe oxidative stress to membrane can be induced by the DA oxidation. Meanwhile, the liposome membrane itself, such as DMPC liposome, can induce the function to reduce the weak ROS, such as $H_2O_2$ (Yoshimoto *et al.*, 2007). Considering the above the findings, an alternative conversion system of ROS from $O_2^-$ to $H_2O_2$ is considered to be demanded for the maintenance of the liposome membrane. In chapter 2, it is suggested that the Aβ can strongly interact with the oxidized liposome membrane, implying the possible formation of Aβ/Cu complex on the liposome membranes. Instead of the toxic ROS such as $O_2^-$ radical and so on, the Aβ/Cu complex could generate the less toxic ROS, $H_2O_2$, together with the stoichometric oxidation of the DA according to the previous report (Opazo *et al.*, 2002). Thus, the Aβ/Cu-induced oxidation of DA might be a promising strategy for a reduction of the toxicity by an auto-oxidaiton of DA on the surface of liposome membranes and consequently for the defense of (bio)membrane from the further oxidative stress.

In this study, the DA oxidation by Aβ(1-42)/Cu complex was investigated in the

presence and absence of some kinds of liposomes. The influence of liposome membrane against a second-ordered kinetic parameter, $k_{cat}/K_m$, was examined to discuss the relationship of reactivity with the membrane property such as the extent of the hydration. A possible regulation of the DA-oxidation by $A\beta$/Cu complex on the liposome surface under oxidative stress condition has finally been discussed.

## 2. Materials and Methods

### 2.1. Materials

$A\beta$(1-42) peptides were purchased from the Peptide Institute (Osaka, Japan). 1,2-Dimyristoyl-*sn*-glycero-3–phosphocholine (DMPC), 1,2-dipalmitoyl-*sn*-glycero- 3–phosphocholine (DPPC), 1,2-dioleoyl-*sn*-glycero-3–phosphocholine (DOPC), sphingomyelin (SM), and 1-palmitoyl-2-oleoyl-*sn*-glycero-3-phosphocholine (POPC) were obtained from Avanti Polar Lipids (Alabaster, AL, USA). Stearic acid (SA) and dichlorofluorescein diacetate (DCF) were purchased from Sigma Aldrich (St. Louis MO, USA). Other reagents used were purchased form Sigma Aldrich and Wako Pure Chemicals (Osaka, Japan).

### 2.2. Liposome Preparation

Liposomes were prepared by the following process as previously reported (Yoshimoto *et al.*, 2006). The lipid composition of liposome at this study was summarized in **Table 3-1**. The lipid mixture was dissolved in chloroform and then dried onto the wall of a round-bottom flask in vacuum and was then left overnight to ensure the removal of all of the solvent. The dried thin lipid film was hydrated with adequate buffer solution to form multilamellar vesicles (MLVs). Large unilamellar vesicles (LUVs) were formed from the MLVs with five cycles of freeze-thaw treatment. The liposomes with different composition were then made in diameter 100 nm.

## 2.3. Preparation of Aβ/Cu Complex

Aβ(1-42) peptide solutions were prepared from powder by dissolve on 0.1% $NH_3$ solution to 200 μM as stock solution at 4 °C. The stock solutions were stored at -80° C until its use. For a preparation of Aβ/Cu complex, 10 μM Aβ(1-42) were independently pre-incubated with 20 μM $CuCl_2$ for 30 - 60 min and were vortexed before reactions. After that, 100 μM EDTA was added for eliminate free Cu(II) ion and further incubated for 15 min. The reactions were carried out at 37 °C in phosphate-buffered saline (PBS), pH 7.4, under ambient conditions containing preincubated Aβ (0.2 μM), $CuCl_2$ (0.4 μM). The Aβ/Cu complex on liposome membrane was prepared as following: the solution containing 2 μM Aβ(1-42) and 4 μM $CuCl_2$ was pre-incubated at 37 °C for 30-60 min. The free Cu ion inactivated by addition of EDTA at final concentration of 10 μM and further incubated for 15 min. All solution was deoxygenated by purging with high-purity nitrogen.

## 2.4. Hydrogen Peroxide Assay

Dichlorofluorescein diacetate (DCF) was dissolved (5 mM) in 100% dimetyl sulfoxide (bubbled with $N_2$ gas for 30 min to remove oxygen), deacetylated with 0.25 M NaOH for 30 min, and then neutralized, pH 7.4, to a final concentration of 1 mM. Horse radish peroxidase (HRP) stock solution was prepared to 1 μM in PBS, pH 7.4. The oxidative reactions for DA by Aβ/Cu complex were carried out in PBS, pH 7.4, under ambient conditions. $H_2O_2$ concentrations were measured by fluolescence spectrometer (FP-6500 SpectroFluoroMeter) (Ex: 485 nm, Em: 520 nm). During the reaction, there is no fibril was formed confirmed with SEM observation and ThT fluorescence measurement.

## 2.5. Dielectric Dispersion Analysis

The dielectric spectrum was measured using an HP4291B impedance analyzer

(Hewlett Agilent Tech.) according to the previous reports (Schrader *et al.*, 2001; Morita *et al.*, 2003). A spectrum of relative permittivity and dielectric loss were measured in a frequency range between 1 MHz and 1 GHz. The characteristic frequency observed at around 50 MHz was obtained with the fitting analysis of the obtained spectra using Debye's equation. The difference in frequency for liposomes between the absence and presence of Aβ/Cu was utilized as an index of the Aβ/Cu-liposome interaction.

## 2.6. Fourier Transforms Infrared Spectroscopy (FT-IR)

The FT-IR measurement was performed as follows. 1 mM of various liposome were prepared in 100 nm in diameter. Samples for infrared spectroscopy analysis were prepared in 50-μm-thick cells with $CaF_2$ windows. The infrared spectra were measured with a FT/IR-4100ST (Nihon Bunko Co. Ltd.) at 25 °C. The temperature of sample was controlled by means of a block assembly equipped with a circulating water jacket and monitored by a thermosensor placed at the edge of the cell window. The resolution was 4 $cm^{-1}$. The subtraction of spectra in buffer was carried out to remove the contribution from water bands. The accuracy of the frequency reading was better than $\pm 0.1$ $cm^{-1}$.

## 3. Results and Discussion

### 3.1. Oxidation of Dopamine by Aβ/Cu Complex

*3.1.1. Metalloenzyme-like Function of Aβ/Cu Complex*

The role of oxidative stress on Alzheimer disease (AD) has recently become an important issue among the researchers. Amyloid β-peptide (Aβ) has been shown to contribute to the oxidative stress that accompanies AD (Bush *et al.*, 2003; Barnham *et al.*, 2004). The Aβ/Cu complex generates $H_2O_2$ through the reduction of copper ion (Cu(II) → Cu(I)), accompanied by the oxidation of biological reducing agents such as vitamin, DA, and
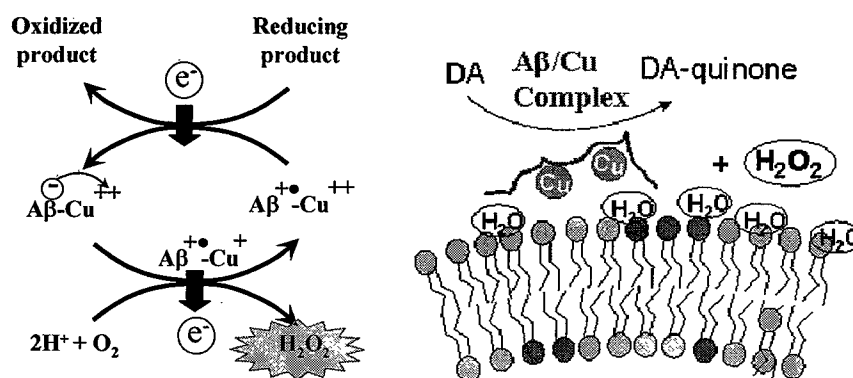
**Fig.3-1** Model for Aβ/Cu-catalyzed oxidation of DA in a bulk phase (left, Opazo *et al.,* 2002) and on liposome membrane (right, this study).

cholesterol (Opazo *et al.,* 2002). The metalloenzyme function of Aβ/Cu complex has also been reported to oxidize a cholesterol on biomembrane and its reactivity was dependent on the physical states of the cholesterol/POPC (liquid disordered phase) and cholesterol/DPPC (liquid ordered phase) liposomes (Yoshimoto *et al.,* 2005).

The liposome membrane is therefore expected to regulate the reactivity of Aβ/Cu-catalyzed oxidation of DA (**Fig.3-1**).

### 3.1.2. Oxidation of Dopamine by Aβ/Cu Complex in Bulk Solution

As shown in **Fig.3-1**, $H_2O_2$ is generated by an oxidation of DA with 1 to 1 stoichiometry. The generation rate of $H_2O_2$, $V_{H2O2}$, can herewith be regarded as an oxidation rate of DA. The reaction system was first optimized in terms of Cu concentration. The concentration of Aβ(1-42) was set at 200 nM considering its soluble concentration in the AD brain (McLeen *et al.,* 1999). The $H_2O_2$ generation were monitored at different Cu(II) concentration (0-600 nM) with the constant Aβ(1-42) concentration (200 nM). In the case of 10 μM of DA, the $V_{H2O2}$ value reached the saturated value at molar ratio of 2 Cu : 1 Aβ (**Fig.3-2**), suggesting that there could be two copper binding sites in monomeric Aβ at pH 7.4 according to the previous reports (Atwood *et al.,* 2000; Opazo *et al.,* 2002). In the following,
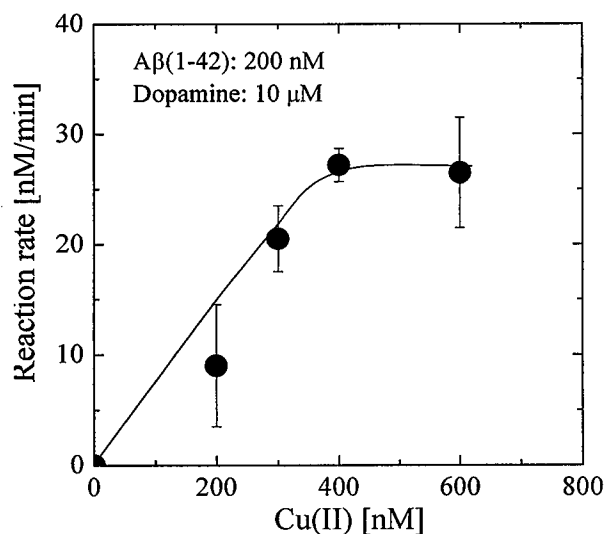
**Fig.3-2** Optimal stoichiometry of Aβ(1-42)/Cu complex. Aβ(1-42) (200 nM) was incubated at the different concentration of Cu(II) (0-600 nM) in the presence of 10 μM DA. $H_2O_2$ generation was confirmed to be associated with the dopamine oxidation by Aβ(1-42)/Cu complex. All the reaction was performed at 37 °C.

all the experiments were performed by using Aβ/Cu complex at the molar ratio of 2:1.

The reaction rate $V_{H2O2}$ was then estimated at various DA concentrations (1 to 10 μM) as shown in **Fig.3-3(a)**. The slope of $H_2O_2$ concentration against the time gives the $V_{H2O2}$ value and those reciprocal values were plotted against the reciprocal DA concentration (**Fig.3-3(b)**). The resulting linear relationship between both values indicated that the reaction mechanism with Michaelis-Menten type can be applied for the DA oxidation catalyzed by Aβ/Cu in bulk phase (Opazo *et al.*, 2002). According to the Lineweaver-Burk equation, the catalytic property of Aβ/Cu complex was investigated. The $K_m$ and $V_{max}$ was 8.9 μM and 34.6 nM/min, respectively. These values are considerably consistent with the previous finding (8.9 μM and 34.5 nM/min) (Opazo *et al.*, 2002).

## 3.2. Membrane Enhanced Activity of Aβ/Cu Complex for Dopamine Oxidation.

### 3.2.1. Reaction on Liposome Membrane

In the first series of experiment, the Aβ/Cu-catalyzed oxidation of DA was examined in the presence of liposome. The ratio of Aβ/Cu to lipid was, in general, considered to be an important factor for the observation of the target reaction. Our experimental conditions were set in the presence of 200 nM Aβ(1-42) and 1 mM total lipid (roughly corresponding with 8.1 Aβ/Cu molecule per one vesicle assuming the average lipid area as previously reported) (Papahadjopoulos and Kimeberg, 1973). Therefore, the reaction catalyzed by Aβ/Cu is considered to completely occur on the liposome membrane and the contribution of reaction in bulk phase can be negligible because of the partitioning of DA on the liposome surface.

At the DA oxidation catalyzed by Aβ/Cu, an equi-molar $H_2O_2$ with the DA oxidation is generated (Opazo et al., 2002). The incubation of DMPC liposome with $H_2O_2$ for 24 h resulted in the $H_2O_2$ decomposition (Yoshimoto et al., 2007). It was confirmed that no degradation of $H_2O_2$ was observed in the incubation of $H_2O_2$ with DMPC liposome for 30 min.
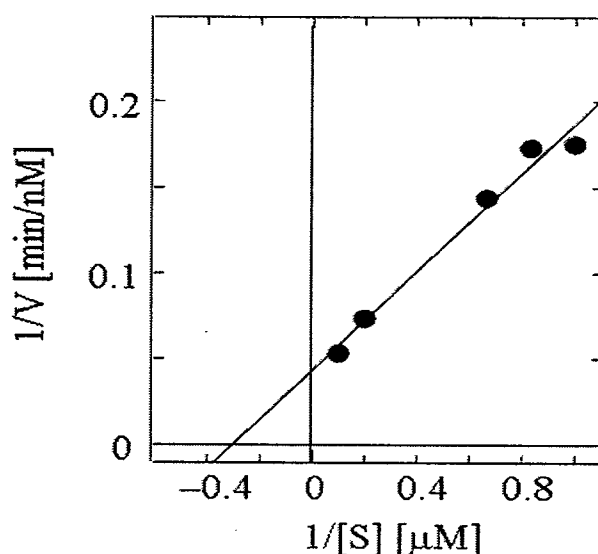


**Fig.3-3** Time course of produced $H_2O_2$ concentration catalyzed by Aβ/Cu complex: Aβ(1-42): 200 nM, $Cu^{2+}$: 400 nM. DA concentration: 1-10 μM.

Although the $H_2O_2$ at milimolar level affected the oxidation by Aβ/Cu, the $H_2O_2$ level in our experiments was the micromolar range, showing that the reaction of Aβ/Cu with $H_2O_2$ was negligible. The decomposition of $H_2O_2$ by liposome occurred in the time range in hours (Yoshimoto *et al.*, 2007). No effect of liposome on the degradation of $H_2O_2$ was, however, observed in our experimental conditions.

From these preliminary experiments, the initial velocity during the first 30 min of the reaction is reasonable for the kinetic analysis on Aβ/Cu-catalyzed DA oxidation. Since $H_2O_2$ is produced in a stoichiometric to DA with 1:1, the rate of $H_2O_2$ production was analyzed with DCF method. $H_2O_2$ production as a product of the stoichiometry of Cu bound to Aβ(1-42) was first optimized. Aβ(1-42) (200 nM) with Cu(II) (0 to 800 nM) was incubated and the concentration of resultant $H_2O_2$, generated in the presence of DA (5 mM), EDTA and DMPC liposome, was assayed (**Fig.3-4(a)**). $H_2O_2$ production by Aβ/Cu complex on the liposome membrane was reached to the saturated value at a molar ratio of 2 Cu : 1 Aβ, as well as that in bulk phase (Opazo *et al.*, 2002). These results suggest that two Cu atoms coordinating to Aβ monomer could support the redox activity even in the presence of liposome. The saturation of $H_2O_2$ production in this experiment suggests that only the Cu(II) bound to Aβ, and not free Cu(II), contributed to the production of $H_2O_2$.

The data obtained were plotted according to the Lineweaver-Burk equation in order to investigate the catalytic property of Aβ/Cu complex (**Fig.3-4(b)**). The distinct linear relationships were observed both in the absence and the presence of liposome. The kinetic parameters were $V_{max}$ = 22.8 nM/min and $K_m$ = 3.3 μM in the absence of liposome, roughly consistent with the previously reported data of $V_{max}$ = 34.5 nM/min and $K_m$ = 8.9 μM (Opazo *et al.*, 2002). On the other hand, $V_{max}$ = 15.9 nM/min and $K_m$ = 2.88 μM were yielded in the presence of liposome. There is a possibility that the liposome membrane could affect the reactivity of DA oxidation by Aβ/Cu complex.
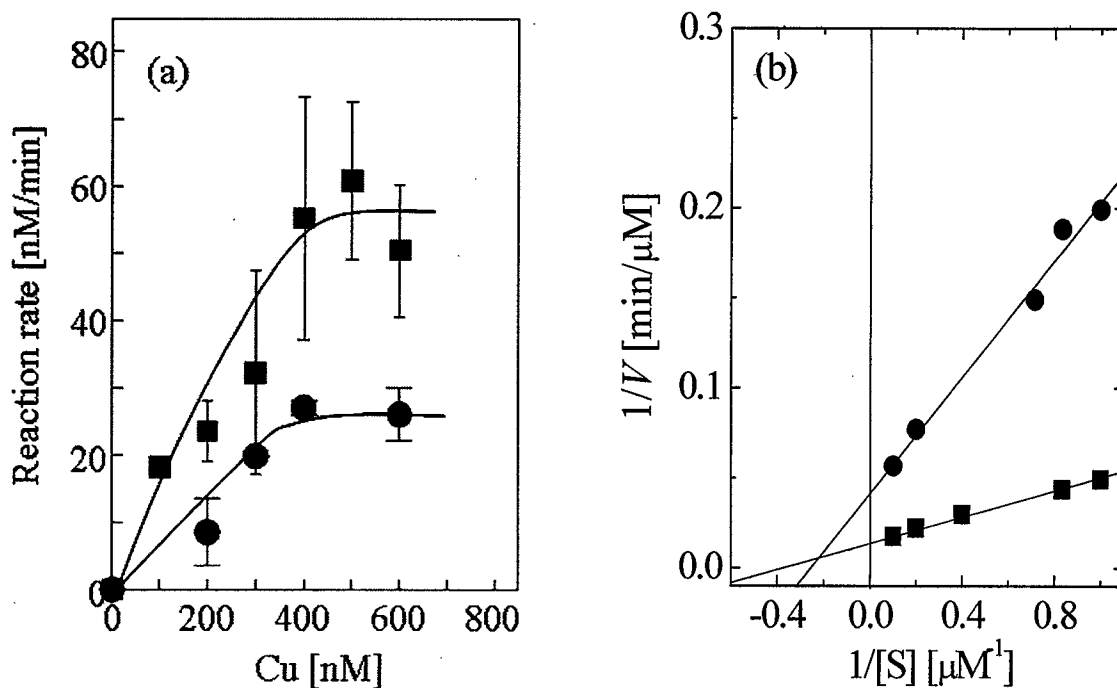
**Fig.3-4 (a)** Effect of liposome on the stoichiometry of Cu to Aβ(1-42) on $H_2O_2$ generation associated with the dopamine oxidation by Aβ/Cu complex. **(b)** Lineweaver-Burk plot of dopamine oxidation catalyzed by Aβ/Cu complex (Aβ : Cu = 1 : 2) in the absence and presence of DMPC liposome. Circle: no liposome (n=3), Square: DMPC liposome (n=3). Concentration of Aβ(1-42) and dopamine were 200 nM and 10 μM, respectively. 1 mM DMPC was added to the reaction solution. All the reaction was performed at 37 °C.

### 3.2.2. Regulation of Enzyme-like Activity of Aβ/Cu Complex on Liposome Membrane

The effect of liposome against the reactivity was investigated as shown in **Table 3-1**. The $k_{cat}/K_m$ value was used for the comparison of reactivity among various liposomes. DPPC and DOPC liposome showed the similar reactivity ($k_{cat}/K_m$) as that of DMPC liposome (5 ~ 6×10⁻⁵min⁻¹ · nM⁻¹). In the case of DMPC/Stearic acid (SA), the reactivity was promoted in a dependent manner on the SA concentration. DOPC/SM and POPC/SM liposomes at liquid-disordered ($l_d$)+solid-ordered ($s_o$) phase also indicated the higher $k_{cat}/K_m$ value as compared with the control condition ($k_{cat}/K_m$ = 2.12±0.3 ×10⁻⁵ min⁻¹ · nM⁻¹). These results may show that the enzyme-like activity for Aβ/Cu complex was controlled on the surfaces of liposomes with different phase states.

79

**Table 3-1** Comparison of reactivity of Aβ/Cu in the presence of eight kinds of liposomes

| | Liposome system | $k_{cat}/K_m$ $[10^5 \times min^{-1} \cdot nM^{-1}]$ | $k_{cat}$ $[min^{-1}]$ | $K_m$ $[\mu M]$ | $v_{max}$[a] $[cm^{-1}]$ |
|---|---|---|---|---|---|
| | No liposome | 2.12±0.3 (n=3) | 0.173 | 8.9 | - |
| 1 | DMPC | 5.52±0.71 (n=3) | 0.159 | 2.88 | 1238 |
| 2 | DMPC/SA (9:1) | 7.52±0.4 (n=3) | 0.131 | 1.74 | 1234±0.5 (n=3) |
| 3 | DMPC/SA (2:1) | 8.23±0.035 (n=3) | 0.101 | 1.23 | 1229±0.8 (n=3) |
| 4 | DMPC/LA (2:1) | 4.15±0.3 (n=2) | 0.109 | 2.62 | 1239±0.4 (n=3) |
| 5 | DPPC | 6.05±0.45 (n=2) | 0.206 | 3.41 | 1239±0.5 (n=2) |
| 6 | DOPC | 5.61±0.42 (n=2) | 0.159 | 2.84 | 1236±0.7 (n=2) |
| 7 | DOPC/SM (1:1) | 2.52 | 0.062 | 2.46 | 1243±0.6 (n=3) |
| 8 | POPC/SM (1:1) | 4.23 | 0.058 | 1.37 | 1241±0.5 (n=3) |
| 9 | DMPC/SAPC$_{ox}$ (6:4) | 0.5 | 0.011 | 2.20 | 1231±0.8 (n=3) |

[a] The antisymmetric stretching vibration of $PO_2^-$ ($v_{max}$) was evaluated from the FT-IR spectra at around 1230 $cm^{-1}$.

From the above results, the phase state of liposome membranes or the relating characteristic might control the reactivity. In the following, the membrane property of liposomes was examined.

### 3.2.3. Effect of Bound Water of Liposome Membrane on DA Oxidation by Aβ/Cu Complex.

The key mechanism of the oxidative reaction mediated by Aβ/Cu is the proton-coupled electron transfer (PCET) mechanism (Haeffner et al., 2005). Two electrons and two protons must be transferred between DA and $O_2$ to generate both DA-quinone and $H_2O_2$. In principle, the proton transfer is promoted by the water molecule based on Grotthuss's typed

mechanism. It is confirmed that the $D_2O$ reduced the $H_2O_2$ generation, indicating the proton transfer relating to the water molecule. Furthermore, the reduction of the $H_2O_2$ generation was significantly large relative to the bulk phase, suggesting that the bound water might be responsible for the proton transfer in $A\beta/Cu$-induced oxidation of DA.

In lipid membranes, the unsterilized phosphate oxygen form hydrogen bonds with adjacent molecules through water molecules (Yamamoto *et al.*, 1995). The antisymmeteric stretching band for the $PO_2^-$ double bond of PC obtained from FT-IR study is useful index to monitor the hydration state of the polar head group (Casal *et al.*, 1987; Yamamoto *et al.*, 1996). Therefore, the hydration in liposome membrane was investigated by using the dielectric dispersion analysis and FT-IR.

In order to investigate the difference between water in bulk and the bound water, the relaxation time reflecting the mobility of water molecule was estimated, for water in bulk ($10^{-12}$ sec) and water bound to DMPC liposome membrane ($10^{-9}$ sec) by using the dielectric
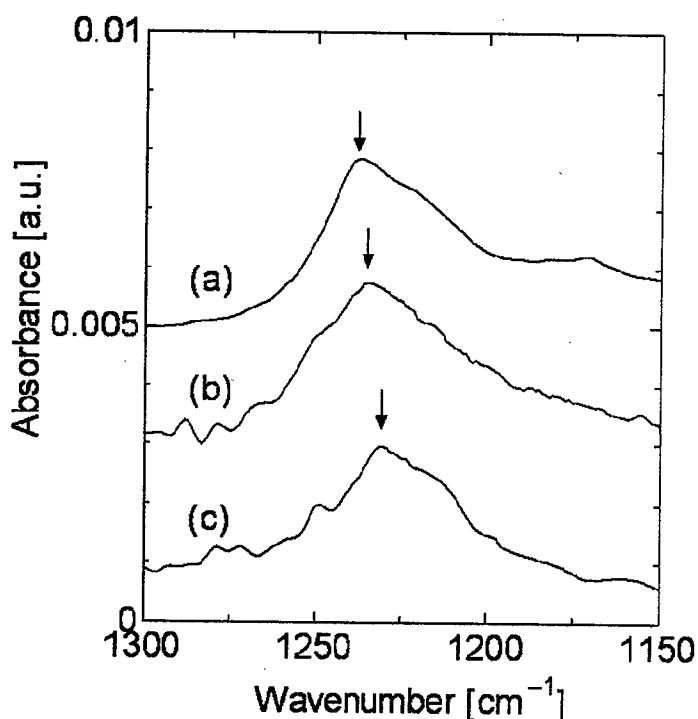


**Fig.3-5** Infrared spectra of (a) DMPC, (b) DMPC/SA (9:1), and (c) DMPC/SA (2:1), liposomes for the $PO_2^-$ double bond stretching region at 25 °C. Arrows show the maximum frequencies of the antisymmetric stretching band ($v_{as}$).

dispersion analysis (data not shown). These were consistent with the previous report (Klosgen et al., 1996). The activation energy $\Delta E$ for both waters was evaluated according to Arrhenius's law: $(2\pi\tau)^{-1} = A \exp(-\Delta E /RT)$. The resulting $\Delta E$ value was ~21 kJ/mol for bulk water and 31 kJ/mol for water bound to liposome membrane, respectively. This indicates that the polarization of O-H bond in bound water is stronger than that in bulk water. The bound water favors the polarization in O-H bond. It is, therefore, considered that the proton transfer via waters on a basis of Grotthuss's mechanism could be reasonable.

The bound water to phospholipids was investigated by using FT-IR. **Figure 3-5** shows the infrared spectra of various liposomes for the $PO_2^-$ double bond stretching bands (1000-1300 cm$^{-1}$). The assignment of spectra has been already studied (Inoue et al., 2001). In the case of liposome, the symmetric and antisymmetric stretching modes had the maximum frequencies at 1238 cm$^{-1}$. These values are consistent with those of Egg PC liposomes (Yamamoto et al., 1996) and dipalmitoylphosphatidylcholine liposome at liquid crystalline state (Asher et al., 1977). The incorporation of stearic acid in DMPC liposome shifted the $PO_2^-$ antisymmetric stretching band to lower frequency. It seems that the bandwidth slightly decreases. However, an accurate estimation of the bandwidth was difficult because of overlapping with the C-O stretching band of the ester group at approximately 1170 cm$^{-1}$ (Yamamoto et al., 1996). The shift to lower frequency by incorporation of stearic acid was therefore caused by an enhanced hydration of $PO_2^-$ group of DMPC on the membrane surface. These results show that the water was strongly immobilized at the phosphorous group. This immobilization of water is advantageous for the polarization of O-H bond in water molecule.

From both approaches using a dielectric dispersion analysis and FT-IR, it can be considered that the bound waster favors the polarization of O-H bond, suggesting that the bound water could play a key role for promotion of the PCET based on Grotthuss's mechanism. Then, the $k_{cat}/K_m$ value for various liposomes was plotted against those $\Delta v_{max}$ value as shown in **Fig.3-6(a)**. A linear correlation was observed in almost all liposomes,
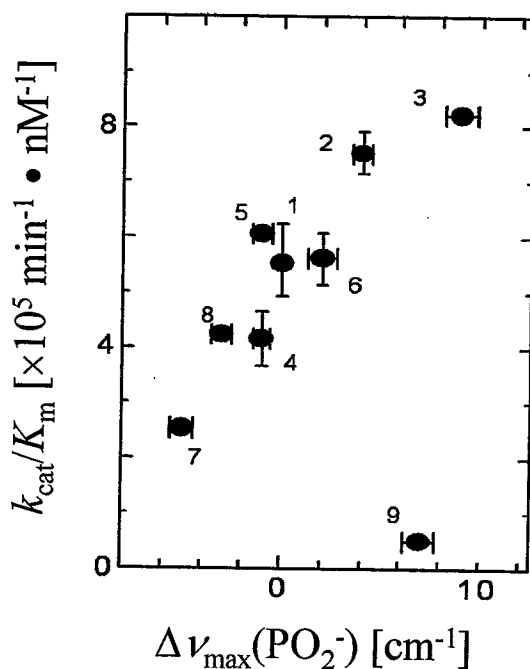
**Fig.3-6** Relationship between kinetic parameter of dopamine oxidation by Aβ(1-42)/Cu complex and (a) $\Delta v_{max}$ value, (b) $m_{lip}$ value for three liposomes. [Aβ/Cu$_2$] = 200 nM, [substrate] 1-10 μM, [lipid] = 1 mM, 37 °C. The second-rate constant $k_{cat}/K_m$ for dopamine was obtained with Michaelis-Menten equation. 1: DMPC, 2. DMPC/SA (9:1), 3: DMPC/SA (2:1), 4: DMPC/LA (2:1), 5: DPPC, 6: DOPC, 7: DOPC/SM (65:35), 8: POPC/SM (1:1), DMPC/SAPC$_{ox}$ (6:4).

except for the oxidized liposome (no.9), suggesting that the bound water could promote the PCET mechanism for enhancement of the reactivity. In the case of oxidized liposome, the $k_{cat}/K_m$ value deviated from the desired line might be caused by the conformational change of Aβ(1-42) via the Schiff-base formation as dscived in the following.

It is therefore considered that the liposome membrane with bound waters promoted the reactivity of Aβ/Cu–induced oxidation of DA in comparison with that at bulk phase.

## 3.3. Possible Function of Liposome Membrane against Oxidative Stress

From the results obtained before, the significance of reaction on the liposome membrane was discussed here. The $k_{cat}/K_m$ values for bulk phase, the non-oxidized liposome,

and the oxidized liposome were plotted (**Fig.3-7**). In the case of DMPC and DMPC/SA (2:1) liposomes, the enhanced effect was observed. Meanwhile, the oxidized liposome, DMPC/SAPC$_{ox}$, showed the inhibitory effect. It is likely that Aβ might take the different secondary structure from ordinal one by a formation of Schiff-base with lipid oxidants such as a 4-hexanonenal (HNE) (Axelsen *et al.*, 2008) or an aldehyde-type lipid as an intermediate of lipid oxidation. Therefore, it can be expected that the Aβ/Cu complex could reduce the ROS level by modulation of DA concentration under non-oxidative stress conditions while superoxide dismutase (SOD) can directly modulate the ROS level independent of DA concentration. It is thus considered that the Aβ/Cu complex has the possible function to defend the biomembranes from the oxidative stress. Under the oxidative stress conditions, the fragmented SOD could convert the $O_2$ ˙ radical to $H_2O_2$ for the reduction of ROS level (Tuan *et al.*, 2009). As described in the following chapters, it is considered that Aβ can contribute to the alternative function under the oxidative stress condition.

For the other compounds as substrates for Aβ/Cu complex, the $k_{cat}/K_m$ value was summarized in **Table 3-2**. The $k_{cat}/K_m$ value for DA, L-DOPA, and cholesterol in bulk showed the similar value at around $2.2 \times 10^{-5}$ min$^{-1}$ · nM$^{-1}$. In the presence of DMPC liposome, the $k_{cat}/K_m$ value for DA is obviously larger than that for L-DOPA. If the conformation of the Aβ/Cu complex on the liposome membrane is similar, the reactivity expressed by the second-order rate constant depends on the effective concentration on the surface of liposome membrane. The membrane environment is also likely to promote an oxidation of substrate such as DA, as described in chapter 1. DA favors the partitioning into the liposome membranes in comparison with L-DOPA. Therefore, the reaction process as a whole is considered to be affected by the membrane environment.

In the case of cholesterol incorporated into the liposome membrane, the reactivity was dependent on the phase state of liposome membrane. The behavior of cholesterol within a lipid membrane depends on its concentration. In the case of DPPC liposome, below 33 mol%
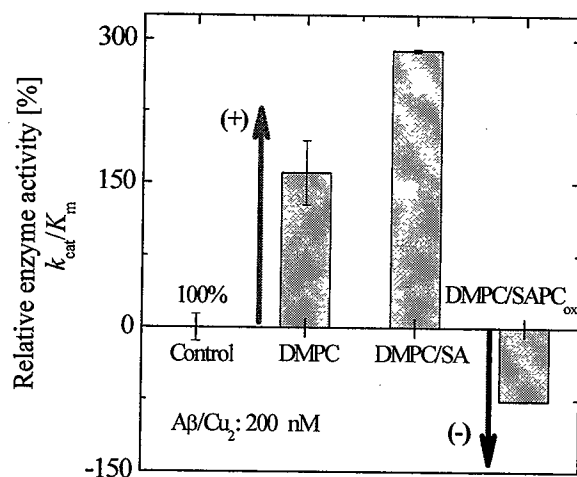
**Fig.3-7** Comparison of the kinetic parameter of DA oxidation by Aβ/Cu complex for three liposomes. [Aβ/Cu2] = 200 nM, [DA] = 1-10 μM.

of cholesterol, it favors the dispersed state on the liposome membrane (called as $s_o$ phase or

$s_o$+liquid-ordered ($l_o$) phase). The resulting $k_{cat}/K_m$ value was $2.1 \times 10^{-5} \text{min}^{-1} \cdot \text{nM}^{-1}$.

Meanwhile, a concentrated cholesterol on the liposome membrane (called as $l_o$ phase)

promoted the $k_{cat}/K_m$ value up to $4.8 \times 10^{-5} \text{min}^{-1} \cdot \text{nM}^{-1}$.

**Table 3-2** Summary of reactivity of various substrates controlled by liposomes

| Substrate | Conditions# | $k_{cat}/K_m$ [$\times 10^{-5} \text{min}^{-1} \cdot \text{nM}^{-1}$] |
|---|---|---|
| Dopamine (DA) | Bulk | 2.12±0.3 ($n$=3) |
| | (+) DMPC | 5.52±0.71 ($n$=3)** |
| L-DOPA | Bulk | 2.18 ($n$=2) |
| | (+) DMPC | 2.56 ($n$=1) |
| Cholesterol | Bulk* | 2.59## |
| | DPPC/Ch (2:1) | 2.1~4.8 ($n$≤4) |

# the concentration of lipid was 1 mM. * Free cholesterol was dissolved in chloroform, dried under nitrogen, re-dissolved in ethanol, and brought into PBS buffer (24 volumes of PBS, pH 7.4, per volume of ethanol extract) by sonication. ## Puglielli *et al.*, 2005. ** All the data for various liposomes were referred to **Table 3-1**.
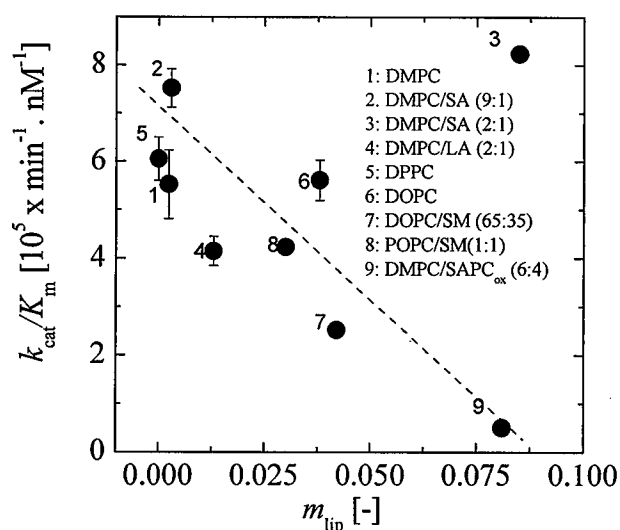
85

**Fig.3-8** Relationship between the reactivity of Aβ/Cu complex on various liposomes and their $m_{lip}$ value.

From these results, it is concluded that the behavior of the substrates on/in liposome membrane is dependent on their partitioning behaviors (See chapter 1), resulting in the modulation of the reactivity of Aβ/Cu complex on the liposome surface (Aβ/Cu-LIPOzyme). It is also considered that the Aβ/Cu-LIPOzyme is effective to the processing of DA.

Finally, the mechanism of the regulation of the Aβ/Cu activity by liposome membrane was discussed from the physicochemical aspects. The Aβ/Cu-liposome membrane interaction is expected to be dominated the enzymatic activity because the interaction between both might induce the variation in secondary structure of Aβ/Cu. In the discussion for the relation of bouond water to the reaction mechanism, the $k_{cat}/K_m$ value for DMPC/SA liposome was adjusted to the desired line (**Fig.3-8**). Meanwhile, in the discussion about the physicochemical mechanism, the DMPC/SA lipsome was deviated from the desired line in **Fig.3-8**. The interaction of Aβ/Cu with the liposome with high $m_{lip}$ value might result in the conformational change to reduce its reactivity.

86

# 4. Summary

In this chapter, the enzymatic function of Aβ/Cu on the liposome membrane was examined. Aβ can form the complex with Cu by a stoichiometric manner of 1:2 of Aβ:Cu. Aβ/Cu complex could catalyze the oxidation of DA, so that the toxicity level of ROS could be reduced as compared with that in the auto-oxidation pathway. Since Aβ/Cu-catalyzed oxidation of DA is dominated by a proton-coupled electron transfer (PCET) mechanism, water molecule with considerably polarized O-H bonds is advantageous for the proton transfer from DA to $O_2$ to generate both DA-quinone and $H_2O_2$. The liposome membrane can accumulate the bound water with considerably polarized O-H bonds prior to PCET. Consequently, the liposome membrane could promote the DA–oxidation by an enhancement of PECT mechanism. This could result in the reduction of toxicity level of the ROS by modulation of DA concentration. The enzyme-like activity of Aβ/Cu ($k_{cat}/K_m$) was found to be dependent on the hydrogen bond instability of lipospome ($m_{lip}$). It is also consisdersd that the Aβ/Cu complex on membrane could act as a modulator of (i) the formation of DA-quinone for its release from membrane and (ii) the formation of less toxic ROS ($H_2O_2$) instead of $O_2^-$ in auto-oxidaiton. In such a sense, it suggested that the Aβ/Cu complex has the possible function for the defense of (bio)membranes from the ROS.

# Chapter 4. Interactive Behavior of DA with Aβ on Liposome Membrane ~ Quantity Control of DA and Aβ Fibrils ~

## 1. Introduction

Amyloid β (Aβ) secreted from amyloid precursor protein is a peptide of 39-43 amino acids that some scientists suspect to be the main constituent of amyloid plaques in the brains of Alzheimer's disease patients. As is the case with other amyloidgenic proteins, Aβ originates as a soluble and constitutive protein found in biological fluids, such as cerebrospinal fluid, blood, and tissue (Haass *et al.*, 1992; Soji *et al.*, 1992). The aggregation of the soluble Aβ monomer into toxic oligomeric or fibrillar species is considered to be a crucial step in the pathology of the disease (Dahlgren *et al.*, 2002; Resende *et al.*, 2008). It has been reported that the most neurotoxic species are oligomers acting as intermediates during the formation of fibrils (Dahlgren *et al.*, 2002; Kayed *et al.*, 2003). Until now, there is no way to cure Alzheimer's disease or to stop its progression. Some researchers were encouraging advances in Alzheimer's treatment, including medications and non-drug approaches to improve symptom management. Therefore, the prevention of formation of Aβ oligomers and fibrils are promising strategies for the prevention and treatment of AD (Hard *et al.*, 2002).

In previous studies, a number of inhibitors of fibril formation have been described to prevent the formation of a biologically active species of peptide. It has been shown that various compounds as summarized in **Table 4-1** can inhibit the amyloid fibril formation.

On the other hand, the identification of the molecules that could initiate the *"reverse"* reaction to the fibril formation may be a key step toward the better understanding of the pathology of inclusions and deposits in human diseases, which allows us to evaluate the role of fibrils in neurodegenerative processes and disease progression. If these molecules could exert neuro-protective effects, their discovery could open new avenues for the therapeutic

**Table 4-1** Summary of the inhibitory factors and suggested mechanisms of inhibition of amyloid fibril formation

| Chemical Compounds | Peptide | Proposed Mechanism | Reference |
|---|---|---|---|
| Pyrroloquinoline (PQQ) | α-synuclein | PQQ, which contains quinone group, bind to α-synuclein via a Schiff-base to form a PQQ-conjugated-α-synuclein adduct which prevent fibril formation. | Kobayashi et al., 2006 |
| Salvianolic acid B (Sal B) | Aβ(1-40) | Sal B has many hydroxyl groups that might interact with the peptide side chain to inactivate fibril aggregation. Sal B inhibits elongation process | Durairajan et al., 2008 |
| Baicalein | α-synuclein | Baicalein quinone (oxidized baicalein) binds to α-synuclein by formation of a Schiff-base with a lysine side chain in α-synuclein to inhibit α-synuclein nucleation. | Zhu et al., 2004 |
| Curcumin | Aβ(1-40) Aβ(1-42) | The compact and symmetric structure of curcumin (Cur) might be suitable for the specially binding to free Aβ and subsequently inhibiting polymerization of Aβ into Aβ fibrils. | Ono et al., 2004a |
| Tannic acid (TA), Myricetin (Myr) | Aβ(1-40) Aβ(1-42) | TA and Myr could bind to the ends of short fibrils and then inhibit the extension of fibrils. TA and Myr would bind to Aβ monomers and consequently inhibit of polymerization. | Ono et al., 2004b |
| Dopamine L-DOPA | α-synuclein | Oxidized product of DA (DAQ) form coupling with Tyr to form a covalent adduct. The DAQ-α-synuclein covalent adduct formation by nucleophilic attack of DAQ to Lys side-chains (Lys forming a Schiff base with DAQ). DAQ-α-synuclein covalent adduct induced the stabilization of protofibrils. | Conway et al., 2001; Li et al., 2004 |

intervention. The formed amyloid fibrils have been reported to be disaggregated by various compounds, such as DA and L-DOPA (Li et al., 2004), nordihydroguaiaretic acid (NDGA), rifampicin (RIF), tannic acid (TA), quercetin (QUE) (Matsuzaki et al., 2007a), and Salvianolic acid B (Durairajan et al., 2008), Anti-Aβ$_{1-11}$ antibody (Mamikonyan et al., 2007). The disaggregation of Aβ fibrils also seems to be a promising strategy for the treatment of AD (Soto et al., 1998). From in vivo experiments using dyes specific to amyloid, Aβ fibrils are commonly observed on cell membranes (Okada et al., 2007). It has also been reported that the

liposome membrane could recruit not only the fragmented or short peptides (Tuan *et al.*, 2008; Tuan *et al.*, 2009) but also Aβ fibrillar aggregates (Avdulov *et al.*, 1997). In the neural cell system, varieties of catecholamine derivatives are secreted and some hydrophobic derivatives, such as DA, are subject to partition into the lipid membrane. It is therefore expected that the disaggregation of Aβ fibrils on the liposome membranes by catecholamine derivatives would occur and might be useful for the understanding of the physiological phenomena of AD.

The aggregation of Aβ also occurs in lipid raft mediated by a cluster of monosialoganglioside GM1. The membrane has played a "seed" role during the Aβ fibril formation (Matsuzaki *et al.*, 2007b). It has also been reported that, a toxic form of Aβ is generated during the aggregation with GM1-contanning raft-like liposomes, and the existence of GM1-bound Aβ in AD brains was confirmed (Hayashi *et al.*, 2004). The secondary structure of Aβ fibrils formed in the presence of GM1 containing-membrane has reported to be different in the absence of membrane (Kakio *et al.*, 2004). It therefore seems that the membrane has a strong effect on the fibril formation and properties of fibrils.

Amyloid fibrils are deposited on the neuronal cell membranes, whereby the catecholamines, such as DA was found to partition (adsorb) onto the lipid membrane. It is well known that the DA is easily to form the reactive DA-quinone, which was closely linked to other hypothesis, such as mitochondrial, inflammation, generation of oxidative stress, dysfunction of the ubiquitin-proteasome system, and degeneration of dopaminergic neurons (Miyazaki *et al.*, 2009). Therefore, some molecules or reagents to prevent quinone formation or quench generated DA-quinone would be potential therapeutic approaches against DA-quinone-related diseases.

In this chapter, the interactive behavior of DA with Aβ proteins on the liposome membrane were investigated, mainly focusing on: *(i)* inhibition of Aβ fibril formation by DA; *(ii)* disaggregation of Aβ fibrils by DA; and *(iii)* reduction of DA/ DA-quinone concentration

via Aβ fibrils though its interaction with DA. The function of biomembrane to defend itself from toxicity were finally summarized and discussed. Main focusing points are *(1)* the modulation of the DA concentration on *"membrane"* through the regulation of the enzyme-like activity of Aβ/Cu complex in order to reduce toxicity induced by ROS generation and toxic DA-quinone, *(2)* regulation of the Aβ fibril level by *"membrane"* in order to reduce the toxicity induced by Aβ fibrils, and *(3)* the possibility of *"membrane"* to prevent toxicity or recover itself under stress condition.

## 2. Materials and methods

### 2.1. Materials

Aβ(1-40) and Aβ(1-42) peptides were purchased from the Peptide Institute (Osaka, Japan). The phospholipids, such as 1-palmitoyl-2-oleoyl-*sn*-glycero-3-phosphocholine (POPC) and 1,2-dimyristoyl-*sn*-glycero-3–phosphocholine (DMPC), were obtained from Avanti Polar Lipids (Alabaster, AL, USA). Cholesterol (Ch) was obtained from Wako Pure Chemical (Osaka, Japan). Stearic acid (SA) was purchased from Sigma Aldrich (St. Louis, MO, USA). Thioflavin T (ThT) was obtained from Dojindo (Kumamoto, Japan). Dopamine hydrochloride, L-tyrosine (Tyr), catechol (Cat), 3,4-dihydroxyphenylacetic acid (L-DOPA), norepinephrine (NE) and epinephrine (EP) were purchased from Sigma-Aldrich. Other reagents used were purchased form Sigma Aldrich and Wako Pure Chemical (Osaka, Japan).

### 2.2. Liposome Preparation

Liposomes were prepared by the following process as previously reported (Yoshimoto *et al.,* 2006). The lipid mixture was dissolved in chloroform and then dried onto the wall of a round-bottom flask in vacuum and was then left overnight to ensure the removal of all of the solvent. The dried thin lipid film was hydrated with adequate buffer solution to form multilamellar vesicles (MLVs). Large unilamellar vesicles (LUVs) were formed from the

MLVs with five cycles of freeze-thaw treatment. For the preparation of oxidized lipid, the SAPC$_{ox}$ was prepared by mixing SAPC vesicles with CuSO$_4$/H$_2$O$_2$ (1mM) solution over night at 25 °C. After that, the lipid was extracted in chloroform/MeOH phase by Folch's method (Folch *et al.*, 1957). The oxidized liposomes were prepared by mixing SAPC$_{ox}$ with DMPC or DMPG lipid in the molar ratio 4:6.

## 2.3. Fibril Preparation

Aβ(1-40) and Aβ(1-42) peptide solutions were prepared from powder by dissolve in 0.1% NH$_3$ solution to 200 μM as stock solution at 4 °C. The stock solutions were stored at -80 °C until its use. Just before the experiment, the Aβ stock solutions were thawed and then diluted 20-fold by Tris-HCl buffer (Tris-HCl buffer: 50 mM and 100 mM NaCl, pH 7.4) to a final concentration 10 μM. The fibrils were prepared by incubating Aβ monomer solution at 37 °C for at least 24 h. For the inhibition of Aβ fibril formation experiment, the inhibitor, such as DA or other catechol derivatives, was added at beginning of incubation time. The processes were monitored as a function of time via ThT fluorescence.

## 2.4. Aβ Seed Preparation

Seed stock solutions were prepared by the following procedure as previously reported (Andersen *et al.*, 2009). In brief, the seed was prepared from 10 μM of already fibrillated sample solution prepared as the conditions described above. Fibrils were disrupted into seeds by sonication of the fibril solution by a probe sonication in a 10-ml plastic tube on an ice-bath at 40 W for 10 min with 1 min intervals for each 1 min. The seed stocks were kept at 4 °C and briefly vortex mixed before use.

## 2.5. Fibril Disaggregation Experiment

Preformed Aβ fibrils were incubated with catechol derivatives at various concentrations at 37 °C. The dissociation of Aβ fibril was monitored by ThT fluorescence measurement as a function of time. The TEM images and TIRFM images were also obtained as a function of time. Fluorescence spectroscopy data for disaggregation of Aβ fibrils were fitted to a first order-exponential decay equation (Mamikonyan *et al.*, 2007).

$$F(t) = F_i \exp(-k_d t) \tag{4-1}$$

where F($t$) represents the ThT fluorescence at time $t$, F$_i$ is the initial level of fluorescence, and $k_d$ is the pseudo-first order rate constant of disaggregation.

## 2.6. Fluorescence Measurement

The fibrils formation and existing fibril disaggregating processes were monitored by measuring the ThT fluorescent intensity. The fluorescence measurements were carried out at 37 °C by using JASCO, PF-6500 fluorescence spectroscopy at an excitation wavelength of 442 nm and an emission wavelength of 485 nm. To account for the background fluorescence, the fluorescence intensity for each control solution containing Aβ was also measured.

## 2.7. Transmission Electron Microscopy (TEM)

The Aβ fibrils formation and degradation of Aβ fibrils were monitoring by transmission electron microscopy (TEM). The TEM images were obtained by the following procedure as previously reported (Sasahara *et al.*, 2007). In brief, a 5 μl aliquot of diluted solution was placed on a copper grid (400-mesh) covered with a carbon-coated collodion film for 1 min and the excess sample solution was removed by blotting with filter paper. After the residual solution had been dried up, the grid was negatively stained with a 2% (wt/vol) uranyl acetate solution. Again, the liquid on the grid was removed with filter paper and dried. EM

images were acquired using a JEOL 100CX transmission microscope (JEOL, Tokyo, Japan) with an acceleration voltage of 80 kV.

## 2.8. Total Internal Reflection Fluorescence Microscope (TIRFM)

The TIRFM system used to observe amyloid fibrils degradation was developed based on an inverted microscope (IX70, Olympus, Tokyo, Japan) as previously described (Ozawa *et al.*, 2009). The ThT molecule was excited at 442 nm by a helium-cadmium laser (IK5552R-F, Kimmon, Tokyo, Japan). The laser power was 4-80 milliwatt, and the observation period was 3-5s. The fluorescence image was filtered with a bandpass filter (D490/30, Omega Optical, Bratteboro, VT) and visualized using a digital steel camera (DP70, Olympus).

## 2.9. CD Spectroscopy

Variation in the secondary structural content of Aβ with and without DA was recorded by using a circular dichroism spectrometer (J-720W, JASCO, Tokyo, Japan). CD spectra were measured by using a quartz cell from 195 to 250 nm with a step interval 0.1 nm bandwidth, a scanning at speed of 10 nm $min^{-1}$.

## 2.10. Cell Culture and Neurotoxicity Assay

For the cytotoxicity of Aβ experiment, Human Glioblastoma (A172 DSP) cells were cultured, maintained, differentiated and assayed as previously described (Durairajan *et al.*, 2008) and briefly described as follows: Human Glioblastoma (A172 DSP) cells were plated in 24 wells plate at a density of $5\times10^4$ cells/ml in 2 ml Dulbecco's modified Eagle's medium (MEM) medium containing 10% fetal bovine serum, plus 0.3 ml 3% L-glutamine solution and incubated for 24 h at 37 °C with 5% $CO_2$ in $CO_2$ incubator. After 24 h, the cell were treated with the aggregated Aβ for 18 h in a medium solution in $CO_2$ incubator at 37 °C. After that,

the medium was carefully decanted off, and then 1 ml Dulbecco's PBS containing 0.05% EDTA and 0.05% Trypsin was added. 50 μl of aqueous MTT solution (5 mg/ml) were then added to each well, and the mixture was incubated at 37 °C for 3 h. The formazan was extracted from the cells with 1 ml DMSO in each well. Finally, color intensity was measured at 570 nm. All MTT assays were repeated three times.

## 2.11. QCM Measurement

Liposomes were immobilized on modified QCM electrode as described in the chapter 2. In briefly, the DMPC/SA (10:4) liposomes were immobilized on amino undecanthiol-self assembled monolayer (AUT-SAM) modified QCM sensor in the presence of DMTMM as catalysis. For other kinds of liposome, the liposomes were modified with 2% molar of PE lipid for binding with mercaptou-undecanoic acid -self assembled monolayer (MUA-SAM). A 10 μM solution of monomeric Aβ(1-40) were injected onto the immobilized liposome for 45 min with flow rate of 0.06 ~ 0.07 ml/min. The adsorbed mass of monomeric Aβ was estimated equal to change in frequency of QCM signal at saturated value.

## 2.12. Statistical Analysis

Results are expressed as mean ± standard derivation (SD). All experiments were performed at least in triplicate. The data distribution was analyzed, and statistical differences were evaluated using the Student's t-test. A P value of $< 0.05\%$ was considered significant.

## 3. Results and Discussion

## 3.1. Liposomes Regulate Aβ Fibril Formation

### 3.1.1. Aβ Fibril Formation

It has been reported that the Aβ toxicity in Alzheimer's disease was well correlated

with the formation of fibrillous and/or amorphous aggregation of Aβ. The fibril formation experiment was performed by incubation 10 μM Aβ monomer on Tris-HCl buffer solution at 37 °C. The kinetic of Aβ fibril formation was monitored by ThT fluorescence intensity measurement. The ThT fluorescence intensity against of time shows the characteristic sigmoidal curves (**Fig.4-1(a)**). From the previous report (Nuria *et al.*, 2007), this curve consists of two processes: (i) a nucleation process and (ii) an elongation process. In the process (i), the oligomers/protofibril formation or the nucleation occurs while the fluorescence variation was not detected. This duration is defined as "lag phase" and its time is a "lag time" ($t_{lag}$), and the nucleation rate was estimated as $1/t_{lag}$. In the process (ii), the fibrils grow by the binding of monomers to the ends of fibrils and the ThT fluorescence intensity increased. This duration is called as "elongation phase" and its rate is an "elongation rate".

In order to confirm the significance of the nucleation process, the fibrils formed in this process was directly observed with a scanning electron microscopy (SEM), a total internal reflection fluorescence microscopy (TIRFM) and a transmission electron microscopy (TEM). Firstly, the fibrils obtained in **Fig.4-1** were observed with a SEM because SEM observation is advantageous to grasp the macroscopic and steric structure of the target. The fibrillar aggregates were observed as shown in **Fig.4-1(b)**. In order to clarify if these fibrillar aggregates were amyloid fibrils, the modification by ThT was performed. In the observation with a TIRFM combining with ThT, the fibrillar aggregates with ThT fluorescence were observed (**Fig.4-1(c)**). These fibrillar aggregates could be considered as amyloid fibrils of Aβ(1-40), consistent with the previous reports (Ban *et al.*, 2004; Yagi *et al.*, 2007). The microscopic structure of these fibrillar aggregates was confirmed with a TEM observation (**Fig.4-1(d)**). The fibrillar structure with a characteristic structure of amyloid fibrils previously reported (Ban *et al.*, 2004; Yagi *et al.*, 2007) was observed.

The sonication of fibrils was then performed to obtain the short fibrils. That TEM image shows the short fibrils with 100 nm in length or so (**Fig.4-1(e)**). From the histogram

analysis of seeds, these length distributions were found to show a mono-dispersion with 101.8 nm of median length. In order to check the importance of the seeds, the seeds were added to the process of the amyloid fibril formation (**Fig.4-1(a)**). It is obvious that the lag time disappeared by the addition of seeds, implying that the seeds can act as an alternative intermediate of nuclei formed during the lag phase, consistent with the previous reports (Nichols *et al.*, 2002; Yagi *et al.*, 2007).
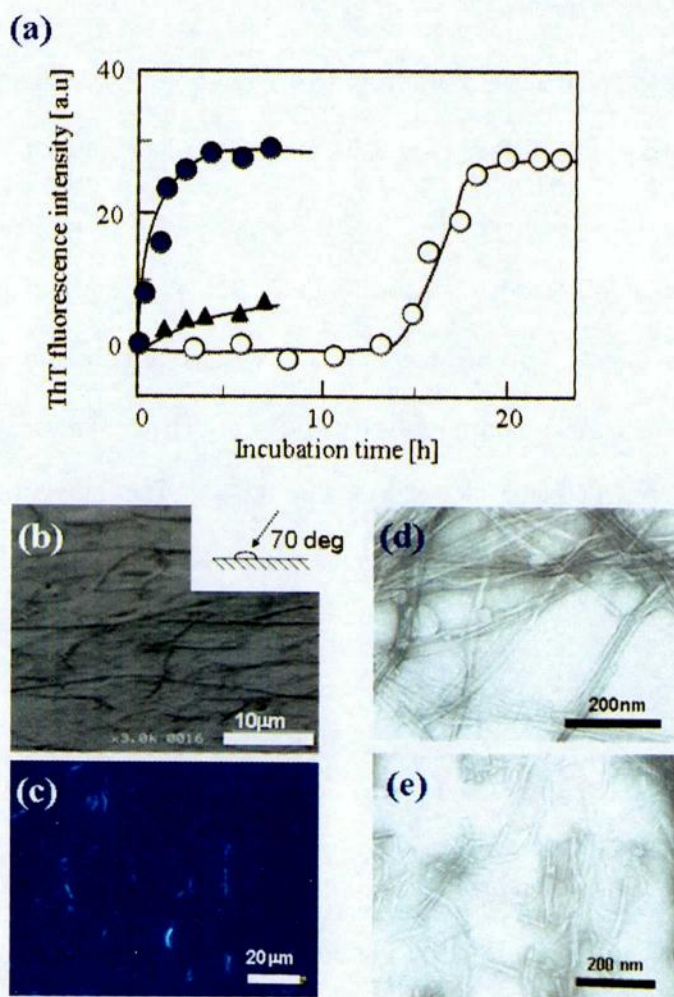


**Fig.4-1** (a) Growth of Aβ fibrils. Open circle: spontaneous growth, closed circle: growth from seeds, closed triangle: growth from seeds in the presence of Triton X-100 (0.25 wt%). 5 μM of Aβ(1-40) was used. Direct observation of fibrils of Aβ(1-40) with (b) SEM (observation angle was 70 deg.), (c) TIRFM, and (d) TEM. (e) TEM image of seeds of Aβ(1-40) fibrils. Fibrils were prepared by incubation monomeric Aβ on 50 mM Tris-HCl, 100 mM NaCl pH 7.4 at 37 °C.

The formation of seeds-like aggregate (nuclei) is considered to be sensitive against the presence of liposome because the nucleation process is one of the association of Aβ molecules via hydrophobic interaction and the stabilization of hydrogen bonds within Aβ molecules. Therefore, the effect of liposome membrane on the nucleation process was investigated in the followings.

### 3.1.2. Liposomes Modulate Aβ Fibril Formation

It was found that liposome with different hydrogen bond instability shows the different ability to accumulate Aβ on its surface (**Fig.2-9**), which is a key step for Aβ fibril formation. In order to investigate effect of liposomes on Aβ fibril formation, 250 μM various kinds of liposomes were independently added in the 5 μM Aβ(1-40) solution at the beginning of incubation time. The kinetic of Aβ fibril formation was measured and plotted against the fibril formation time. The effect of liposome on the amyloid fibril formation was investigated on both of nucleation step ($t_{lag}$) and elongation step ($k_{app}$). The elongation rate ($k_{app}$) was calculated by fitting following equation (Nielsen *et al.*, 2001).

$$Y = y_i + m_i x + \frac{y_f + m_f x}{\{1 + \exp[-(x - x_0)/\tau]\}} \tag{4-2}$$

$$t_{lag} = x_0 - 2\tau, \ k_{app} = 1/\tau$$

where $Y$ is the fluorescence intensity, $x$ is time, and $x_0$ is the time of 50% maximal fluorescence. $y_i$ and $m_i$ are the initial fluorescence and its slope at the nucleation phase, respectively. $y_f$ and $m_f$ are the final saturated fluorescence and its slope at the maturation phase.

The lag time ($t_{lag}$) and elongation rate ($k_{app}$) were plotted against the hydrogend bond instability of liposome ($m_{lip}$) as shown in **Fig.4-2.** The liposome with high hydrogen bond instability shows the ability to promote Aβ fibrils formation at both of nucleation and elongation step. In the case of non-oxidized liposomes, the nucleation process was not
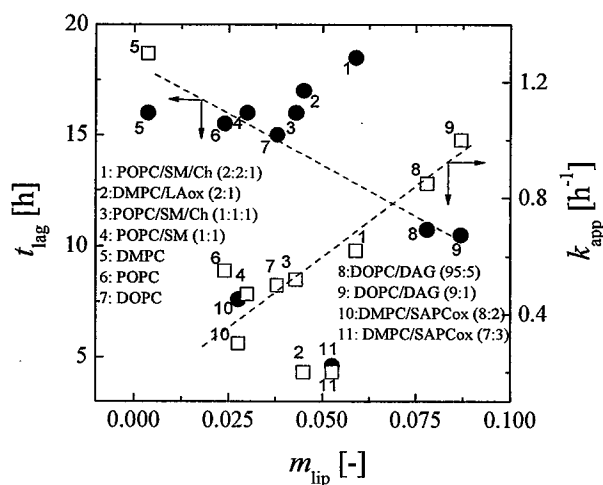
**Fig.4-2** Effect of liposomes on Aβ fibril formation. The relationship between membrane property ($m_{lip}$) and kinetic parameters of Aβ fibril formation ($t_{lag}$ and $k_{app}$).
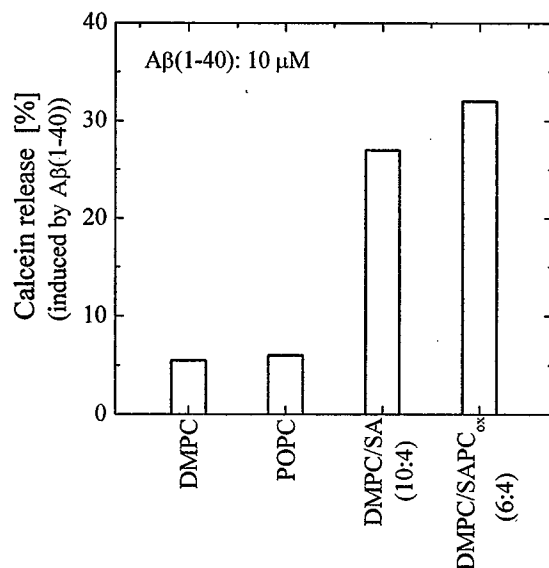


**Fig.4-3** Aβ-liposome interaction evaluated by the calcein leakage.

promoted significantly, whereas the oxidized liposome such as DMPC/SAPC$_{ox}$ (6:4) showed the significant promotional effect of nucleation. Then, the liposome-Aβ interaction was examined by using the calcein leakage experiment. The liposome entrapping calcein as a lipid fluorescence probe is a useful tool to evaluate the interaction strength between the membrane and the target material because the calcein leakage behavior is sensitively proportional to the

target-induced membrane perturbation. As shown in **Fig.4-3**, the release of calcein entrapped inside various liposomes was also observed after the addition of the Aβ(1-40) in order to investigate the Aβ-liposome interaction. The DMPC and POPC liposomes showed the weak interaction, whereas DMPC/SA and DMPC/SAPC$_{ox}$ liposomes showed the significant strong interaction between the liposome and Aβ(1-40). However, it is coarse that the liposome-Aβ interaction could directly result in the rapid nucleation. Therefore, the accumulation of Aβ on the liposome membrane was examined with an IL-QCM developed in chapter 2.

### 3.1.3. Evaluation of Adsorbed Mass of Aβ(1-40) on Liposome

The effect of liposome on the nucleation process may involve at least two steps: (i) accumulation of Aβ monomer on the surface of fibril which leads to critical concentration of Aβ monomer to form nuclei and (ii) the effect on transformation form α-helix structure onto β-sheet structure of Aβ monomer. In order to clarify these possibility, the adsorbed mass of monomeric Aβ(1-40) on the liposome membrane was measured by using immobilized liposome-QCM developed in the chapter 2. The adsorbed mass of Aβ on each liposome
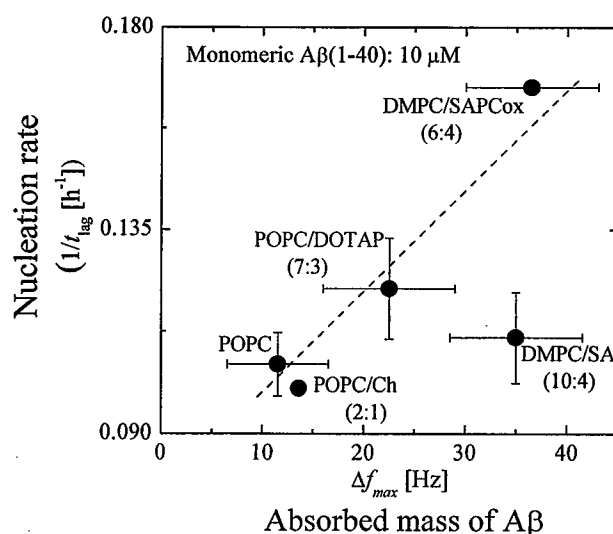
**Fig.4-4** Effect of liposome on nucleation step of Aβ(1-40) fibril formation.

membrane was plotted against nucleation rate for Aβ fibril formation on those liposomes. As shown in **Fig.4-4**, there is a relationship between adsorbed mass of Aβ(1-40) on liposomes and its nucleation rate. The nucleation rate shows the tendency to increase with increasing the adsorbed mass of monomeric Aβ. It may explain the effect of liposome on the nucleation step of Aβ fibril formation through the accumulation of Aβ monomer on its surface and make Aβ easy to form nuclei.membrane was plotted against nucleation rate for Aβ fibril formation on those liposomes. As shown in **Fig.4-4**, there is a relationship between adsorbed mass of Aβ(1-40) on liposomes and its nucleation rate. The nucleation rate shows the tendency to increase with increasing the adsorbed mass of monomeric Aβ. It may explain the effect of liposome on the nucleation step of Aβ fibril formation through the accumulation of Aβ monomer on its surface and make Aβ easy to form nuclei.

## 3.2. Effect of DA on Aβ Fibril Formation

### 3.2.1. DA and Its Derivatives Could Inhibit Aβ Fibril Formation

The prevention of amyloid fibril formation is believed to be a promising strategy for the treatment of AD (Soto *et al.*, 1998). The possibility of prevention of the Aβ fibril formation by DA and its derivatives, such as Catechol, L-DOPA, NE and EP, was confirmed by incubating Aβ monomer in Tris-HCl at 37 °C in the presence and absence of catechol derivatives. The fibrils formation processes were monitored by ThT fluorescence intensity in order to minimize the potential interactions between the dye and catecholamines. The ThT fluorescence was measured immediately after the addition of an aliquot of the incubation sample to the dye. The results were shown in **Fig.4-5**. After 24 h incubation, the ThT fluorescence intensity was high in the solution without catechol derivatives, implying the fibril formation. The fluorescence in the absence of any compounds was set to 100%. However, in the presence of 100 µM catechol derivative compound, the ThT signal did not
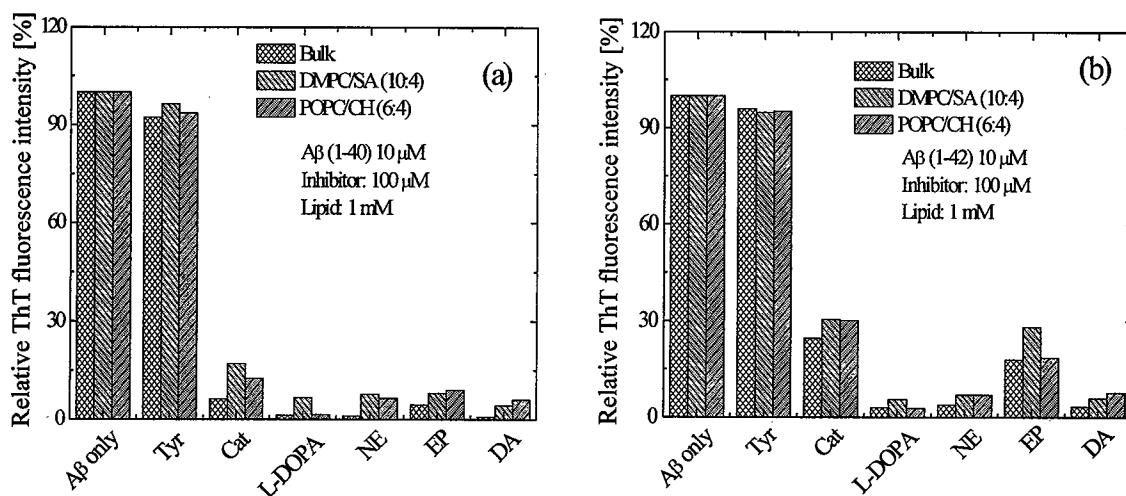
**Fig.4-5** Effect of various compounds on fibril formation of Aβ(1-40) (a) and Aβ(1-42) (b) in the absence and in the presence 1 mM DMPC/SA (10:4) or 1 mM POPC/CH (6:4) liposomes. Aβ fibrils were prepared by incubating 10 μM Aβ monomer in Tris-HCl buffer solution at 37 °C for 24 h Fibril formation was estimated by ThT assay, and the ThT fluorescence intensity in the absence of any compound was set to 100%.

increase, indicating the inhibition of fibril formation. Such effect was also examined in the presence of Tyr. The experiment was also performed by using Tyr as inhibitor. The ThT fluorescence intensity in the solution with and without 100 μM Tyr was similar, indicating that Tyr had no effect on the inhibition of fibril formation. This result suggested that the catechol group was required for the inhibitory effect on the Aβ fibril formation. However, the inhibitory effect of catechol derivative was found to be dependent on its chemical structure. Its dependence on the concentration of catechol derivatives was also investigated. Catechol and its derivatives showed the dose-dependent inhibitory effect on Aβ fibril formation (Data not shown).

In order to compare the inhibitory activity of these compounds, the concentration of these compounds necessary for half-maximal effect ($IC_{50}$) was estimated, the result shows in order: DA < L-DOPA < NE < EP < Catechol for both of Aβ (1-40) and Aβ (1-42) (**Table 4-2**). DA was thus found to show the strongest inhibitory effect against both Aβ (1-40) and Aβ (1-42) fibril formation. Therefore, the DA-induced inhibition of fibril formation was selected for further experiments.

**Table 4-2** The inhibition concentration (IC$_{50}$) of Catechol, DA, L-DOPA, NE and EP for the Aβ(1–40) and Aβ(1-42) fibril formation

| Inhibitor | IC$_{50}$* [μM] | |
|:---:|:---:|:---:|
| | Aβ(1-40) | Aβ(1-42) |
| Catechol | 5.2 | 26.4 |
| DA | ~ 1 | 3.4 |
| L-DOPA | 1.3 | 3.8 |
| NE | 1.4 | 7.4 |
| EP | 2.3 | 8.1 |

* IC$_{50}$ (μM) was defined as the concentration of Catechol, DA, L-DOPA, NE and EP to inhibit the fibril formation to 50% of the control value.

### 3.2.2. Direct Observation of Inhibition of Aβ Fibril Formation by Dopamine

In order to demonstrate the inhibition of Aβ fibril formation by DA, a direct observation of Aβ fibrils was performed with a TIRFM combined with ThT fluorescence (**Fig.4-6**). TIRFM is a useful technique to evaluate a population and a length of fibrils on a quartz slide. As shown in **Fig.4-6(a1)**, a considerable Aβ(1-40) fibrils with 10.2 μm in average length was observed without any inhibitor. The fibrils observed by a TEM were confirmed to possess the micro-structures peculiar to amyloid fibrils (**Fig.4-6(b1)**), consistent with the previous reports (Li et al., 2004). On the contrary, the samples of Aβ monomers co-incubated with 100 μM DA (for 24 h) showed no ThT fluorescence intensity in the observation field of TIRFM, indicating the inhibitory effect of DA on the fibril formation of Aβ (**Fig.4-6(c1)**). At a microscopic observation with TEM, the Aβ fibrils could not be observed and small amorphous aggregates were observed in the samples of 10 μM Aβ monomers co-incubated with 100 μM DA for 24 h (**Fig.4-6(d1)**). The similar results were obtained for Aβ(1-42) as shown in **Fig.4-6(a2-d2).** The samples of Aβ(1-42) monomers
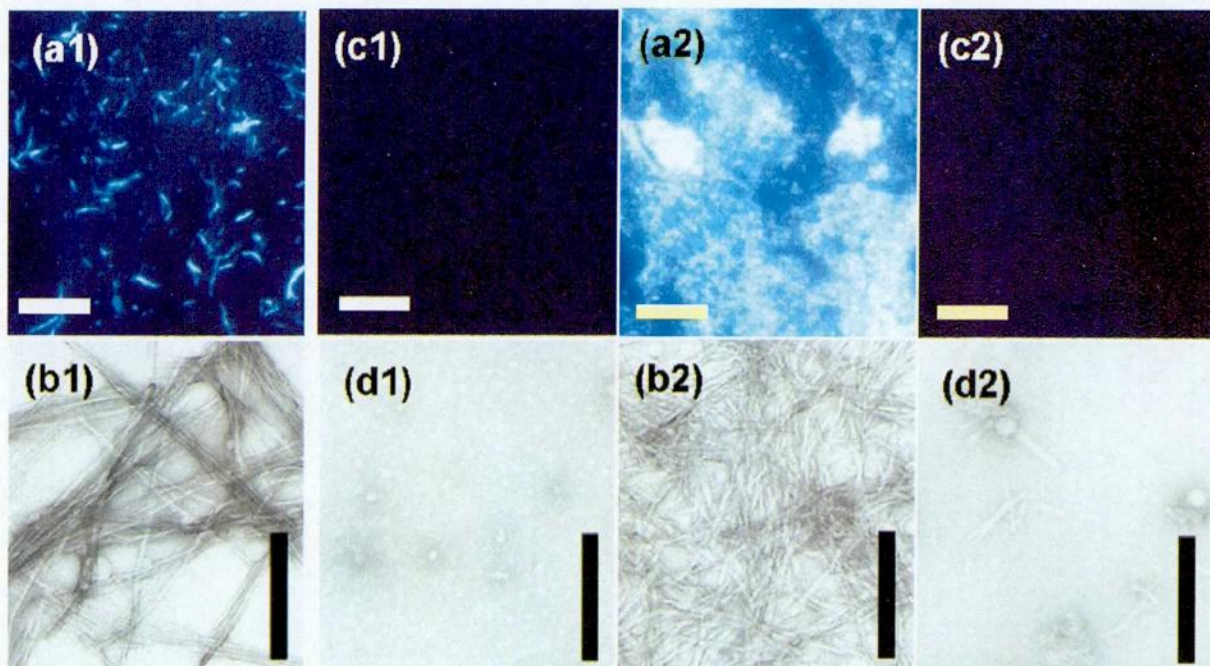
103

**Fig.4-6** The direct observation with two different microscopic techniques. The TIRFM images (scale: 10 μm) of fibrils formed in the absence of DA (a1, a2) and in the presence of 100 μM DA (c1, c2) for Aβ(1-40) and Aβ(1-42), respectively. The TEM images (scale: 200 nm) of fibrils formed in the absence of DA (b1, b2) and in the presence of 100 μM DA (d1, d2) for Aβ(1-40) and Aβ(1-42), respectively. Aβ fibrils were prepared by incubating 10 μM Aβ monomer in Tris-HCl buffer solution at 37 °C for 24 h.

co-incubated with 100 μM DA (for 24 h) showed a slight ThT fluorescence intensity in the observation field of TIRFM (**Fig.4-6(c2)**) and a few very short fibrils coexisting with small amorphous aggregates were obtained by TEM (**Fig.4-6(d2)**), indicating that the DA also shows the inhibitory effect on Aβ(1-42) fibril formation. It is thus considered that DA could inhibit the fibril formation of Aβ.

*3.2.3. Effect of DA on the Kinetics of Aβ Fibril Formation*

The ThT fluorescence intensity was measured during the fibril formation (**Fig.4-7**) in order to investigate the effects of DA on the kinetics of Aβ fibril formation. The control experiment was performed by incubating 10 μM Aβ monomers without any inhibitor. The time-course of ThT fluorescence intensity was measured and shown in the **Fig.4-7**. As shown

in the **Fig.4-7(a)** and **(c)**, the presence of 5 μM DA induced decrease in ThT intensity compare to control samples (without DA) and the presence of 100 μM induced inhibit completely Aβ fibril formation. The inhibition of Aβ fibril formation by DA may involve two broadly different mechanisms, in inhibition of either a nucleation process or an elongation process. In order to clarify whether DA could inhibit a nucleation process or elongation process or both of these processes, the effect of DA on kinetic of Aβ fibril formation was investigated by using the seeds of Aβ fibrils. The seeds were added to Aβ monomer solution
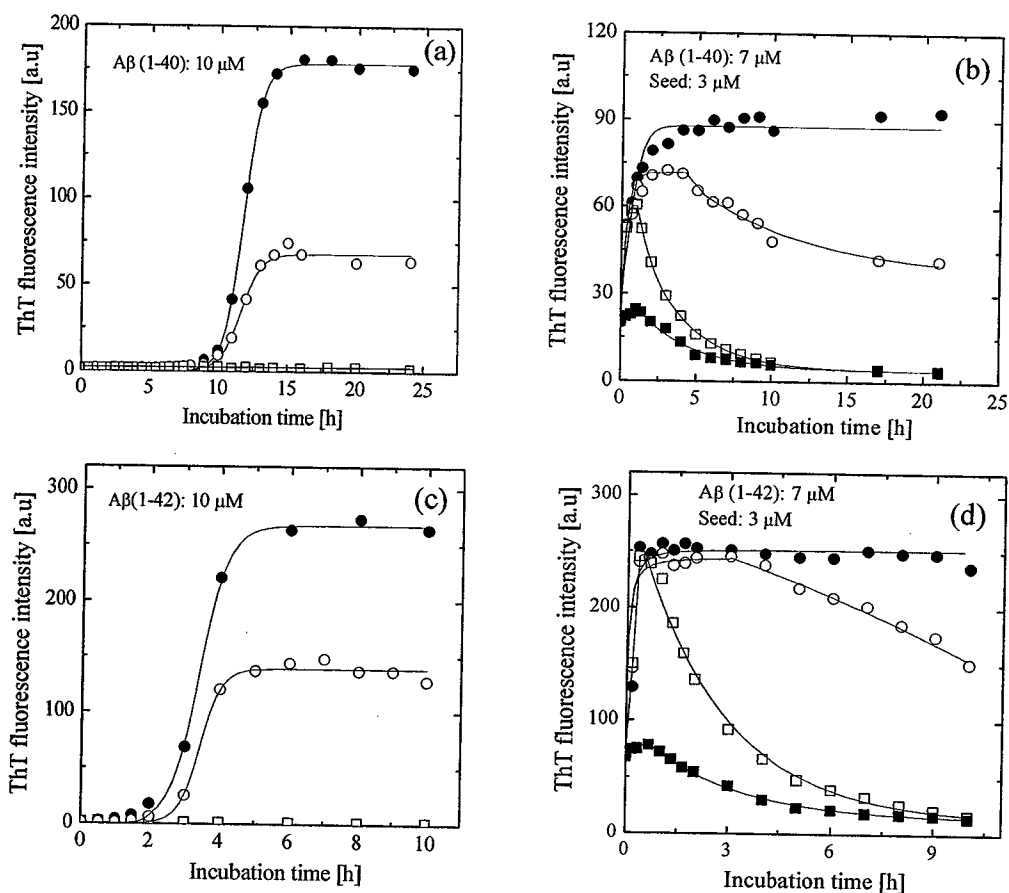


**Fig.4-7** Effect of DA on kinetics of Aβ fibril formation. The time-course of the ThT fluorescence during Aβ(1-40) (a) and Aβ(1-42) (c) fibril formation without DA (*filled circles*) and with 5 μM DA (*open circles*), with 100 μM DA (*open squares*) from Aβ monomer solutions. The time course of the ThT fluorescence during Aβ(1-40) (b) and Aβ(1-42) (d) fibril formation without DA and with 5 μM, 100 μM DA, from 7 μM Aβ monomer and 3 μM Aβ seed solution. Aβ seed + Aβ only (*filled circles*); Aβ seed + Aβ monomer + 5 μM DA (*open circles*); Aβ seed + Aβ monomer + 100 μM DA(*open squares*); Aβ seed + 10 h pre-incubated solution containing 100 μM DA and 7 μM Aβ monomer (*filled squares*). All the solution were prepared in Tris-HCl buffer solution and incubated at 37 °C.

to make the final concentrations of seeds and monomers at 3 μM and 7 μM, respectively. The kinetic of Aβ fibril formation in the presence of seeds were also measured and shown in the Figs.4-7(b) and (d) for Aβ(1-40) and Aβ(1-42), respectively. In the absence of DA, the fluorescence intensity significantly increased without a lag phase and reached to plateau more rapidly in contrast to the sample without seeds. These curves are consistent with the previous first-order kinetic model (Naiki et al., 1996). The addition of seeds to the monomer solution in the presence of 5 μM DA also shows the similar increase of the ThT fluorescence intensity to the case in the absence of DA. The elongation of Aβ(1-40) fibrils was induced up to 4 h. The addition of 100 μM DA could not inhibit the elongation up to 1 h or in the presence of seeds (Fig.4-7(b)) although 100 μM DA could completely inhibit the spontaneous Aβ fibril formation (Fig.4-7(a)). The initial rate in ThT fluorescence intensity (apparent elongation rate) was similar in the experiments with 5 and 100 μM of DA. It is thus considered that the DA did not inhibit the elongation process of Aβ fibril formation and that DA inhibited the nucleation process in the fibril formation of Aβ(1-40). The similar results were obtained for Aβ(1-42) (Fig.4-7(d)). From the results, it is considered that DA inhibits the nucleation process, rather than the elongation process. The decrease in ThT fluorescence intensity may be resulted from the disaggregation of Aβ fibrils induced by DA. Both the decrement in ThT intensity and the transition time from elongation phase to disaggregation phase depend on the concentration of DA, which strongly supports the DA-induced disaggregation of fibrils.

### 3.2.4 Proposed Mechanism of DA Inhibition of Aβ Fibril Formation

The obtained results clearly show that the DA could inhibit the Aβ fibril formation. The remaining problem is the mechanism responsible for the inhibition of amyloid fibril formation. It has been reported that, for inhibition of α-synuclein fibril formation, the oxidized product of DA (DA-quinone, DAQ) stabilized the protofibrils of α-synuclein,

leading to an inhibition of fibril formation, where 5-10% of the α-synuclein molecules formed a covalent adduct with DAQ by a reaction of DAQ with Tyr of α-synuclein (Conway *et al.*, 2001; Li *et al.*, 2004). In the other chemical compounds, it has been reported that the formation of a Schiff-base between quinone group of inhibitory compounds and Lys-side chain of α-synuclein induced the inhibition of fibril formation (Zhu *et al.*, 2004; Kobayashi *et al.*, 2006). On the other hands, a nucleophilic attack of DAQ to Lys (Lys forming a Schiff base with DAQ) is also considered as another possible mechanism to form the complex formation between proteins and compounds (Conway *et al.*, 2001; Li *et al.*, 2004). It is therefore supposed that the oxidized product of catechol derivatives (catechol quinone and its derivatives) bound to Aβ monomer to form the covalent adduct-like complex. The effect of DA on the secondary structure of Aβ monomer was investigated though the circular dichroism measurement. **Figure 4-8(a)** shows that the structure of DAQ-Aβ(1-40) complex (incubated for 24 h) was similar to that of Aβ(1-40) monomer, suggesting that DA/DAQ retains the secondary structure of Aβ. Therefore, the catechol ring of catechol derivatives as a common
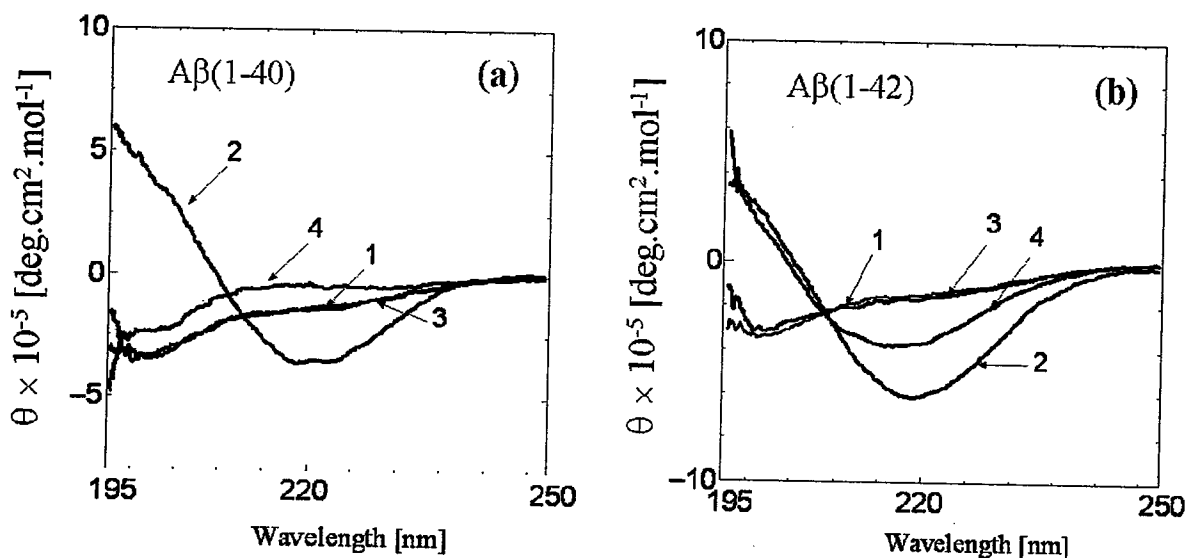


**Fig.4-8** CD spectra of Aβ(1-40) (a) and Aβ(1-42) (b) at the beginning (0 h) and the end (24 h) of incubation in the absence and the presence of 100 μM DA. Aβ only at 0 h (curve 1), Aβ only at 24 h (curve 2); Aβ and 100 μM DA at 0 h (curve 3); and Aβ and 100 μM DA at 24 h (curve 4). The solutions were prepared by incubating 10 μM Aβ monomer on PBS buffer pH 7.4 at 37 °C.

chemical structure might contribute to their interaction with Aβ. The sequence of Aβ(1-40) and Aβ(1-42) involves two Lys residues (Lys[16] and Lys[28]) (Petkova *et al.*, 2002). It is therefore likely that the DA-quinone could forms a Schiff-base with Aβ molecule although no direct evidence has not been obtained. This conjugated adduct might stabilize the disordered conformation and be advantageous for a prevention of the conversion to a β-sheet-rich structure. The addition of seeds to a 10 h pre-incubated sample of 7 μM Aβ monomer and 100 μM DA inhibited the formation of intermediate of Aβ fibrils (closed square in **Figs.4-7(b)** and **(d)**). No increase in ThT fluorescence intensity was observed, strongly suggesting that the conjugated adduct has the structure disadvantageous for a binding to the seeds for fibril growth. The similar results were obtained for inhibition of Aβ(1-42) fibril formation but the effect of DA on Aβ(1-42) fibril formation was less than that of Aβ(1-40) (**Table 4-2** and **Fig.4-8(b)**). Aβ(1-42) has been reported to show the higher propensity to form fibrils by showing the shorter lag time as compared with that of Aβ(1-40). Therefore, this data also confirmed the inhibitory effect of DA on the nucleation process rather than the elongation process.

### 3.2.5. Effect of Liposome on Dopamine Inhibit Aβ fibril formation

In the presence of liposome membranes, the DA prefers to partition(adsorb) into the liposome membrane (as shown in the chapter 1). Otherwise, as shown in the **section 3.1.2**, the liposomes could modulate the Aβ fibril formation. Therefore, the liposomes may affect on both of DA concentration and Aβ fibril formation, and may affect on the DA-monomeric Aβ interaction in term of inhibitory activity of DA for Aβ fibril formation. In order to investigate the influence of liposomes on inhibitory effect of DA, the serial experiment was performed. The inhibitory activity of DA (defined as $IC_{50}$-**Fig.4-9(a)**) for Aβ fibril formation was investigated in the presence of 0.5 mM several kinds of liposomes. As shown in **Fig.4-9(b)**, for the switterionic liposomes, the influence of liposomes on inhibitory activity of DA is not

so strong athought these liposomes showed influences on both of DA and Aβ fibril formation. In contrary, the charged liposomes show strong effect on inhibitory activity of DA on Aβ fibril formation by showing very high IC50 values of DA. These rerults may cause from electrostatic interaction of liposome surface with positively charge DA (Tuckerman *et al.*, 1959) and negatively charge Aβ(1-40) (Kuboi *et al.*, 2006) at pH 7.4. In the presence of negatively charge POPA liposomes, DA could be enhanced on surface of POPA liposomes where Aβ monomers look like difficult to adsorb on. Inveserly, Aβ monomers interact very strong with positively charge DOTAP liposomes' surface and rapidly formation of fibrils, where DA is difficult to bind. Althought DA and Aβ could bind to each other because of their charge properties. In the presence of liposomes with high concentration compare to that of DA and Aβ monomers, the strong electrostatic interaction in the presence of liposomes may induce separation of DA from Aβ monomers leading to decrease inhibitory activity of DA.
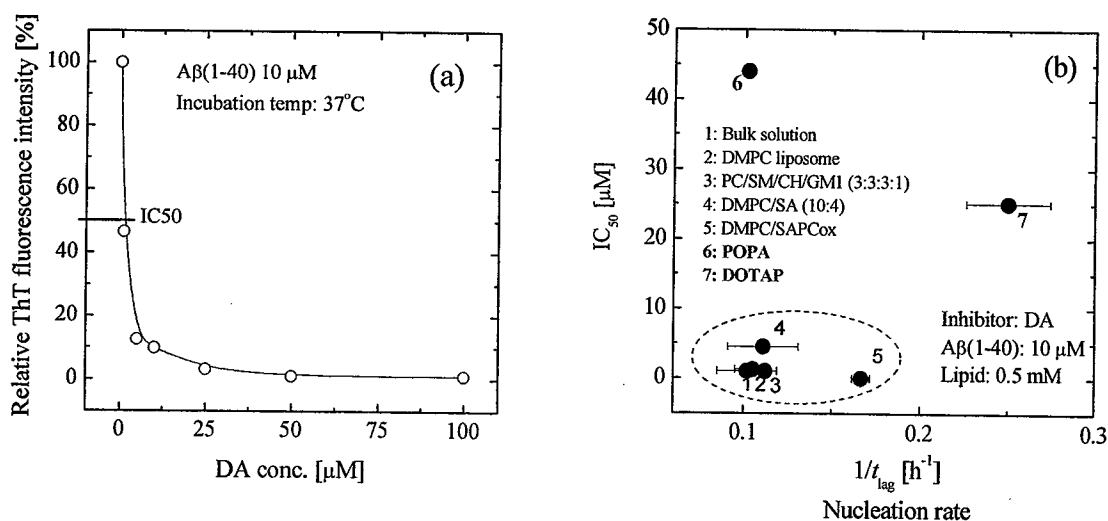


**Fig.4-9** Effect of liposome on inhibitory effect of DA (IC50) for Aβ(1-40) fibril formation.

## 3.3. Dopamine Disaggregate Aβ Fibril – Effect of Liposomes

### 3.3.1. Dopamine and Its Derivatives Induced Destabilization of Aβ Fibrils in the Absence and Presence of Liposomes

As shown in the **Figs.4-7(b)** and **(c)**, the decrease in ThT fluorescence intensity may be resulted from the disaggregation of Aβ fibrils induced by DA. Therefore, the effect of DA and its derivatives on stabilization of DA were performed. The addition of DA or its derivatives onto Aβ fibril solution to final concentration of 100 μM was performed. The time-course of the ThT fluorescence intensity was monitored and shown in **Fig.4-10(a)**. As can be seen in **Fig. 4-10(a)**, the ThT fluorescence intensity significantly decreased in the presence of 100 μM DA or its derivatives. On the contrary, no significant decrease in ThT fluorescence intensity was observed in the presence of 100 μM Tyr, indicating that Tyr had no effect on the Aβ fibrils (data not shown). These results suggest that the catechol group is necessary for the disaggregation both of Aβ(1-40) and Aβ(1-42) fibrils. Furthermore, the disaggregation activity of these compounds on Aβ fibrils was examined in the presence of fatty acid-containing domain-like liposomes (DMPC/SA (10:4 in molar ratio)) as a model biomembrane. Since DMPC/SA liposomes can interact strongly with Aβ fibrils (Avudulov *et al.*, 1996), the additive effect of liposomes can be expected. **Figure 4-10(a)** showed that a significant enhancement effect for disaggregation was observed in the case of dopamine (DA) and L-DOPA except for catechol (Cat), noepinephrine (NE) and epinephrine (EP). Furthermoe, the apparent disaggregation rate constant, $k_d$, was analyzed with a first-order kinetic analysis using equation (4-1). In the case of Cat, NE, and EP, the $k_d$ value was $(23 \sim 38) \times 10^{-6}$ $s^{-1}$ **(Fig.4-10 (b))**. It is obvious that the addition of liposomes raised the $k_d$ value in the case of DA and L-DOPA. From these results, DA among various catechol derivatives was found to show the strongest effects. In the following, the DA-induced disaggregation of fibrils was further investigated.

It has been reported that the oxidative product of DA and other catecholamines are

major factors for inhibit fibril formation (Li *et al.*, 2004) and the Schiff-base formation between catechol-quinone group of oxidative product of catecholamines and Lys residues of protein was proposed to be the key factor for inhibition of fibril formation. Therefore, it is proposed that schiff-base formation may be a key factor for disaggregation of Aβ fibril. Therefore, in this experiment, the effect of oxidative product of DA (DA-quinone) on Aβ(1-40) fibril disaggregation was investigated and was compared with that of DA. The oxidation
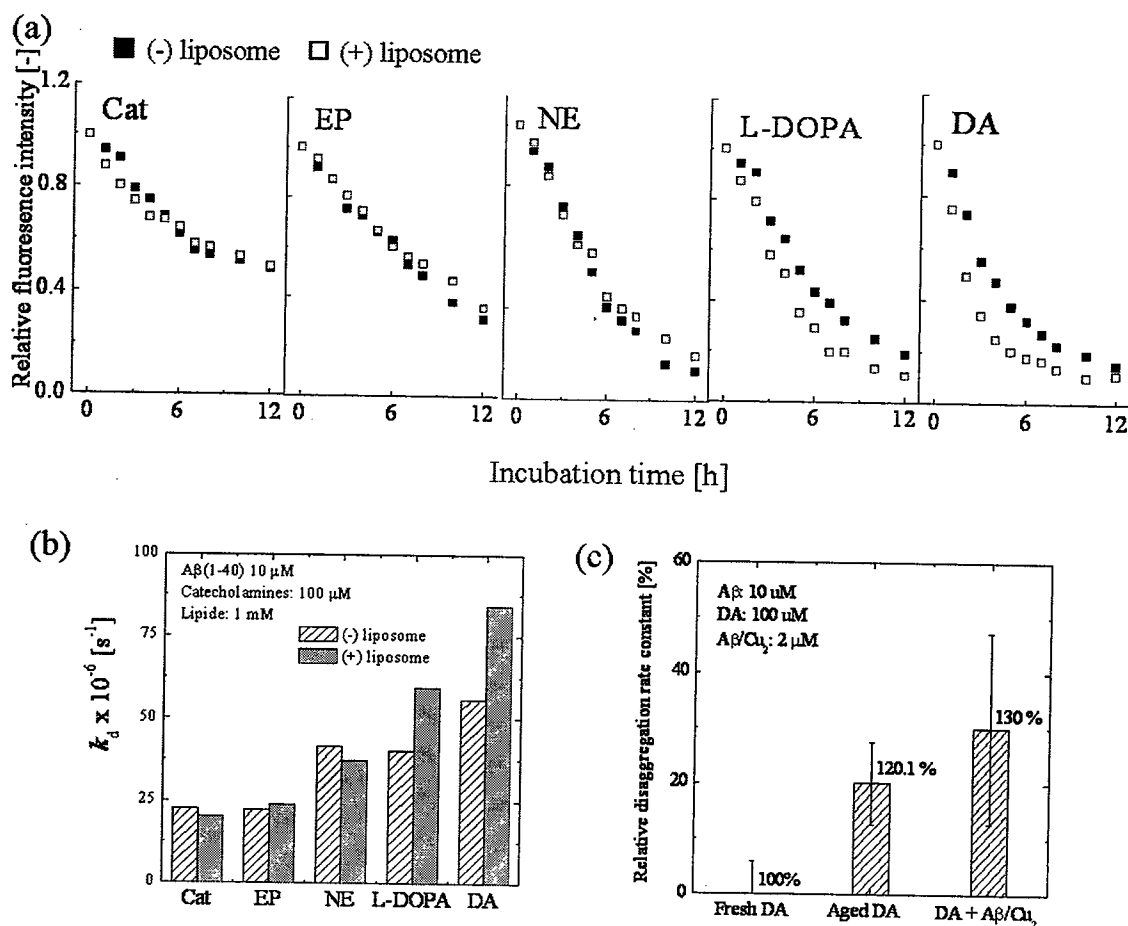


**Fig. 4-10** (a) Time-course of ThT fluorescence intensity in the presence and the absence of liposome. (b) Disaggregation rate constant for Aβ(1-40) fibrils in the absence and the presence of liposome. Aβ fibrils were prepared by incubating 10 μM Aβ monomer solution at 37 °C for 24 h in Tris-HCl buffer containing 100 mM NaCl, pH 7.4. Aβ(1-40) (10 μM) and DMPC/SA (10:4) liposome with 100 nm in diameter (1 mM) were used. All the experiments were performed at 37 °C. (c) Comparison of DA and oxidation product of DA on disaggregation of Aβ fibrils. Oxidation product of DA was prepared either incubation at 37 °C for 12 h in aerobic condition for auto-oxidation or oxidation by Aβ/Cu complex. All experiments were performed at 37 °C.

product of DA was prepared either incubation at 37 °C for 12 in aerobic condition for auto-oxidation or oxidation by Aβ/Cu complex. As shown in **Fig.4-10(c)**, the oxidation product of DA, DA-quinone, expresses higher activity on disaggregation of Aβ fibril. It could be conclude that oxidation product of DA is major factor for disaggregation of the Aβ fibril. Athough this result is not enough evidence; it may support the above proposal.

Form view point of the DA, the effect of liposomes on enhancement of disaggregation of Aβ fibrils by DA may be explained by following: *(i)* enhancement of DA concentration by partitioning (adsorbtion) on the liposome membrane (**Table 1-5**) where Aβ was reported to strongly interact with (Avdulov *et al.*, 1997), and (ii) enhancement of DA-oxidation to form DA-quinone (**Fig.1-10**) which showed higher activity on disaggregation of Aβ fibrils than that of DA.

As shown in **Table 4-3**, an apparent rate constant, $k_d$, of disaggregation was estimated according to equation (4-1) to be $(5.07\pm0.2)\times10^{-5}$ s$^{-1}$ and the $k_d$ for Aβ(1-42) fibrils was $(8.05\pm0.2)\times10^{-5}$ s$^{-1}$. Aβ(1-42) fibrils showed larger $k_d$ value than Aβ(1-40) fibrils, which may be induced by the difference on the values of molecular weight per length value of Aβ(1-40)

**Table 4-3** Summary of disaggregation behavior of Aβ(1-40) and Aβ(1-42) fibrils induced by DA

| | | Aβ(1-40) | Aβ(1-42) |
|---|---|---|---|
| Molecular weight per length [kDa/nm] | | 30.3 | 19 |
| DA-induced disaggregation rate constant, $k_d$ [s$^{-1}$] | No liposome | 50.74 | 80.45 |
| | With liposome DMPC/SA(10:4) | 84.26 | 152.92 |
| D$_2$O isotope effect, $k_{D2O}/k_{H2O}$ [-] | No liposome | 0.42±0.01 | 0.60±0.05 |
| | With liposome DMPC/SA(10:4) | 0.35±0.01 | 0.51±0.01 |

and Aβ(1-42) were estimated to be 30.3 kDa/nm (Petkova *et al.,* 2005) and 19 kDa/nm

(Antzutkin *et al.,* 2002), respectively, and by the difference in conformation of fibrils between

double layered structure with in registered parallel β-sheet of Aβ(1-40) (Petkova *et al.,* 2002)

and in registered parallel β-sheet of Aβ(1-42) (Antzutkin *et al.,* 2002), which has been

clarified with a solid-state NMR experiments. These findings suggests that the Aβ(1-40)

fibrils indicated the solid-like nature as compared with Aβ(1-42) fibrils. It is, therefore,

considered that the DA could disaggregate the Aβ(1-42) fibrils faster than Aβ(1-40) fibrils.

*3.3.2. Direct Observation of Aβ Fibril Disaggregation in the Absence and the Presence of*

*Liposomes*

In order to demonstrate the disaggregation of Aβ fibril by DA, the direct observation

was performed with TIRFM combined with ThT fluorescence and TEM. A 10 μM Aβ(1-40)

fibrils were incubated with 100 μM DA at 37 °C. The TIRFM images showed the progressive

loss of 10 μM Aβ(1-40) fibrils in the presence of 100 μM DA **(Figs.4-12(a1)-(a3))**. The fibrils

almost disappeared after 6 h of the incubation **(Fig.4-12(a3))**, indicating the completed

disaggregation of Aβ fibrils by DA. These results provide the strong evidence for the DA-

induced disaggregation of Aβ fibrils. However, the remaining Aβ fibrils, at 6 h later, was

unclear. Then, the microscopic structure of these aggregates was confirmed with a TEM

observation. TEM images of the aggregate at each period were shown in **Figs.4-11(b1)-(b3)**.

At 2 h later after the DA addition, many short fibrils with several hundreds nm in length were

observed **(Fig.4-11(b2))** and at 6 h after DA addition, not only the length but also the number

of fibrils decrease significantly, indicating the disaggregation of Aβ fibrils by DA. On the

other hands, the presence of DMPC/SA liposome promoted the disaggregation of fibrils

**(Figs.4-11(c1)-(c3))**. Especially, the magnification of TEM image gave the insight that the

DA-induced disaggregatin of fibrils was induced by their fragmentation, not only by the

dissolution from the both ends (see arrows in **Fig.4-11(c3)**).

In order to confirm the DA-induced disaggregatin from the viewpoints of fragmentation, the size distribution of fibrils was monitored. **Figure 4-12** shows the TEM images on fragmented fibrils by DA. In the case of disaggregatin of fibrils by DA, the size distribution showed the 40 to 60 nm in length (**Figs.4-12(a)** and **(b)**). Meanwhie, the mean length of fragmented fibrils by an ultrasonication was 100 nm or so (**Fig.4-12(c)**). These
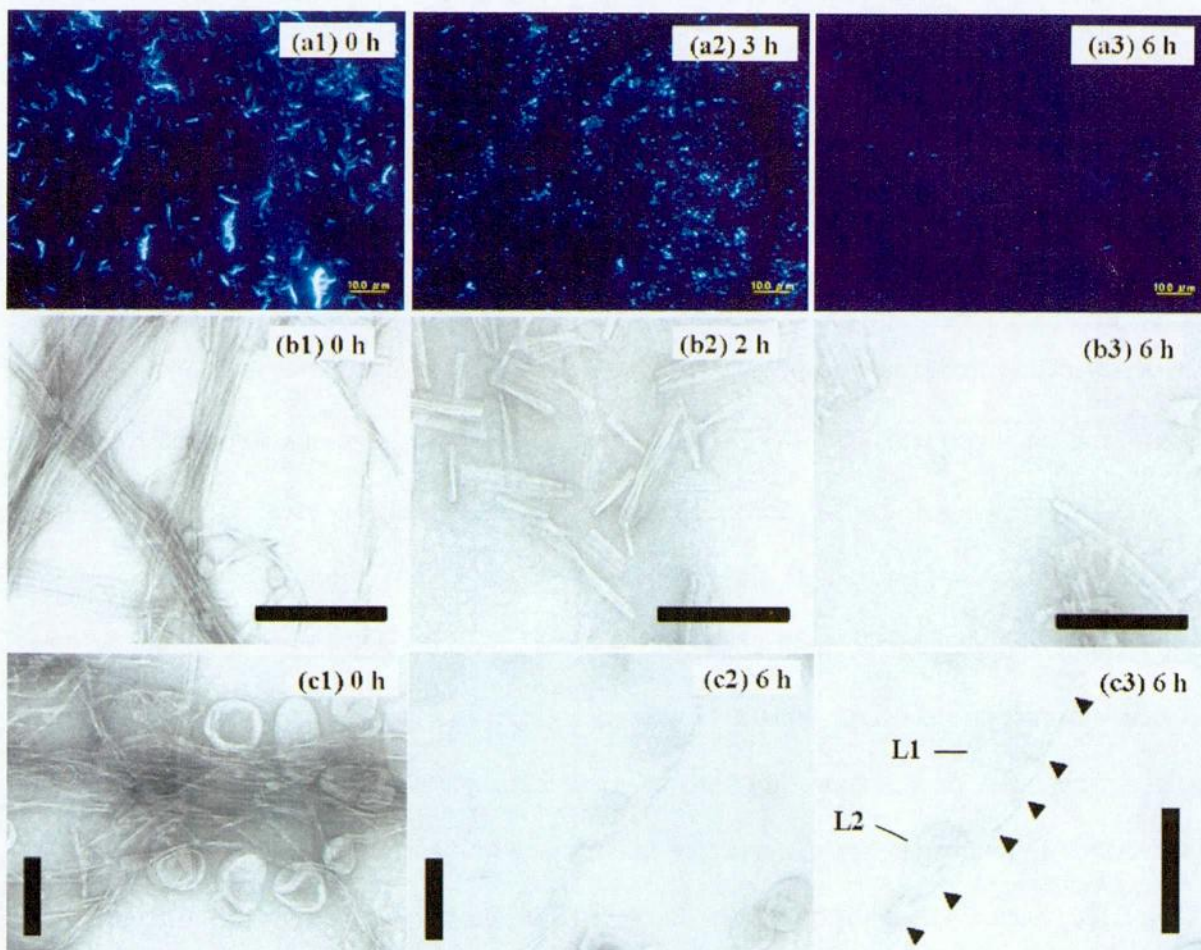


**Fig.4-11** Direct observation of disaggregation of Aβ fibrils by DA in the absence and the presence of DMPC/SA (10:4) liposome. (a) Disaggregation of fibrils of Aβ(1-40) monitored by TIRFM (scale 10 μm). The preformed fibrils of Aβ were incubated in the presence of 100 μM DA at 37 °C for (a1) 0 h, (a2) 3 h, and (a3) 6 h. (b) Disaggregation of fibrils of Aβ(1-40) monitored by TEM (scale 200 nm). The preformed Aβ fibrils were incubated in the presence of 100 μM DA at 37 °C for (b1) 0 h, (b2) 2 h, and (b3) 6 h. (c) Disaggregation of fibrils of Aβ(1-40) monitored by TEM for (c1) 0 h, (c2) 6 h, and (c3) its magnification. Arrows indicates the fragmentation sites of fibrils. L1 and L2 indicate DMPC/SA liposomes.
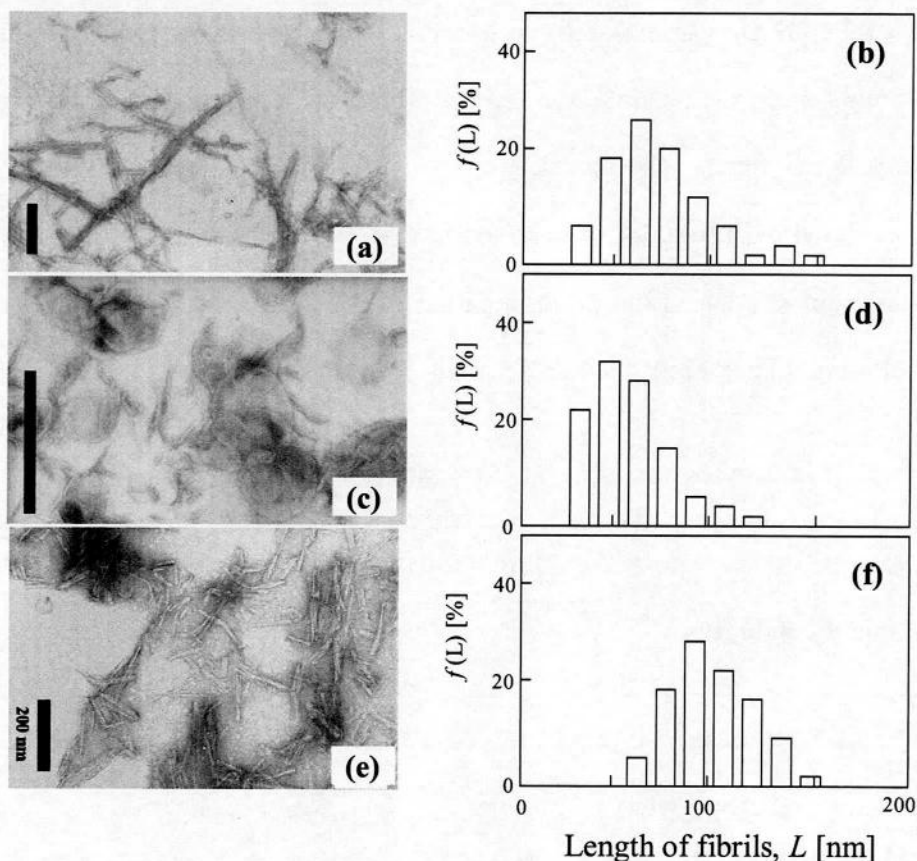
**Fig.4-12** TEM images of fragmented Aβ(1-40) fibrils and their length distribution. (a, b) Fibrils disaggregated by DA for 6 h at 37 °C. (c, d) Fibrils disaggregated by DA in the presence of 1 mM DMPC/SA (10:4) for 6 h at 37 °C. (e, f) Fibrils sonicated for 2 min. Aβ fibrils were prepared by incubating 10 μM of monomeric Aβ(1-40) in 50 mM Tris-HCl buffer (100 mM NaCl, pH 7.4) at 37 °C for 24 h.

indicated that DA-treated disaggregation was obviously different from the conventional fragmentation process.

Secondly, the existence of DMPC/SA liposome resulted in the effective disaggregation (40 nm and 60 nm in mean length of fibrils). As shown in **Fig.4-11(c3)**, DMPC/SA liposomes might play role for the field of the fragmentation of fibrils since the DA molecule favors the partition to lipid membrane as described in chapter 1.

### 3.3.3. Liposomes-Regulated Disaggregation of Aβ Fibrils

In order to understand the role of liposomes on the disaggregation of Aβ fibrils,

various liposomes were systematically prepared, where the prepared liposomes include normal liposomes, charged liposome and oxidized liposomes. The effect of liposomes on the disaggregation of Aβ fibrils was investigated in order to evaluate the disaggregation rate constant, $k_d$, as shown in **Table 4-4**. It was found that, the addition of the different liposomes showed the different effects on the disaggregation of Aβ fibrils by DA. In brief, the normal liposome (including single lipid or micro-domain liposome) enhanced the disaggregation of

**Table 4-4** Effect of liposomes on disaggregation rate constant

| Experiment conditions | | Membrane properties | | $k_d[s^{-1}]\times10^{-6}$ | |
|---|---|---|---|---|---|
| | | $m_{lip}[-]$ | $Z/A^*$ $[Q.nm^{-2}]$ | Aβ(1-40) | Aβ(1-42) |
| **DA only** | | | | 50.74±5.7 | 80.45±7.92 |
| **DA + liposome** | | | | | |
| Normal liposomes | 1 | POPC/SM (7:3) | 0.030 | | 53.75 | 92.93 |
| | 2 | PC/SM/CH (4:3:3) | 0.043 | | 66.84 | 97.65 |
| | 3 | PC/SM/CH/GM1 (3:3:3:1) | 0.070 | | 60.87 | 94.12 |
| | 4 | POPC | 0.024 | 0 | 69.45±6.90 | 102.60±7.52 |
| | 5 | POPC/Ch (6:4) | 0.033 | | 61.30±8.10 | 106.04±7.10 |
| | 6 | DMPC | 0.0024 | 0 | 62.59±2.70 | 106.71±4.20 |
| | 7 | DMPC/SA (10:2) | N.Y** | | 64.22±1.74 | 150.48±4.82 |
| | 8 | DMPC/SA (10:4) | 0.065 | | 84.26±1.20 | 152.92±10.51 |
| Oxidized liposomes | 9 | DMPC/SAPC$_{ox}$ (6:4) | 0.081 | 0 | 115.74±11.40 | 168.54±12.7 |
| | 10 | DMPG/SAPC$_{ox}$ (6:4) | 0.074 | -0.84 | 164.90±8.23 | 160.35±7.65 |
| Charged liposomes | 11 | POPA | N.Y | -1.40 | 76.96 | 105.24 |
| | 12 | DOTAP | N.Y | +1.40 | 34.40±2.41 | 54.5±4.54 |
| | 13 | POPC/DOTAP (7:3) | N.Y | +0.42 | 42.35±3.71 | 68.06±4.67 |

* Surface charge density of liposomes was calculated assuming unilamellarity, spherical shape, a bilayer thickness of 3.7 nm (Tahara et al., 1994), and a mean head group area of 0.72 nm² (Tazan et al., 1996), and considering that the head group of POPG; POPA and DOTAP are fully ionized at pH 7.4 (Vechettt et al., 1997). **N.Y: Not yet evaluated.
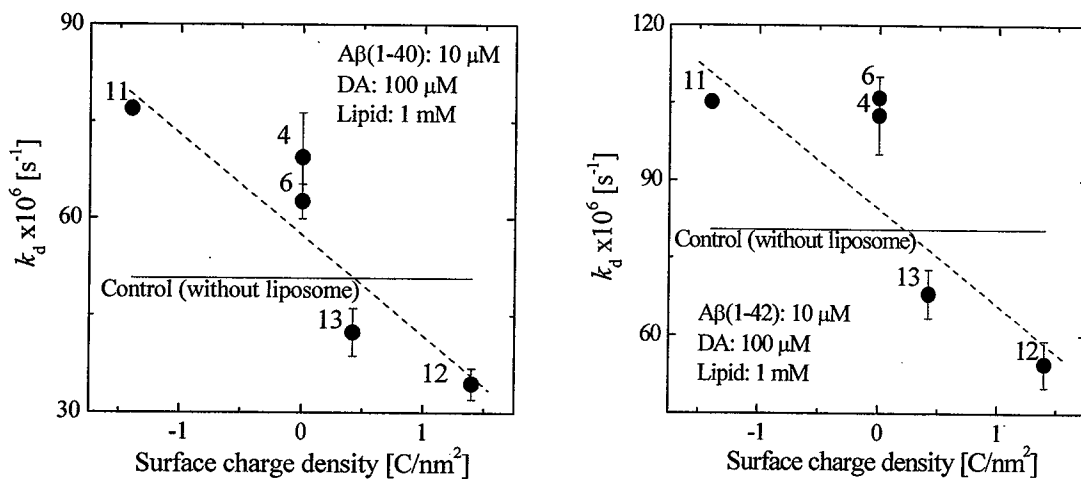
**Fig.4-13** Effect of surface charge density of liposome on disaggregation of Aβ fibrils. The liposomes were numbered as shown in the **Table 4-4**.

Aβ fibrils and the disaggregation process was enhanced significantly in the case of oxidized liposomes. The addition of the charged liposomes showed an opposite effect on the disaggregation of Aβ fibrils. The anionic liposome could enhance the disaggregation process while the cationic liposomes suppressed. Therefore, the effect of liposome may be contributed by both of hydrogen bond stability of liposome ($m_{lip}$) and surface charge density of liposomes. The effect of surface charge density of liposomes was also analyzed. **Figure 4-13** shows the effect of surface charge density of liposomes on the disaggregation rate constant, implying that the electrostatic interaction may play very important role for the liposome effect. It is well known that, at pH 7.4, DA mainly exists as a cationic form (Tuckerman *et al.*, 1959). Therefore, the DA concentration could be enhanced on the surface of the negatively-charged liposome and could be reduced on the surface of positively-charged liposomes because of the electrostatic interaction.

Furthermore, the effect of liposome on the disaggregation of Aβ fibrils was plotted as the function of membrane properties - hydrogen bond stability of liposome ($m_{lip}$) as shown in **Fig.4-14**. The addition of liposomes could enhance the disaggregation of Aβ fibrils by DA in the range of $m_{lip} > 0.06$. This may be considered by the following effects: (i) a contribution of

hydrated water against a stabilization of hydrogen bonds inside Aβ fibril, which has been reported to be key factor for stabilization of Aβ fibrils (Fernandez *et al.*, 2002) and (ii) the enhancement of DA concentration on liposome membrane in which Aβ fibrils have been reported to favor the interaction (Kremer *et al.*, 2003). As for the case (i), the liposome membrane with the high $m_{lip}$ value is considerably hydrated at around $PO_2^-$ as described in chapter 2.

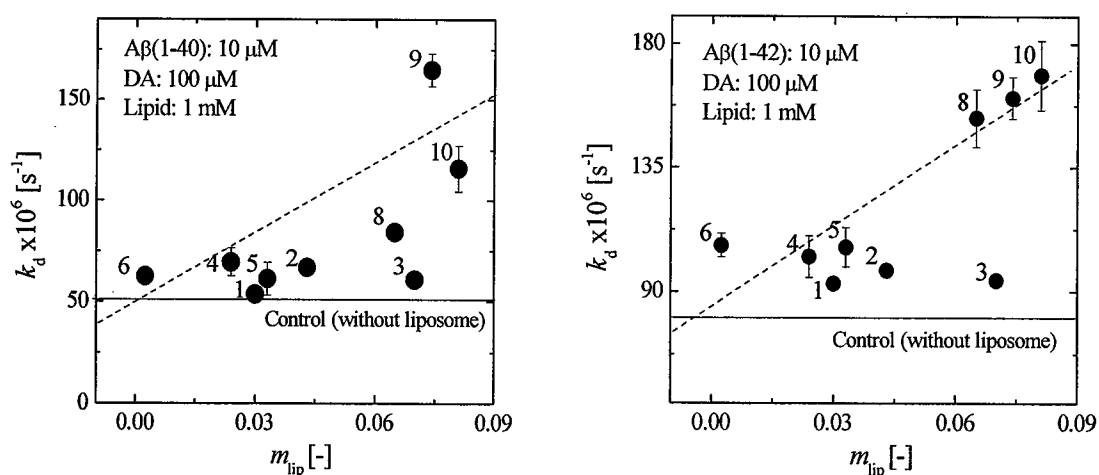The possibility of the enhancement of DA concentration on liposome membrane was



**Fig.4-14** Disaggregation rate constant of Aβ fibrils in the presence of various liposomes. Correlationship of membrane property ($m_{lip}$) and disaggregation rate constant. The liposomes were numbered as shown in the **Table 4-4**.
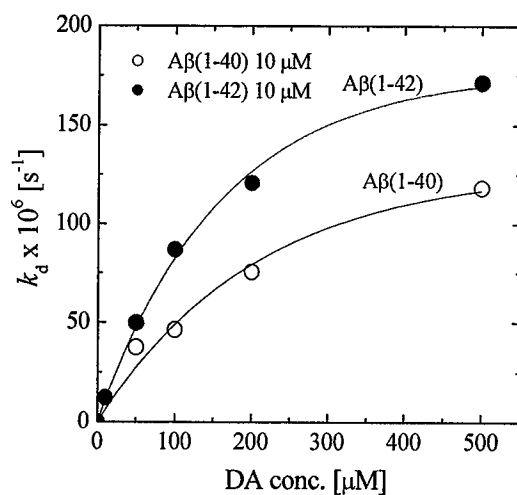


**Fig.4-15** Dependence-DA concentration on disaggregation rate constants of Aβ fibrils.

118

already shown in the chapter 1 (**Fig.1-8**), where the higher concentration of DA leads to higher disaggregation rate constant (**Fig.4-15**). **Figure 4-15** shows the effect of the DA concentration on the disaggregation rate constant. The $k_d$ value monotonously increased with the DA concentration from 10 µM up to 500 µM. This result will also support the explanation on the effect of surface charge of liposome at various disaggregation rate constant of Aβ fibrils by DA.

### 3.3.4. Proposed Mechanism of Disaggregation of Aβ Fibril Induced by Dopamine

Previous study indicates that the bound water to the liposome membrane promoted the enzymatic hydrolysis reaction on the liposome membrane (Yamamoto *et al*, 1995). The bound water might be effective for the disaggregation of fibrils. The bound water to DMPC (un)modified the stearic acid (SA) was then investigated since SA preferably binds to Aβ fibril (Avdulov *et al.*, 1997). The liposome membrane includes the waters bound to the phosphoester group ($PO_2^-$) (Yamamoto *et al.*, 1995). The peak shift of $PO_2^-$ antisymmetric stretching band observed at around 1230 cm$^{-1}$ to lower frequency corresponds well with the increase in the bound water (Yamamoto *et al.*, 1995). **Figure 4-16** indicated that the peak for DMPC/SA shifted to lower frequency with increasing the SA molar ratio, suggesting that the SA could pool the bound water within liposome membranes. In the experiment with a dielectric dispersion analysis, the relaxation times of bulk water and bound water could be also estimated (Klosgen *et al.*, 1996). The activation energy $\Delta E$ was estimated to be 22 kJ/mol for bulk water and 31.8 kJ/mol for bound water according to Arrhenius's law: $(2\pi\tau)^{-1} = A \exp(-\Delta E/RT)$ (Klosgen *et al.*, 1996). The $\Delta E$ value indicates the extent of polarization of O-H bond in water molecule because the strong polarization along O-H bond results in the increase in intermolecular interaction between water molecules (Klosgen *et al.*, 1996). The O-H bond in bound water is strongly polarized by its binding to phospholipid. It is considered that the bound water with strong polarization along O-H bond is advantageous to attack the HBs

119

within fibrils. Thus, the bound water is anticipated to be "*active*" water in contrast to bulk water. Therefore, the DMPC/SA with much bound water is expected to enhance the disaggregation of Aβ fibrils, in comparison with its disaggregation in bulk phase.

The addition of DMPC liposome promoted the $k_d$ value (**Fig.4-16**). Furthermore, the induction of SA into DMPC liposomes promoted the disaggregation of Aβ(1-40) fibrils, depending on the concentration of SA (**Fig.4-16**). It is confirmed, in this study, that the addition of liposomes by itself could not disaggregate the Aβ fibrils (data not shown), although there is a report that a neutral phospholipid vesicle could disaggregate Aβ(1-42) fibrils into protofibrils (Martins *et al.*, 2008). It is, therefore, concluded that the promoting effects of DMPC/SA liposomes on the disaggregation of fibrils resulted from the other factors.

In order to clarify the role of the bound water to DMPC/SA liposome towards the disaggregation of fibrils, a solvent isotope effect was examined by using $D_2O$. The polarization of O-D bond in $D_2O$ needs more energy than that in O-H bond in $H_2O$. The resulting $k_{d,D2O}/k_{d,H2O}$ value was 0.40±0.03 for DMPC ~ 0.34±0.05 for DMPC/SA(28.6 mol%),
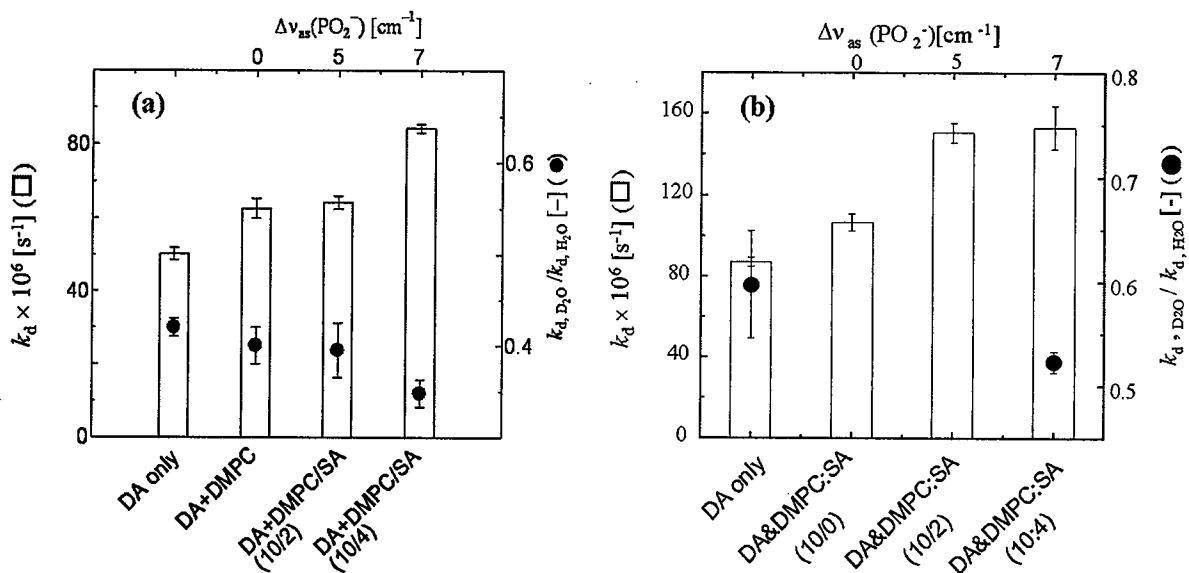


**Fig.4-16** Effect of liposome on the rate of disaggregation (a) Aβ(1-40) fibrils and (b) Aβ(1-42) fibrils. Fibrils were disaggregated by 100 μM DA in the absence and presence of 1 mM SA containing DMPC liposome. Aβ fibrils were prepared by incubating 10 μM Aβ monomer solution at 37 °C for 24 h in Tris-HCl buffer containing 100 mM NaCl, pH 7.4. The data were obtained from at least three independent experiments.

which were obviously smaller than that in bulk phase (0.42±0.01). On the other hand, the $k_{d,D2O}/k_{d,H2O}$ value for Aβ(1-42) fibrils in the presence of DMPC/SA(28.6 mol%) was 0.52±0.02, which is larger than the case of Aβ(1-40) (**Table 4-3**). This finding is consistent with the result in the absence of liposomes. The $k_{d,D2O}/k_{d,H2O}$ value also agreed with the extent of the bound water measured by the FT-IR technique ($\Delta v_{max}$) as shown in **Fig.4-16**, suggesting that the bound water could preferably contribute to the disaggregation of fibrils. The bound water weakened the HB within the fibrils associating with the liposome membrane, thus enhancing the DA-dependent disaggregation of fibrils.

### 3.3.5. Aβ Fibril Reduced Level of DA/DA-Quinone

It has been clearly shown that the DA could reduce level of the Aβ fibril by disaggregation of Aβ fibrils. Inversely, Aβ may also reduce the level of DA. In order to check this possibility, the remained DA concentration was analysised after its incubation at 37 °C for 12 h to disaggregate the Aβ(1-40) fibril, separated by ultra-filtration with membrane to cut off 3 kDa molecules as shown in **Fig.4-17(a)**. The effect of the DA concentration on the disaggregation was examined by using electrochemical sensor developed on the chapter 1, showing that the DA concentration after 12 h incubates with 10 µM Aβ fibrils was reduced at its magnitude of about 40 µM although Aβ concentration was 10 µM (**Fig.4-17(b)**). The DA concentration could be reduced much more in the presence of 1 mM DMPC/SAPC$_{ox}$ (6:4). This result lead to two possibilities: *(i)* more than one DA molecules are necessary to attach on Aβ fibril per one Aβ monomer molecules during the fibril disaggregation, and *(ii)* Aβ fibrils may induce the DA oxidation to convert onto non-toxic melanin. The second possibility may become proper because of the appearance of melanin-like polymer structure in the sample solution after the incubation up to 24 h (data not shown).
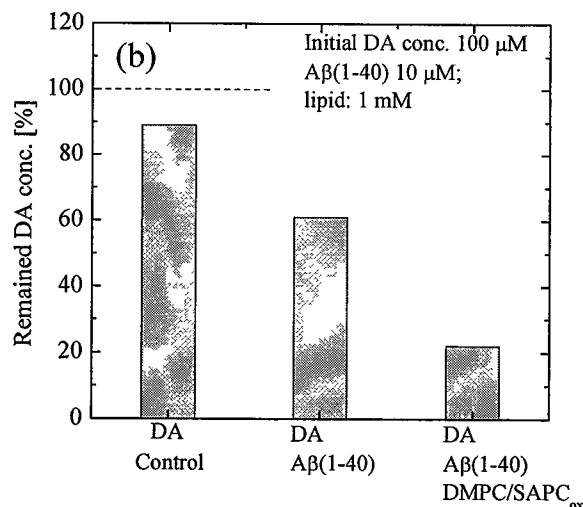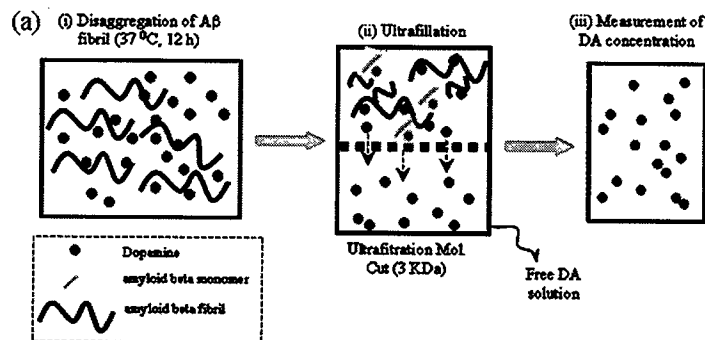
**Fig.4-14** (a) Conceptual illustration for ultra-filtration for separation of free DA from Aβ solution. (b) Remain DA concentration after 12 h incubate with 10 μM Aβ(1-40) fibril solution at 37 °C in the presence and the absence of 1 mM DMPC/SAPC$_{ox}$ (6:4). The control sample was prepared by DA only. Initial DA concentration: 100 μM.

## 3.4. Role of Membrane on Prevention and Removal of Toxicity

### 3.4.1. Liposome Could Regulate Aβ Fibril's Toxicity

It has been reported that the liposomes membranes could regulate the Aβ fibril formation. The difference in the kinetic constant of Aβ fibril formation resulted in the difference in morphology (data not shown) and in the difference in characteristics of the Aβ fibril, especially in toxicity of Aβ fibrils. In order to confirm this hypothesis, the toxicity of Aβ fibrils was studied by using the Glial cell as the target cell. The toxicity of Aβ fibrils on the cells was measured thought the cell viability by using MTT assay method. As shown in
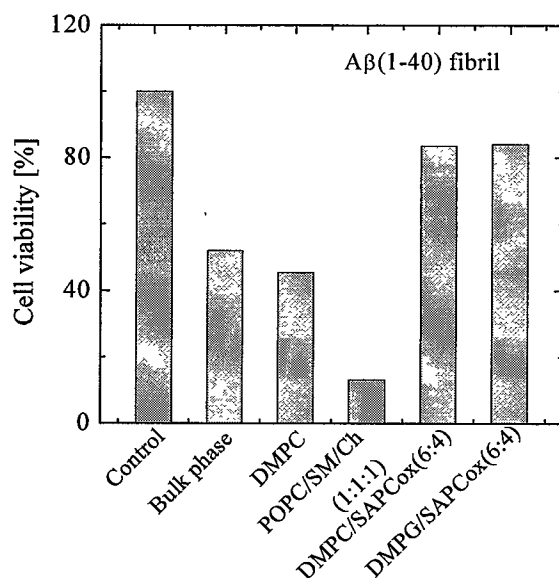
122

**Fig.4-18** Toxicity of Aβ formed on liposome membrane for Glial cells. The cell viability was measured by MTT assay method.

**Fig.4-18**, it was found that the liposomes could regulate the toxicity of Aβ fibrils, which may cause the difference in the dependent manner on the morphology of Aβ fibrils regulated by liposome membrane.


### 3.4.2. Summary of Role of Liposome Membrane - A Hypothesis that Membrane Could Protect and Repair Itself

First, the state of liposome membrane should be classified by the physicochemical parameters, such as stability of hydrogen bond ($m_{lip}$), local hydrophpbicity ($LH_{lip}$), and so on. In chapter 2, the oxidized liposome showed the high $m_{lip}$ value in comparison with the normal liposomes, depending on the concentration manner of oxidized lipid. Then, the $m_{lip}$ value was adopted as an index for the state of oxiditively damage. Based on the findings obtained in this study, the characteristic parameters were summarized as a function of $m_{lip}$ as shown in **Fig.4-19**.

The DA partitioning into liposome membrane was roughly correlated with the $m_{lip}$ value for various liposomes, suggesting that oxidized liposomes favors the partition of DA in
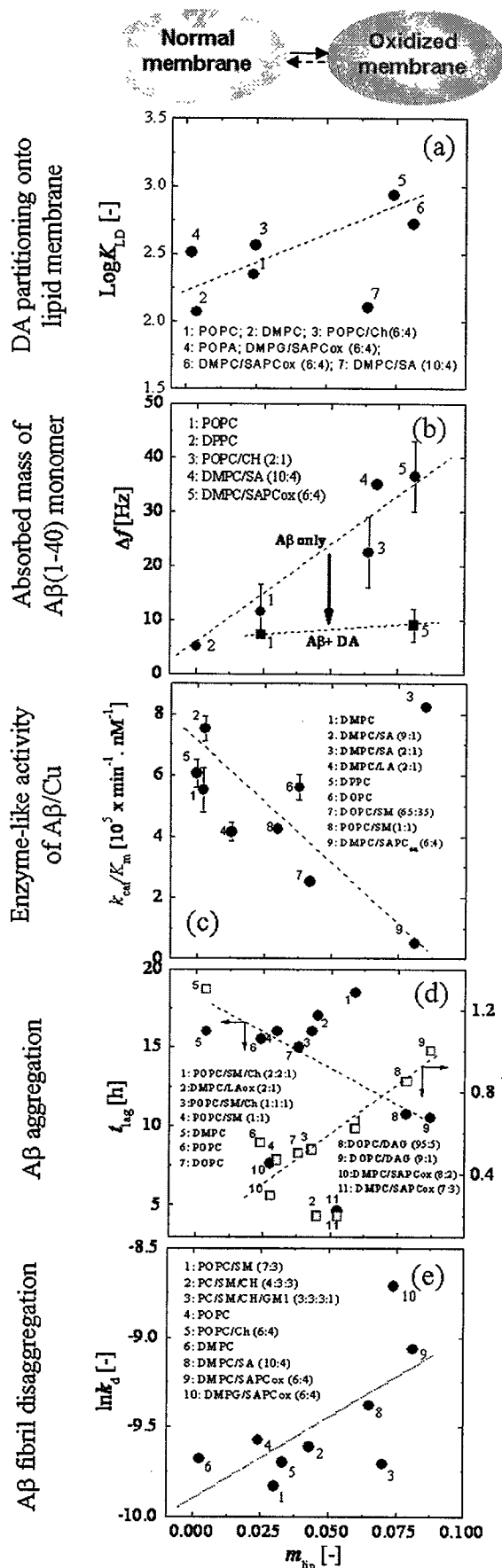
**Fig.4-19** The $m_{lip}$ dependency of (a) DA partition into liposome, (b) A$\beta$ accumulation on liposome membranes, (c) the reactivity of A$\beta$/Cu complex on liposome membranes, (d) Fibril formation kinetics ($t_{lag}$ and $k_{app}$), and (e) DA-induced disaggregation of fibrils on liposomes. (a) is referred to Chapter 1. The calculation of $K_{LD}$ for various liposomes and their values were summarized in the **Table 1-5**. (b) is referred to Chapter 2. Accumulation of A$\beta$(1-40) was estimated with an IL-QCM (**Fig.2-11**). (c) is referred to Chapter 3 (**Fig.3-8**). (d) and (e) are referred to Chapter 4. The lag time and the apparent elongation rate constant were estimated from a fitting of the time-course of ThT fluoresence intensity with an equation (4-2) (**Fig.4-2**). The disaggregation rate constant of A$\beta$ fibrils was estimated from a fitting of the time-course of ThT fluorescence intensity with an equation (4-1) (**Table 4-4**).

124

comparison with normal liposomes (**Fig.4-19(a)**). Oxidized liposomes favor not only DA but also Aβ accumulation as shown in **Fig.4-19(b)**. Among the liposomes used here, DMPC/SAPC$_{ox}$ (6:4) liposome shows the highest $m_{lip}$ value enough to interact with Aβ(1-40). The Aβ accumulation could be linearly correlated with the $m_{lip}$, being consistent with the principle of $m_{lip}$ described in chapter 2. Under low DA concentration, the DA-induced oxidation of liposome membrane is not significant. Meanwhile, the excess DA partitions into liposome membrane enough to give the oxidative damages. The resulting oxidative damaged liposome membrane reduced the reactivity of Aβ/Cu on membranes (**Fig.4-19(c)**), indicating that the excess DA under oxidative stress remains there. Furthermore, a secretion of Aβ and its accumulation could be promoted, resulting in the rapid nucleation on oxidized liposome membrane (**Fig.4-19(d)**). The nucleated Aβs is advantageous for their elongation since the elongation rate constant $k_{app}$ was correlated with the $m_{lip}$ value. Finally, the rapidly formed fibrils could be rapidly, on the (oxidized) liposome membranes, disaggregated by remained DA.

From the viewpoints of the interactive responses of DA and Aβ on membrane, systematic studies have been carried out by exemplifying the two representative cases from **Fig.4-19**.

**[Non-Oxidative Membrane]**

In the case of non-oxidative membranes, the DA partitioning and the associating accumulation of Aβ is unlikely to occur. Even though an increase in DA concentration would occur, the Aβ/Cu complex on the liposome with low $m_{lip}$ value can effectively convert into DA-quinone to control the DA concentration, resulting in the reduction of ROS from an auto-oxidation of DA. Non-oxidative stress condition is disadvantageous for the amyloid fibril formation although the formed fibrils on the liposome surface showed strong cytotoxicity (**Fig.4-20**).

**[Oxidative Damaged Membrane]**

Under the excess DA, the DA-induced toxicity could be developed based on the auto-oxidation of DA leading the formation of the oxidized membrane. Although the further auto-oxidation of DA might not be inhibited, the DA-Aβ adduct formation could alternatively result in the control of the DA concentration. DA-Aβ adduct is also advantageous for the inhibition of the formation of amyloid fibrils with strong cytotoxicity since an accumulatin of DA-Aβ adduct on the liposomes and a nucleation of Aβ could be suppressed as shown in **Fig.4-19(b)**. Once the oxidized lipid species are generated by the excess DA, a rapid nucleation for fibril formation with low cytotoxicity (See **Fig.4-18**) was induced, followed by a rapid disaggregation of fibrils including DA-Aβ adduct. This process is expected to be as a part of the removal of both the oxidized lipids and the exess DA from the membranes and its recovery.
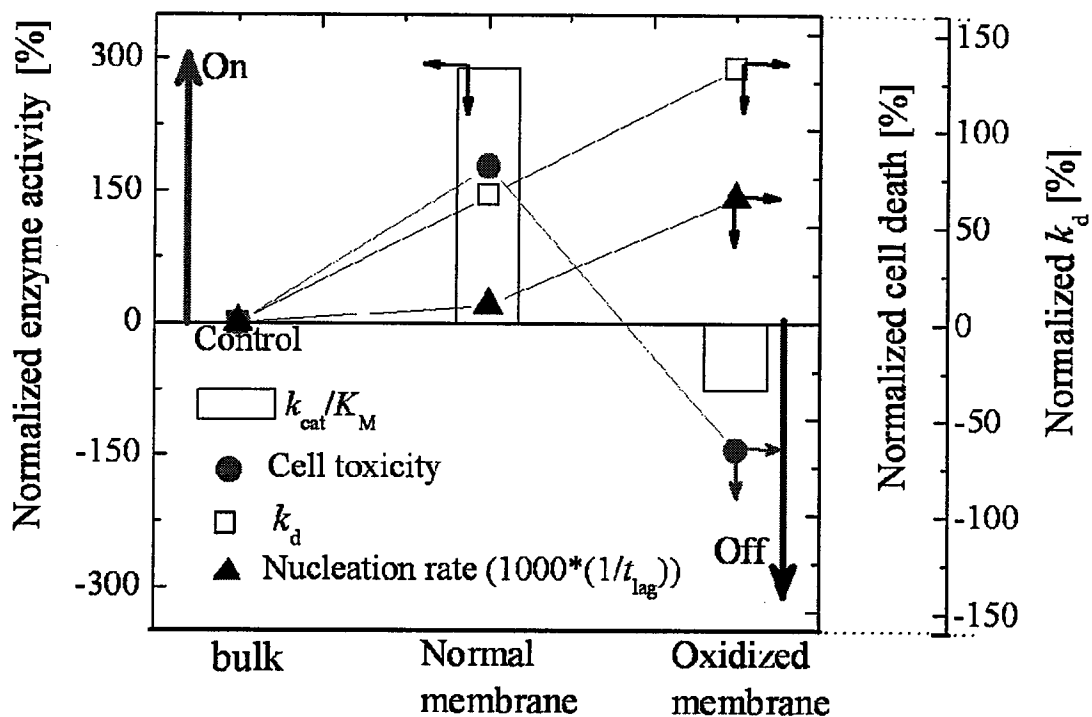


**Fig.4-20** Membrane regulates (i) the enzyme-like function of Aβ/Cu complex, (ii) Aβ fibril formation, (iii) toxicity of Aβ fibrils, and (iv) disaggregation of Aβ fibril induced by DA.

As summarized in **Fig.4-20**, the normal membrane could protect ifself by enhancement of the Aβ/Cu complex-enzyme like activity to reduce ROS generation from auto-oxidation of DA. When the membrane was exposed to such oxidative stress conditions (oxidative damaged membrane), it can make responses against the stress by several pathways, such as (a) recruilt Aβ to quickly form Aβ fibrils with less toxicity and then (b) promote the disaggregation of Aβ fibrils by DA/DA-quinone to reduce toxicity induced by both DA/DA-quinone and aggregated Aβ. The above results lead to hypothesis that the "*membrane*" could protect and recover itself under stress condition. The role of liposome membrane was summarized and was schematically shown in the **Fig.4-21**.

It was found that monomeric Aβ protein has high affinity to bind to oxidized membrane, suggesting the specific interaction between monomeric Aβ protein with oxidized membrane. By its adsorption on the oxidized membrane and rapidly formation of fibrils together with formation of cluster of oxidized lipid (Lee, 2005), Aβ may show its ability to
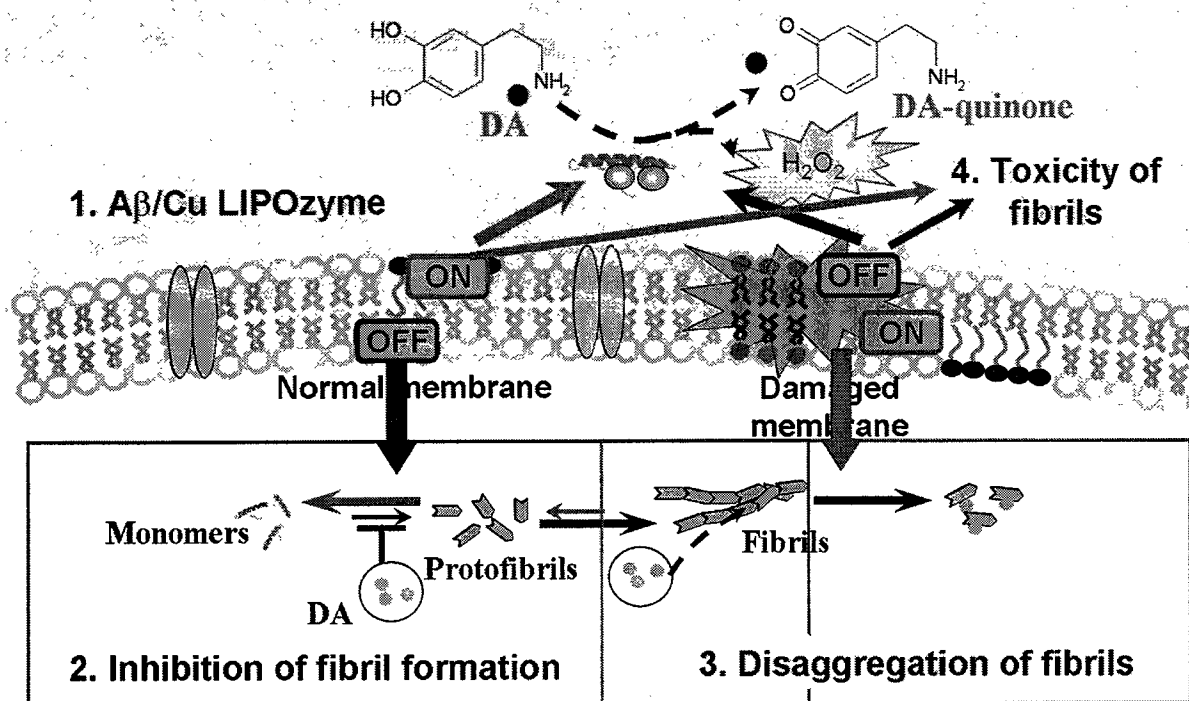


**Fig.4-21** Schematic of liposome membrane regulates DA concentration, level of Aβ fibril, and toxicity of Aβ fibrils.

recruit oxidized lipid from membrane. Taken together with disaggregation of Aβ fibrils by DA, it is expected that the Aβ may remove the oxidized lipid from membrane to repair membrane.

## 4. Summary

In this chapter, the effect of DA against Aβ on liposome membranes was investigated, focusing on (i) the inhibition of fibril formation on liposome membrane and (ii) the disaggregation of Aβ fibril on the liposome membrane. The DA showed the ability to reduce the toxicity of the Aβ fibril both by the inhibition of fibril formation and by the fibril disaggregation. Inversely, Aβ may have the effect to inactivate the toxic DA-quinone. Finally, the functions of biomembrane to defend itself from toxicity under the oxidative stress were summarized and discussed.

In brief, the membrane could modulate the DA concentration by regulating the enzyme-like activity of Aβ/Cu complex or by regulating the DA-Aβ interaction. The membrane possesses the ability to regulate the Aβ fibril level by promoting both of Aβ fibril formation and the disaggregation of Aβ fibril. When the membrane was exposed to such oxidative stress conditions, it can make responses against the stress by several pathways, such as (a) the enhancement of the Aβ/Cu complex-enzyme like activity to reduce ROS generation from auto-oxidation of DA or (b) the promotion of the disaggregation of Aβ fibrils by DA/DA-quinone to reduce toxicity of both DA-quinone and aggregated Aβ. Although the damaged membrane (oxidized membrane) could not enhance such enzyme activities, it could make response on the other ways by (c) accelerating the formation of less toxic Aβ fibrils and by (d) accelerating the disaggregation of Aβ fibril which could remove toxic DA-quinone. (e) By removing Aβ fibrils, it may remove the oxidized lipids associating with Aβ fibrils. The above response of DA and Aβ on the membrane were found to be regulated by the "membrane" under stress condition, depending on the "state" of membrane (i.e. hydrogen

bond instability).

The obtained results lead to the hypothesis that the *"membrane"* could make response to protect and recover itself under the oxidative stress condition.

# General Conclusion

Dopamine (DA) has been reported to play a important role in neuronal system as neurotransmitter. The lack of DA in neuron was well known to induce the dementia symptom although the existence of DA at extremely high level induces the oxidative stress, together with the formation of toxic DA-quinone through the "auto-oxidation" pathway. On the other hand, the Aβ deposition on the neuronal cell membrane has been reported to be related with the "oxidative stress". In a biological system, the cells could be protected from the oxidative stress by antioxidative enzymes, such as superoxide dismutase (SOD) and catalyses. However, in some cases, the antioxidant enzymes may lose their functions by the reactive oxygen species (ROS), leading to the loss of their protective function. Furthermore, it is necessary to remove the toxic species for the recovery the cells themselves.

In this thesis, systematic studies have been performed, mainly focusing on: *(i)* the interactive behaviors of DA with Aβ on the liposome membrane in order to reduce toxicity of both of them and *(ii)* the potential function of membrane against the toxicity induced by DA and Aβ. The appropriate methodology to analyze the interactive behaviors of DA with Aβ peptide on the liposome surface has been developed prior to the investigation on the mechanism of above studies.

In chapter 1, the DA sensors were developed based on the electrochemical method by using conducting polymer film and composition of Nafion, and conducting polymer film modified GC electrode. Electrochemical response of DA at GC/PMeT was compared with that at a GC/Nafion/PMeT electrode in terms of the signal amplitude. The GC/Nafion/PMeT electrode was found to show the superior characteristics over GC/PMeT. The heights of the current peaks for DA oxidation increased linearly with a DA concentration in the range of $5 \times 10^{-7}$ to $2 \times 10^{-4}$ M. A mechanism of the DA detection by using the above method was discussed, where (i) the partitioning of the DA in the polymer film and (ii) the DA oxidation

accompanied with the transfer of two electrons could be important for the selective detection of DA. Then, the DA sensor was utilized for the monitoring of the DA concentration to evaluate the DA-liposome interaction. The DA was found to show the propensity to partition (adsorb) onto the liposome membrane. Through its partitioning on the liposome membrane, the DA was found to induce the membrane damage, caused by auto-oxidation together with the generation of ROS (OH$^{\bullet}$, O$_2^-$). Inversely, the addition of the liposomes was found to promote the DA-oxidation indicated by decreased DA concentration significantly as compared without liposome. These results are very helpful for the deeper understanding of the phenomena, which will be shown and discussed in the chapter 4.

In chapter 2, the membrane sensor was designed and developed by the immobilization of liposome onto the surface of the modified QCM electrode in order to evaluate the membrane - protein interaction, focusing on the amyloidogenic proteins. The method for immobilization of liposome on the SAM-modified QCM (Au) electrode was investigated by modifying both of surface electrode and membrane components. The large decrease in the resonance frequency of quartz crystals observed was dependent on the liposome diameter, showing that the small liposomes are proper for immobilization. The incorporation of other compounds in membrane induced the fixation of membrane, and was found to the induce stabilization of the immobilized liposomes, resulting that the amount of immobilized liposomes increased with the increase of percent of other component on liposomes. On the other hand, the electrostatic interaction could enhance the amount of immobilized liposomes by attractive force or to prevent immobilization by repulse. By using amino coupling method, intact liposomes could be immobilized on solid surface and immobilized liposomes could stabilize for 10 h with frequency changes less than 5 %. It was finally found that, by using the covalent binding methods, the liposomes could be immobilized with "intact" shape and high density for long time. The immobilized liposomes were applied to evaluate: *(i)* the interaction between liposomes and proteins, specially Aβ peptide, and *(ii)* the DA-Aβ interaction on the liposome membrane, in order to clarify the mechanism of Aβ fibril formation and its

interaction with DA. It was found that the interaction of amyloidgenic Aβ could basically be governed by the hydrogen bond stability in the hydrophobic environment inside the liposome membrane and could be modulated by the variation of the surface properties (i.e. hydrogen bond instability) of the liposome membrane in the presence of DA under the oxidative stress condition. It is considered that the DA could play an important role in the regulation of the Aβ and liposome interaction to create some important values such as LIPOzyme function (Chapter 3) and Aβ fibril formation (Chapter 4).

In chapter 3, the Aβ-Cu-LIPOzyme (liposome with enzyme-like function) was found to be utilized for the regulation of the DA-oxidation as an enzymatic-like pathway, instead of auto-oxidation pathway. Aβ can form the complex with Cu by a stoichiometric manner of 1:2 of Aβ:Cu. Aβ/Cu complex could catalyze the oxidation of DA, so that the ROS level could be reduced as compared with that of the auto-oxidation pathway. Since Aβ/Cu-catalyzed oxidation of DA is dominated by a proton-coupled electron transfer (PCET) mechanism, water molecule with considerably polarized O-H bonds is advantageous for the proton transfer from DA to $O_2$ to generate both DA-quinone and $H_2O_2$, which can be regarded as "less-toxic" ROS in comparison with superoxide ($O_2^-$). The liposome membrane can accumulate the bound water with considerably polarized O-H bonds prior to PCET. Consequently, the liposome membrane could promote the DA–oxidation by a enhancement of PECT mechanism. This could result in the reduction of toxicity level of the ROS by modulation of DA concentration. In such a sense, it can be considered that the Aβ/Cu complex has the possible function for the defense of (bio)membranes from the ROS.

In chapter 4, the effect of DA against the Aβ on liposome membranes were investigated, focusing on *(i)* the inhibition of fibril formation on liposome membrane and *(ii)* the disaggregation of Aβ fibril on the liposome membrane. DA showed the ability to reduce the toxicity of Aβ fibril both by the inhibition of fibril formation and by the fibril disaggregation. Inversely, Aβ may have the effect to deactivate the toxic DA-quinone. Finally,

the function of biomembrane to defend itself from toxicity under the oxidative stress were summarized and discussed. It was found that the membrane could modulate the (1) partitioning(adsorption) of DA and Aβ, (2) enzyme-like function of Aβ/Cu complex (Aβ/Cu LIPOzyme), (3) nucleation and elongation of Aβ fibril formation, and (4) disaggregation of Aβ fibrils by DA/DA-quinone, depending on the hydrogen bond instability of membrane ifself. After summary of the above general tendency, two kinds of case studies on "normal membrane" and "oxidized membrane" were described. In briefly, the "normal membrane" could protect ifself by enhancement of the Aβ/Cu complex-enzyme like activity to reduce the ROS generation from auto-oxidation of DA. When the membrane was exposed to oxidative stress conditions and became the oxidatively damaged membrane, it can make responses against the stress by several pathways, (a) by recruiting the Aβ to rapidly form Aβ fibrils with less toxicity and then (b) by promoting the disaggregation of Aβ fibrils by DA/DA-quinone to reduce toxicity induced by both DA/DA-quinone and aggregated Aβ, and (c) by removing Aβ fibrils together with the oxidized lipids for the recovery of membrane itself.

The obtained results lead to the hypothesis that the membrane could make response by interactively utilizing the DA and Aβ as the "potentially functional elements" in order to protect and recover itself under oxidative stress condition.

# Suggestions for the Future Works

The following studies are recommended in order to extend the findings obtained in this work.

## 1. Membrane Chip for the Diagnostics of Alzheimer's Disease

In this study, a possible role of DA in Alzheimer's disease (AD) has been investigated based on its interactive behaviors with stressed membrane, together with its recruiting behaviors of Aβ and other elements. By combining the DA sensor (described in chapter 1) and membrane (liposome) sensor (described in chapter 2), the "*state*" of the lipid membrane surface, which can waken the potential functions of the biomolecules (DA and Aβ) and molecular assemblies (liposome), could be assessed quantitatively. The obtained results can brighten another aspect of AD from view point of "Membrane". Although some problems should be solved for the practical application in the AD diagnostics, a possibility of the AD diagnostics has been investigated in this thesis by employing the simple case studies.

## 2. Deeper Understanding of Mechanism of Alzheimer's Disease

A hidden mechanism of the Alzheimer's disease has been revealed by regarding the "dopamine" as a key material. Most of the previous researchers considered that the Amyloid fibril formation on the neural cell could induce the toxicity, resulting in the cell death. Some researchers imply the possible roles of the reactive oxygen species against the toxicity of the cells in AD patients. L-DOPA therapy (precursor of the DA) could also be one strategy of the Parkinson's disease and also AD. Although there are many principles, models, and strategies, which have been proposed by others, the total process relating to the AD has not been presented. In this thesis, the interactive

behaviors of DA with Aβ on the liposome membrane were systematically investigated, focusing on the hypothesis that the oxidative stress could play some important roles in the $O_2$-comsuming brain cells. It was found that the lipid membrane, which was commonly distributed in the biological cell, could "waken" the potentials of the biomolecules, depending on the state under the normal and oxidative stress condition (hydrogen bond instability). This basic stance is quite different from the previous findings. A new therapy or new medicine could be developed based on the above Membranomics strategy, together with the conventional genome and proteome strategies.

## 3. Possible Study on "Membrane Repairment" as a Response of Biological Cell at Molecular Assembly Level

It was found that monomeric Aβ protein had high affinity to bind to oxidized membrane, and it may induced by specific interaction between monomeric Aβ with oxidized membrane. By adsorption on the oxidized membrane and the rapid formation of fibrils together with formation of cluster of oxidized lipid (Lee, 2005), Aβ may show its ability to recruit oxidized lipid from membrane. Taken together with disaggregation of Aβ fibrils by DA, Aβ may remove the oxidized lipid from membrane to repair membrane. The above hypothesis could imply the possible significant role of the membrane as both of a modulator of the potential functions of bioelements and a platform to realize it. The conventional research mainly focuses on the metabolism of biomolecules. The above concept could provide us the significance of the metabolism of the "membrane itself" through the interactively induced rearrangement of them on the self-assembly.

# 4. Characterization and Application of Aβ/Cu LIPOzyme to Control the DA Concentration

As shown in the chapter 3, Aβ/Cu complex expressed its ability to regulate DA oxidation as an enzyme-like pathway, where the enzyme-like activity of Aβ/Cu could be regulated by liposome membrane. It was suggested that the distribution and orientation of metal ion and Aβ on the liposome membrane was varied, depending on the membrane properties of liposomes. The regulation of the membrane properties leading to the regulation of the enzyme activity to control the DA concentration, on the brain is promising approach for a medical treatment of neurodegeneration disease patients, such as Alzheimer's disease, Parkinson's disease... For the possible application of Aβ/Cu LIPOzyme for medical treatment, the following objects should be performed: *(i)* Characterization of Aβ/Cu LIPOzyme; *(ii)* Investigation of mechanism of Aβ/Cu complex on DA oxidation; *(iii)* Possibility of application of liposomes as a drug for control the DA concentration through the regulation of Aβ/Cu activity.

# Nomenclature

| | | |
|---|---|---|
| $P$ | = fluorescence polarization of probes embedded in bilayer | [-] |
| $1/P$ | = membrane fluidity of liposome | [-] |
| k' | = capacity factor, (retention volume of the peptide – retention volume of solvent peak) / retention volume of solvent | [-] |
| $\theta$ | = molecular ellipicity | [mdeg/mol] |
| $f_{c1}, f_{c2,}$ | = characteristic parameter of dielectric dispersion analysis | [MHz] |
| $T_m$ | = phase transition temperature | [°C] |
| $k_d$ | = disaggregation rate constant | [s$^{-1}$] |
| $I_{//}$ | = fluorescence intensity of parallel to excited light | [-] |
| $I_{\perp}$ | = fluorescence intensity of perpendicular to excited light | [-] |
| $LH$ | = local hydrophobicity | [-] |
| $m_{lip}$ | = apparent hydrogen bonding stabilization index of protein molecule, by liposome | [-] |
| $\rho_{pr}$ | = hydrogen bonding wrapping of protein | [-] |
| $k_{cat}/K_m$ | = apparent second order rate constant | [-] |
| $k_s$ | = specific capacity factor measured by ILC | [ml/mmol] |
| $t_{lag}$ | = lag time | [h] |
| $k_{app}$ | = elongation rate | [h$^{-1}$] |
| $K_{LD}$ | = partitioning coefficient constant | [-] |
| $V$ | = reaction rate | [nM/min] |
| log$P$ | = hydrophobicity of molecular | [-] |

# List of Abbreviation

| | |
|---|---|
| Aβ(1-40) | Amyloid β-peptide ending at 40 residues |
| Aβ(1-42) | Amyloid β-peptide ending at 42 residues |
| APP | Amyloid precursor protein |
| a.u | Arbitrary unit |
| AUT | 11-Amino undecane thiol |
| CD | Circular dichroism |
| CV | Cyclic voltammetry |
| Cat | Catechol |
| Ch | Cholesterol |
| DA | Dopamine |
| DMPC | 1,2-dimyristoyl-*sn*-glycero-3–phosphocholine |
| DMPE | 1,2-dimyristoyl-*sn*-glycero-3-phosphoethanolamine |
| DMPG | 1,2-ditetradecanoyl-*sn*-glycero-3-phospho-(1'-*rac*-glycerol) (sodium salt) |
| DMTMM | 4-(4,6-Dimethoxy-1,3,5-triazin-2-yl)-4-methyl morpholinium chloride |
| DOTAP | 1,2-Dioleoyl-3-Trimethylammonium-Propane (Chloride Salt) |
| DPH | 1,6-diphenyl-1,3,5-hexatrien |
| DPPC | 1,2-Dipalmitoyl-*sn*-Glycero-3-Phosphocholine |
| DPV | Different pulse voltammetry |
| EDC | N-(3-Dimethyl aminopropyl)-N'-ethylcarbodiimide hydrochloride |
| EP | Epinephrine |
| Egg-PE | L-α-Phosphatidylethanolamine |
| FT-IR | Fourier transform infrared spectroscopy |
| GM1 | Gangliosides |
| ILC | Immobilized liposome chromatography |
| IL-QCM | Immobilized liposome-quartz crystal microbalance |
| L-DOPA | 3,4-dihydroxyphenylacetic acid |
| MUA | 11-Mercaptoundecanoic acid |
| NE | Norepinephrine |
| NHS | N-Hydroxysuccinimide |

| | |
|---|---|
| PCox | Oxidized PC |
| PMeT | Poly(3-methyl thiophene) |
| POPA | 1-Palmitoyl-2-Oleoyl-*sn*-Glycero-3-Phosphate (Monosodium Salt) |
| POPC | 1-palmitoyl-2-oleoyl-*sn*-glycero-3-phosphocholine |
| POPE | 1-palmitoyl-2-oleoyl-*sn*-glycero-3-phosphoethanolamine |
| POPG | 1,2-dimyristoyl-*sn*-glycero-3-phosphoethanolamine |
| QCM | Quartz crystal microbalance |
| ROS | Reactive oxygen species |
| SA | Stearic acid |
| SAM | Self assembled monolayer |
| SAPC | 1-Stearoyl-2-Arachidonyl-sn-Glycero-3-Phosphocholine |
| SEM | Scanning electron microscopy |
| SM | Sphingomyelin |
| SOD | Superoxide dismutase |
| TEM | Transmission electron microscopy |
| TIRFM | Total Internal Reflection Fluorescence Microscope |
| TMA-DPH | N,N,N-Trimethyl-4-(6-phenyl-1,3,5-hexatrien-1-yl)phenyl ammonium p-toluenesulfonat |
| ThT | Fluorescence probe of fibrilous structure (Thioflavin T) |
| TrisHCl | 2-Amino-2-(hydroxymethyl)-1,3-propanediol, hydrochloride |
| Tyr | L-Tyrosine |

# References

Abraham, D. J., Leo, A. J., Extension of the fragment method to calculate amino acid zwitterion and side chain partition coefficients, *Proteins*, **2** (1987) 130-152.

Aleardi, A. M., Benard, G., Augereau, O., Malgat, M., Talbot, J. C., Mazat, J. P., Gradual alteration of mitochondrial structure and function by beta-amyloids: importance of membrane viscosity changes, energy deprivation, reactive oxygen species production, and cytochrome c release. *J Bioenerg. Biomembranes*, **37** (2005) 207–225.

Andersen, C. B., Yagi, H., Manno, M., Martorana, V., Ban, T., Christiansen, G., Otzen, D.E., Goto, Y., Rischel, C., Branching in Amyloid Fibril Growth, *Biophys. J.*, **96** (2009) 1529–1536.

Andorn, A. C., Pappolla, M. A., Catecholamines inhibit lipid peroxidation in young, aged, and Alzheimer's disease brain, *Free Radical Biol. Medicine*, **31** (2001) 315-320.

Antzutkin, O. N., Leapman, R. D., Balbach, J. J., Tycko, R., Supramolecular structural constraints on Alzheimer's β-amyloid fibrils from electron microscopy and solid-state nuclear magnetic resonance, *Biochemistry*, **41** (2002) 15436–15450.

Asanuma, M., Miyazaki, I., Ogawa, N., Dopamine- or L-DOPA-induced neurotoxicity: The role of dopamine quinone formation and tyrosinase in a model of parkinson's disease, *Neurotoxicity Research*, **5** (2003) 165-176.

Asher, I. M., Levin, I. W., Effects of temperature and molecular interactions on the vibrational infrared spectra of phospholipid vesicles, *Biochim. Biophys. Acta*, **468** (1977) 63-72.

Atta, N. F., Galal, A., Karagözler, A. E., Russell, G. C., Zimmer, H., Mark, H. B., J. Electrochemistry and detection of some organic and biological molecules at conducting poly(3-methylthiophene) electrodes, *Biosens. Bioelectron.*, **6** (1991) 333-341.

Atwood, C. S., Scarpa, R. C., Huang, X., Moir, R. D., Jones, W. D., Fairlie, D. P., Tanzi, R. E., Bush, A. I., Characterization of Copper Interactions with Alzheimer Amyloid b Peptides: Identification of an Attomolar-Affinity Copper Binding Site on Amyloid β1–42, *J. Neurochem.*, **75** (2000) 1219-1233.

Avdulov, N. A., Chochina, S. V., Igbavboa, U., Warden, C. S., Vassiliev, A. V., Wood, W. G., Lipid Binding to Amyloid β-Peptide Aggregates: Preferential Binding of Cholesterol as Compared with Phosphatidylcholine and Fatty Acids. *J. Neurochemistry*, **69** (1997) 1746-1752.

Barnham, K. J., Masters, C. L., Bush, A. I., Neurodegenerative diseases and oxidative stress, *Nat Rev Drug Discov.*, **3** (2004) 205-214.

Bors, W., Michel, C., Saran, M., Lengfelder, E., The involvement of oxygen radicals during the autoxidation of adrenalin, *Biochim Biophys Acta*, **540** (1978) 162–172.

Bui, T.H., Study on role of liposome membrane on gene expression of GFP in *E. coli* cell-free translation system, PhD thesis (Osaka University) (2009).

Burke, W. J., Li, S. W., Chung, H. D., Ruggiero, D. A., Kristal, B. S., Johnson, E. M., Lampe,

P., Kumar, V. B., Franko, M., Williams, E. A., Zahm, D. S., Neurotoxicity of MAO metabolites of catecholamine neurotransmitters: Role in neurodegenerative diseases, *NeuroToxicol.*, **25** (2004) 101–115.

Bush, A. I., The metallobiology of Alzheimer's disease, *Trends Neurosci.*, **26** (2003) 207–214.

Bäumle, M., Stamou, D., Segura, J. M., Hovius, R., Vogel, H., Ligand binding to G protein-coupled receptors in tethered cell membranes, *Langmuir*, **20** (2004) 3828.

Cannazza, G., Stefano, A. D., Mosciatti, B., Braghiroli, D., Baraldi, M., Pinnen, F., Sozio, P., Benatti, C., Parenti, C., Detection of levodopa, dopamine and its metabolites in rat striatum dialysates following peripheral administration of L-DOPA prodrugs by mean of HPLC–EC, *J. Pharm. Biomed. Anal.*, **36** (2005) 1079-1084.

Carlsson, A., Nobel Prize on Medicine (2000).

Casal, H. L., Mantsch, H. H., Hauser, H., *Biochem.*, **26** (1987) 4408-4416.

Chang, H. M., Reitstetter, R., Gruener, R., Lipid-Ion Channel Interactions: Increasing phospholipid head group size but not ordering acyl chains alters reconstituted channel behavior., *J. Membrane Biol.*, **145** (1995) 13-19.

Choi, H. Y., Song, J. H., Park, D. K., Ross, G. M., The effects of ascorbic acid on dopamine-induced death of PC12 cells are dependent on exposure kinetics, *Neuroscience Letters*, **296** (2000) 81-84.

Christensen, S. M., Stamou, D., Surface-based lipid vesicle reactor systems: fabrication and applications, *Soft Matter.*, **3** (2007) 828-836.

Ciccotosto, G. D., Tew, D., Curtain, C. C., Smith, D., Carrington, D., Masters, C. L., Enhanced toxicity and cellular binding of a modified amyloid beta peptide with a methionine to valine substitution. *J Biol. Chem.*, **279** (2004) 42528–42534.

Clarke, D. D., Sokoloff, L., Circulation and energy metabolism of the brain. In G. J. Sigel, B. W. Agranoff, R. W. Albers, S. K. Fisher, & M. D. Uhler (Eds.), Basic Neurochemistry: Molecular, Cellular and Medical Aspects (1999) (637–669). Philadelphia: Lippincott-Raven.

Conway, K. A., Rochet, J. C., Bieganski, R. M., Lansbury, P. T., Kinetic stabilization of the α-synuclein protofibril by a dopamine-α-synuclein adduct, *Science*, **294** (2001) 1346-1 349.

Crouch, P. J., Harding, S. M. E., White, A. R., Camakaris, J., Bush, A. I., Masters, C. L., Mechanisms of Aβ mediated neurodegeneration in Alzheimer's disease, *Int'l J. Biochem. Cell Biol.*, **40** (2008) 181–198.

Curtain, C. C., Ali, F., Volitakis, I., Cherny, R. A., Norton, R. S., Beyreuther, K., Barrow, C. J., Masters, C. L., Bush, A. I., Barnham, K. J., Alzheimer's disease amyloid-β binds Copper and Zinc to generate an allosterically ordered membrane-penetrating structure containing superoxide dismutase-like, *J. Biol. Chem.*, **278**, (2001) 20466–20473.

Dahlgren, K. N., Manelli, A. M., Stine, W. B. J., Baker, L. K., Krafft, G. A., LaDu, M. J., Oligomeric and fibrillar species of amyloid-β peptides differentially affect neuronal viability, *J. Biol. Chem.*, **277** (2002) 32046–32053.

Durairajan, S. S. K., Yuan, Q., Xie, L., Chan, W.S., Kum, W. F., Koo, I., Liu, C., Song, Y., Huang, J. D., Klein, W. L., Li, M., Salvianolic acid B inhibits Aβ fibril formation and disaggregates preformed fibrils and protects against Aβ-induced cytotoxicty, *Neurochem. Int.*, **52** (2008) 741-750.

Erdoğdu, G., Karagözler, A. E., Investigation and comparison of the electrochemical behavior of some organic and biological molecules at various conducting polymer electrodes, *Talanta*, **44** (1997) 2011-2018.

Fernandez, A., Berry, R. S., Proteins with H-bond packing defects are highly interactive with lipid bilayers: Implications for amyloidogenesis, *PNAS*, **4**, (2003) 2391-2396.

Folch, J., Lees, M., Stanley, S. H. G., Isolation and purification of total lipids from tissues, *J. Biol. Chem.*, **226** (1957) 497-509.

Fontecha-Cámara, M. A., López-Ramón, M. V., Pastrana-Martínez, L. M., Moreno-Castilla, C., Kinetics of diuron and amitrole adsorption from aqueous solution on activated carbons, *J. Hazardous Materials*, **156** (2008) 472-477.

Frederikse, P. H., Garland, D., Zigler, J. S., Jr, Piatigorsky, J., Oxidative stress increases production of beta-amyloid precussor protein and beta-amyloid (Abeta) in mammalian lenses, and Aβ has toxic effects on lens epithelial cells, *J Biol Chem.*, **271** (1996) 10169-10174.

Fu, W., Luo, H., Parthasarathy, S., Mattson, M. P., Catecholamines potentiate amyloid β-peptide neurotoxicity: Involment of oxidative stress, mitochondrial dysfunction, and perturbed calcium homestasis, *Neurobiol. Disease*, **5** (1998) 229-243.

Grouselle, M., Phillips, J. H., Reduction of membrane-bound dopamine β-hydroxylase from the cytoplasmic surface of the chromaffin-granule membrane, *Biochem. J.*, **20** (1982) 759-770.

Gwinn-Hardy, K., Evidente, V. G. H., Waters, C., Muenter, M. D., Hardy, J., L-dopa slows the progression of familial parkinsonism, *Lancet*, **353** (1999) 1850-1851.

Hard, D. L., Bhatnagar, R. K., Molina, J. R., Anderson, L. L., Secretion of dopamine and norepinephrine in hypophyseal portal blood and prolactin in peripheral blood of Holstein cattle, *Domest. Anim. Endocrin.*, **20** (2001) 89-100.

Hardy, J., Selkoe, D. J. The amyloid hypothesis of Alzheimer's disease: progress and problems on the road to therapeutics, *Science*, **297** (2002) 353-356.

Hayashi, H., Kimura, N., Yamaguchi, H., Hasegawa, K., Yokoseki, T., Shibata, M., Yamamoto, N., Michikawa, M., Yoshikawa, Y., Terao, K., Matsuzaki, K., Lemere, C. A., Selkoe, D. J., Naiki, H., Yanagisawa, K., A seed for Alzheimer amyloid in the brain, *J. Neurosci.*, **24** (2004) 4894-4902.

Hirakura, Y., Lin, M. C., Kagan, B. L., Alzheimer amyloid beta1-42 channels: effects of solvent, pH, and Congo red. *J. Neurosci. Res.*, **57**(1999) 458–466.

Hoyt, K. R., Reynolds, I. J., Hastings, T. G., Mechanisms of dopamine-induced cell death in cultured rat forebrain neurons: Interactions with and differences from glutamate-induced cell death, *Experiment. Neurol.*, **143** (1997) 269–281.

Jung, H. S., Shimanouchi, T., Morita, S., Kuboi, R., Novel Fabrication of Conductive Polymers Contained Micro-Array Gas Sensitive Films Using A Micromanipulation Method, *Electroanal.*,**15** (2003) 1453-1459.

Jung, H. S., Umakoshi, H., Son, S. Y., Shimanouchi, T., Kuboi, R., Characterization of the surface properties of Chitosanse under Heat Stress condition using Aqueous two phase systems and an Immobilized-liposome Sensor System, *Solv. Extr. Res. Dev. Japan*, **10** (2003) 123-132.

Kakio, A., Yano, Y., Takai, D., Kuroda, Y., Matsumoto, O., Kozutsumi, Y., Matsuzaki, K., Interaction between amyloid β-protein aggregates and membranes, *J. Pept. Sci.*, **10** (2004) 612–621.

Kanazawa, K. K, Gordon, J. G., Frequency of a quartz microbalance in contact with liquid, *Anal. Chem.,* **57** (1985) 1771-1772.

Kang, J., Lemaire, H. G., Unterbeck, A., Salbaum, J. M., Masters, C. L., Grzeschik, K. H., The precusor of Alzheimer's disease amyloid A4 protein resembles a cell-surface receptor, *Nature* **325** (1987) 733-736.

Kayed, R., Head, E., Thompson, J. L., McIntire, T. M., Milton, S. C., Cotman, C. W., Glabe, C. G., Common structure of soluble amyloid oligomers implies common mechanism of pathogenesis, *Science*, **300** (2003) 486–489.

Keller, C. A., Kasemo, B., Surface specific kinetics of lipid vesicle adsorption measured with a quartz crystal microbalance, *Biophysical J.*, **75** (1998) 1397-1402.

Kim, B. S., Fukuoka, H., Gong, J. O., Osada, Y., Titration behaviors and spectral properties of hydrophobically modified water-soluble polythiophenes, *European Polymer J.*, **37** (2001) 2499-2503.

Klosgen, B., Reichle, C., Kohlsmann, S., Kramer, K. D., Dielectric spectroscopy as a sensor of membrane head group mobility and hydration, *Biophys. J.*, **71** (1996) 3251-3260.

Klosgen, B., Reichle, C., Kohlsmann, S., Kramer, K. D., Dielectric spectroscopy as a sensor of membrane headgroup mobility and hydration, *Biophys. J.*, **71** (1996) 3251-3260.

Kobayashi, M., Kim, J., Kobayashi, N., Han, S., Nakamura, C., Ikebukuro, K., Sode, K., Pyrroloquinoline quinone (PQQ) prevents fibril formation of α-synuclein, *Biochem. Biophys. Res. Com.*, **349** (2006) 1139-1144.

Kostrzewa, R. M., Kostrzewa, J. P., Brus, R., Neuroprotective and neurotoxic roles of levodopa (L-DOPA) in neurodegenerative disorders relating to Parkinson's disease, *Amino Acids*, **23** (2002) 57-63.,

Kotarek, J. A., Johnson, K. C., Moss, M. A., Quartz crystal microbalance analysis of growth kinetics for aggregation intermediates of the Amyloid-β protein, *Anal. Biochem.*, **378** (2008) 15-24.

Kremer, J. J., Murphy, R. M., Kinetics of adsorption of h-amyloid peptide Aβ(1–40) to lipid bilayers, J. Biochem. Biophys. Methods, **57** (2003) 159-169

Kremer, J. J., Pallitto, M. M., Sklansky, D. J., Murphy, R. M., Correlation of β-amyloid aggregate size and hydrophobicity with decreased bilayer fluidity of model membranes,

*Biochem.*, **39** (2000) 10309-10318.

Kuboi, R., Mawatari, T., Yoshimoto, M., Oxidative refolding of lysozyme assisted by negatively charged liposomes: Relationship with lysozyme-mediated fusion of liposomes, *J. Bioscience Bioeng.*, **90** (2000) 14-19.

Kuboi, R., Shimanouchi, T., Umakohsi, H., Yoshimoto, M., Detection of protein conformation under stress condition using liposome as sensor materials, *Sensors Materials*, **16** (2004) 241-254.

Kuboi, R., Umakoshi, H., Analysis and Separation of Amyloid-β peptides Using Aqueous Two-phase Systems Under Stress Condition ~ From Aqueous Two-phase Systems to Liposome Membrane System ~ *Sol Extr Res Dev Japan*, **13** (2006) 9-16.

Kuboi, R., Yoshimoto, M., Walde, P., Luisi, P. L., Refolding of carbonic anhydrase assisted by 1-palmitoyl-2-oleoyl-sn-glycero-3-phosphocholine liposomes, *Biotechnol. Prog.*, **13** (1997) 828−836.

Kudva, Y. C., Hiddinga, H. J., Butler, P. C., Mueske, C. S., Eberhardt, N. L., Small heat shock proteins inhibit *in vitro* Aβ1-42 amyloidogenesis, *FEBS Letters*, **416** (1997) 117-121.

Lee, B. K., PhD thesis (2005) Osaka University.

Li, J., Zhu, M., Manning-Bog, A. B., Monte, D. A. D., Fink, A. L., Dopamine and L-DOPA disaggregate amyloid fibrils: implications for Parkinson's and Alzheimer's disease, *FASEB J.*, **18** (2004) 962-964.

Liebau, M., Bendas, G., Rothe, U., Neubert, R. H. H., Adhesive interactions of liposomes with supported planar bilayers on QCM as a new adhesion model, *Sensors Actuators B*, **47** (1998) 239-245.

Liu, J., Mori, A. Monoamine metabolism provides an antioxidant defense in the brain against oxidant- and free radical-induced damage, *Arch. Biochem. Biophys.*, **30** (1993) 118–127.

Liu, X., Tu, M., Kelly, R. S., Chen, C., Smith, B. J., Development of a computational to predict blood-brain barrier permeability, The American Society for Pharmacology and Experimental Therapeutics, 32 (2004) 132-139.

Lovell, M.A., Robertson, J. D., Teesdale, W. J., Campbell, J. L., Markesbery, W. R., Copper, iron and zinc in Alzheimer's disease senile plaques, *J. Neurol. Sci.*, **158** (1998) 47-52.

Lundahl, P., Yang, Q., Liposome chromatography: liposomes immobilized in gel beads as a stationary phase for aqueous column chromatography, *J. Chromatography*, **544** (1991) 283-304.

Lüthgens, E., Herrig, A., Kastl, K., Steinem, C., Reiss, B., Wegener, J., Pignataro, B., Janshoff, A., Adhesion of liposomes: a quartz crystal microbalance study, *Meas. Sci. Technol.*, **14** (2003) 1865-1875.

Mamikonyan, G., Necula, M., Mkrtichyan, M., Ghochikyan, A., Petrushina, I., Movsesyan, N., Mina, E., Kiyatkin, A., Glabe, C., Cribbs, D. H., Agadjanyan, M. G., Anti-Aβ1-11 antibody binds to different β-amyloid species, inhibits fibril formation, and disaggregates preformed fibrils but not the most toxic oligomers. *J. Biol. Chem.*, **282** (2007) 22376-22386.

Martins, I. C., Kuperstein, I., Wilkinson, H., Maes, E., Vanbrabant, M., Jonckheere, W., Gelder, P. V., Hartmann, D., D'Hooge, R., Strooper, B. D., Schymkowitz, J., Rousseau, F., Lipids revert inert Aβ amyloid fibrils to neurotoxic protofibrils that affect learning in mice, *EMBO J.*, **27** (2008) 224-233.

Matsuoka, Y., Picciano,M., La Francois, J., Duff, K., Fibrillar beta-amyloid evokes oxidative damage in a transgenic mouse model of Alzheimer's disease, *Neuroscience*, **104** (2001) 609–613.

Matsuzaki, K., Noguch, T., Wakabayashi, M., Ikeda, K., Okada, T., Ohashi, Y., Hoshino, M., Naiki, H., Inhibitors of amyloid beta protein aggregation mediated by GM1-containing raft-like membranes, *Biochim. Biophys.Acta*, **1768** (2007a) 122-130.

Matsuzaki, S., Yasuda, Y., Kobayashi, S., Koyama, Y., Kawamoto, K., Katayama, T., Tohyama, M., Monomeric Aβ and metals reduce their cytotoxicities to each other, *Biochem. Biophys. Res. Com.*, **358** (2007b) 540-544.

Mattson, M. P., Pathways towards and away from Alzheimer's disease, *Nature*, **430** (2004) 631-639.

McLean, C. A., Cherny, R. A., Fraser, F. W., Fuller, S. J., Smith, M. J., Beyreuther K, Bush, A. I., Masters, C. L., Soluble pool of Abeta amyloid as a determinant of severity of neurodegeneration in Alzheimer's disease, Ann Neurol. 46 (1999) 860-866.

Mesulam, M. M., Neuroplasticity failure in Alzheimer's disease: Bridging the gap between plaques and tangles, *Neuron*, **24** (1999) 521–529.

Michikawa, M., The role of cholesterol in pathogenesis of Alzheimer's disease: Dual metabolic interaction between amyloid β-protein and cholesterol, *Mol. Neurobiol.*, **27** (2003) 1-12.

Misonou, H., Kawashima, M., Ihara, Y., Oxidative stress induces intracellular accumulation of amyloid beta-protein (Abeta) in human neuroblastoma cell, *Biochem.*, **39** (2000) 6951-6959.

Miyazaki, I., Asanuma, M., Approaches to Prevent Dopamine Quinone-Induced Neurotoxicity, Neurochem Res, **34** (2009) 698-706.

Mo, J. W., Ogorevc, B., Simultaneous measurement of dopamine and ascorbate at their physiological levels using voltammetric microprobe based on overoxidized poly(1,2-phenylenediamine)-coated carbon fiber, *Anal. Chem.*, **73** (2001) 1196-1202.

Mori, K., Imai, K., Sensitive high-performance liquid chromatography system with fluorometric detection of three urinary catecholamines in the same range, *Anal. Biochem.*, **146** (1985) 283-286.

Moridani, M. Y., Siraki, A., O'Brien, P. J., Quantitative structure toxicity relationships for phenols in isolated rat hepatocytes, Chemico-Biological Interaction 145 (2003) 213-223.

Morita, S., Hamano, Y., Kuboi, R., Effect of fatty acids on interaction between liposome and amyloid β-peptide, *Membrane*, **32** (2007) 215-220.

Morita, S., Nukui, M., Kuboi, R., Immobilization of liposomes onto quartz crystal microbalance to detect interaction between liposomes and proteins, *Colloid Interf. Sci.*,

**298** (2006) 672-678.

Murer, M. G., Dziewczapolski, G., Menalled, L. B., Garcia, M. C., Agid, Y., Gershanik, O., Raisman-Vozari, R., Chronic levodopa is not toxic for remaining dopamike neurons, but instead promotes their recovery, in rats with moderate nigrostriatal lesions, *Ann Neurol.*, **43** (1998) 561-575.

Murray I. V. J., Sindoni, M. E., Axelsen, P. H., Promotion of oxidative lipid membrane damage by amyloid β proteins, *Biochem.*, **44** (2005) 12606-12613.

Nagami, H., Study on metal-Aβ interaction on liposome membrane to control oxidative stress, PhD thesis (Osaka University) (2005).

Nagami, H., Yoshimoto, N., Umakoshi, H., Shimanouchi, T., Kuboi, R., Liposome-assisted activity of superoxide dismutase under oxidative stress, *J. Biosci. Bioeng.*, **99** (2005) 423-428.

Naiki, H., Nakakuki, K., First-order kinetic model of Alzheimer's beta-amyloid fibril extension *in vitro*. *Lab Invest.*, **74** (1996) 374-383.

Navratilova, I., Dioszegi, M., Myszka, D. G., Analyzing ligand and small molecule binding activity of solubilized GPCRs using biosensor technology, *Anal. Biochem.*, **355** (2006) 132-139.

Nielsen, L., Khurana, R., Coats, A., Frokjaer, S., Brange, J., Vyas, S., Uversky, V. N., Fink, A. L., Effect of Environmental Factors on the Kinetics of Insulin Fibril Formation: Elucidation of the Molecular Mechanism, *Biochem.*, **40** (2001) 6036-6046.

Nuria, B. C., Mercedes, C., Josep, C., Conversion of non-fibrillar β-sheet oligomers into amyloid fibrils in Alzheimer's disease amyloid peptide aggregation, *Biochem. Biophys. Res. Com.*, **361** (2007) 916–921.

Oda, T., Wals, P., Osterburg, H. H., Johnson, S. A., Pasinetti, G. M., Morgan, T. E., Rozovsky, I., Stine, W. B., Snyder, S. W., Holzman, T. F., Krafft, G. A., Finch, C. E., Clustering (ApoJ) alters the aggregation of amyloid β-peptide (Aβ1-42) and slowly sedimenting Aβ complexes that cause oxidative stress, *Exp. Neurol.*, **136** (1995) 22-31.

Okada, T., Wakabayashia, M., Ikeda, K., Matsuzaki, K., Formation of toxic fibrils of Alzheimer's amyloid beta-protein-(1-40) by monosialoganglioside GM1, a neuronal membrane component, *J. Mol. Biol.*, **371** (2007) 481-489.

Okuda, T., Kimura, Y., Yoshida, T., Hatano, T., Okuda, H., Arichi, S., Studies on the activities of tannins and related compounds from medicinal plants and drugs: I. Inhibitory effects on lipid peroxidation in mitochondria and microsomes of liver, *Chem. Pharm. Bull. (Tokyo)*, **31** (1983) 1625–1631.

Olivieri, G., Baysang, G., Meier, F., Müller-Spahn, F., Stähelin, H. B., Brockhaus, M., Brack C., N-acetyl-L-cysteine protects SHSY5Y neuroblastoma cells from oxidative stress and cell cytotoxicity: effects on beta-amyloid secretion and tau phosphorylation, *J Neurochem.*, **76** (2001) 224-233.

Ono, K., Hasegawa, K., Naiki, H., Yamada, M., Anti-amyloidogenic activity of tannic acid and its activity to destabilize Alzheimer's β-amyloid fibrils *in vitro*, *Biochim. Biophys.*

*Acta*, **1690** (2004b) 193– 202.

Ono, K., Hasegawa, K., Naiki, H., and Yamada, M., Curcumin has potent anti-amyloidogenic Effects for Alzheimer's β-amyloid fibrils *in vitro.*, *J. Neurosci. Res.*, **75** (2004a) 742-750.

Ono, K., Yoshiike, Y., Takashima, A., Hasegawa, K., Naiki, H., Yamada, M., Potent anti-amyloidogenic and fibril destabilizing effects of polyphenols *in vitro*: implications for the prevention and therapeutics of Alzheimer's disease, *J. Neuro. Chem.*, **87** (2003) 172-181.

Opazo, C., Huang, X., Cherny, R. A., Moir, R. D., Roher, A. E., White, A. R., Cappai, R., Masters, C. L., Tanzi, R. E., Inestrosa, N. C., Ashley I. Bush, Metalloenzyme-like activity of Alzheimer's disease β-amyloid Cu-dependent catalytic conversion of dopamine, cholesterol, and biological reducing agents to neurotoxic $H_2O_2$, *J Biol Chem.*, **277** (2002) 40302-40308.

Ozawa, D., Yagi, H., Ban, T., Kameda, A., Kawakami, T., Naiki, H., Goto, Y., Destruction of Amyloid Fibrils of a $\beta_2$-Microglobulin Fragment by Laser Beam Irradiation, *J. Biol. Chem.*, **284** (2009) 1009-1017.

Papahadjopoulos, D., Kimelberg, H. K., Phospholipid vesicles (liposomes) as models for biological membranes: Their properties and interactions with cholesterol and proteins, *Progress in Surface Science*, **4** (1973) 141-232.

Peat, M. A., Gibb, J. W., High-performance liquid chromatographic determination of indoleamines, dopamine, and norepinephrine in rat brain with fluorometric detection, *Anal. Biochem.*, **128** (1983) 275-280.

Petkova, A. T., Ishii, Y., Balbach, J. J., Antzukin, O. N., Leapman, R. D., Delaglio, F., Tycko, R., A structural model for Alzheimer's β-amyloid fibrils based on experimental constraints from solid state NMR, *Proc. Natl. Acad. Sci. USA.*, **99** (2002) 16742-16747.

Petkova, A. T., Leapman, R. D., Guo, Z., Yau, W. M., Mattson, M. P., Tycko, R., Self-propagating, molecular-level polymorphism in Alzheimer's β-amyloid fibrils, *Science*, **307** (2005) 262-265.

Pignataro, B., Steinem, C., Galla, H. J., Fuchs, H., Janshoff, A., Specific adhesion of vesicles monitored by scanning force microscopy and quartz crystal microbalance, *Biophys. J.*, **78** (2000) 487-498.

Pileblad, E., Slivka, A., Bratvold, D., Cohen, G., Studies on the autoxidation of dopamine: interaction with ascorbate, *Arch Biochem Biophys*, **263** (1988) 447-452.

Pratico, D., Uryu, K., Leight, S., Trojanoswki, J. Q., Lee, V. M., Increased lipid peroxidation precedes amyloid plaque formation in an animal model of Alzheimer amyloidosis, *J Neurosci.*, **21** (2001) 4183-4187.

Reimhult, E., Hook, F., Kasemo, B., Vesicle adsorption on $SiO_2$ and $TiO_2$: Dependence on vesicle size, *J. Chem. Phys.*, **117** (2002) 7401-7404.

Reimhult, E., Höök, F., Kasemo, B., Intact vesicle adsorption and supported biomembrane formation from vesicles in solution: Influence of surface chemistry, vesicle size,

temperature, and osmotic pressure, *Langmuir*, **19** (2003) 1681-1691.

Reiss, B., Janshoff, A., Steinem, C., Seebach, J., Wegener, J., Adhesion kinetics of functionalized vesicles and mammalian cells: A comparative study, *Langmuir*, **19** (2003) 1816-1823.

Resende, R., Ferreiro, E., Pereira, C., Resende, D. O. C., Neurotoxic effect of oligomeric and fibrillar species of amyloid-beta peptide 1-42: Involvement of endoplasmic reticulum calcium release in oligomer-induced cell death. *Neuroscience*, **155** (2008) 725-737.

Richter, R., Mukhopadhyay, A., Brisson, A., Pathways of lipid vesicle deposition on solid surfaces: A combined QCM-D and AFM study, *Biophysical J.*, **85** (2003) 3035-3047.

Rocha, L. S., Carapuca, H. M., Ion-exchange voltammetry of Dopamine at Nafion-coated glassy carbon electrodes: Quantitative features of ion-exchange partition and reassessment on the oxidation mechanism of dopamine in the presence of excess ascorbic acid, *Bioelectrochem.*, **69** (2006) 258-266.

Rosenberg, P. A., Catecholamines toxicity in cerebral cortex in dissociated cell culture, *J Neuroscienece*, **8** (1988) 2887-2894.

Sakurai, Y., Jung, H. S., Shimanouchi, T., Inoguchi, T., Morita, S., Kuboi, R., Natsukawa, K., Novel array-type gas sensors using conducting polymers, and their performance for gas identification, *Sensors Actuators B*, **83** (2002) 270-275.

Sasahara, K., Yagi, H., Naiki, H., Goto, Y., Heat-induced Conversion of $\beta$2-Microglobulin and Hen Egg-white Lysozyme into Amyloid Fibrils, *J. Mol., Biol.*, **372** (2007) 981-991.

Sauerbrey, G., Verwendung von Schwingquarzen zur Wägung dünner Schichten und zur Mikrowägung, *Zeitschrift für Physik.*, **155** (1959) 206-222.

Scheumer, D., Eckman, C., Jensen, M., Song, X., Citron, M., Suzuki, N., Bird, T. D., Hardy, J., Hutton, M., Kukull, W., Larson., E., Levylahad, E., Viitanen, M., Peskind, E., Poorkaj, P., Schellenberg, G., Tanzi, R. E., Wasco, W., Lannfelt, L., Selkoe, D., Tounkin, S., Secrected amyloid-$\beta$ protein similar to that in the senile plaques of Alzheimer's disease is increased *in vivo* by the presenilin 1 and 2 and APP mutations linked to familial Alzheimer's disease, *Nat. Med.*, **2** (1996) 864-870.

Seantier, B., Breffa, C., Félix, O., Decher, G., Dissipation-enhanced quartz crystal microbalance studies on the experimental parameters controlling the formation of supported lipid bilayers, *J. Phys. Chem. B*, **109** (2005) 21755-21765.

Selkoe, D. J, The molecular pathology of Alzheimer's disease, *Neuron*, **6** (1991) 487-498

Selkoe, D. J., Alzheimer's disease: genes, proteins, and therapy, *Physiol. Rev.*, **81** (2001) 741-766.

Shimanouchi, T., Morita, S., Jung, H. S., Sakurai, Y., Suzuki, Y., Kuboi, R., Development of PPy Films Doped with Thiol-SAM-Cu particles for $NH_3$ Gas Sensing, *Sensor. Mater.*, **16** (2004) 255-265.

Smith, M. A., Harris, P. L. R., Sayre, L. M., Perry, G., Iron accumulation in Alzheimer disease is a source of redox-generated free radicals, *Proc. Natl. Acad. Sci. USA*, **94** (1997) 9866-9868.

Song, J. H., Slot, A. J., Ryan, R. W. J., Ross, G. M., Dopamine-induced death of PC12 cells is prevented by a substituted tetrahydronaphthalene, *Neuropharmacology,* **46** (2004) 984-993.

Soto, C., Sigurdsson, E. M., Morelli, L., Kumar, A., Castano, E. M., Frangione, B., β-Sheet breaker pepides inhibit fibrillogenesis in a rat brain model of amyloidosis: Implication for Alzheimer's therapy, *Nat. Med.,* **4** (1998) 822-826.

Spector, A., Review: oxidative stress and disease, *J. Ocul. Pharmacol. Ther.,* **16** (2000) 193–201.

Spencer, J. P., Jenner, A., Butler, J., Aruoma, O. I., Dexter, D. T., Jenner, P., Halliwell, B., Evaluation of the pro-oxidant and antioxidant actions of L-DOPA and dopamine *in Vitro:* Implication for Parkinson's disease, *Free rad. Res.,* **24** (1996) 95-105.

Städler, B., Bally, M., Grieshaber, D., Vörös, J., Creation of a functional heterogeneous vesicle array via DNA controlled surface sorting onto a spotted microarray, *Biointerphases,* **1** (2006) 142-145.

Sugihara, K., Teranishi, T., Shimazu, K., Uosaki, K., Electrochemistry of ordered interfaces. Structure dependence of the surface $pK_a$ of mercaptoundecanoic acid SAM on gold, *Denki Kagaku oyobi Kogyo Butsuri Kagaku.,* **67** (1999) 1172-1174.

Sulzer, D., Zecca, L., Intraneuronal dopamine-quinone synthesis: A review, *Neurotoxicity Reasearch,* **1** (2000) 181-195.

Tahara, Y., Fujiyoshi, Y., A new method to measure bilayer thickness: Cryo-electron microscopy of frozen hydrated liposomes and image simulation, *Micron,* **25,** (1994) 141-149.

Takahashi, S., Gjessing, L. R., A fluorometric method combined with thin layer chromatography for the determination of norepinephrine, epinephrine and dopamine in human urine, *Clinica Chimica Acta,* **36** (1972)369-378.

Takuma, K., Yao, J., Huang, J., Xu, H., Chen, X., Luddy, J., ABAD enhances Abeta-induced cell stress via mitochondrial dysfunction, *FASEB J.,* **19** (2005) 597–598.

Taran, V. D., Wick, R., Walde, P., 1H Nuclear Magnetic Resonance Method for Investigating the Phospholipase D-Catalyzed Hydrolysis of Phosphatidylcholine in Liposomes, *Anal. Biochem.,* **240** (1996) 37-47.

Terland, O., Flatmark, T., Tangeras, A., Gronberg, M., Dopamine oxidation generates an oxidative stress mediated by dopamine semiquinone and unrelated to reactive oxygen species, *J. Mol Cell Cardiol,* **29,** (1997) 1731-1738.

Tse, D. C. S., McCreery, R. L., Adams, R. N., Potential oxidative pathways of brain catecholamines, *J. Med. Chem.,* **19** (1976) 37-40.

Tuan, L. Q., Study on preparation and characterization of antioxidive LIPOzyme, PhD thesis (Osaka University) (2008).

Tuan, L. Q., Umakoshi, H., Shimanouchi, T., Kuboi, R., Liposome-Recruited Activity of Oxidized and Fragmented Superoxide Dismutase, *Langmuir,* **24** (2008) 350-354.

Tuan, L. Q.,, Umakoshi, H., Shimanouchi, T., Kuboi, R., Liposome membrane can act like

molecular and metal chaperones for oxidized and fragmented superoxide dismutase, *Enzyme Microb. Tech.*, **44** (2009) 101–106.

Tuckerman, M. Mayer, M., J. R., Nachod, F.C., Anomalous $pK_a$ values of some substituted phenylethylamides, *J. Am. Chem. Soc.*, **81** (1959) 92-94.

Varadarajan, S., Yatin, S., Aksenova, M., Butterfield, D.A., Alzheimer's amyloid beta-peptide-associated free radical oxidative stress and neurotoxicity, *J. Struct. Biol.*, **130** (2000) 184–208.

Vechettt, G. F., de Arcuri, B. F., Posse, E., Arrondo, J. L. R., Morero, R. D., Aggregation, fusion and aqueous content release from liposomes induced by lysozyme derivatives: effect on the lytic activity. *Mol. Membr. Biol.*, **14** (1997) 137-142.

Vladimir, P. T., Recent advances with liposomes as pharmaceutical carriers, *Nat. Rev. Drug Discovery*, **4** (2005) 145.

Wang, H. S., Li, T. H., Jia, W. L., Xu, H. Y., Highly selective and sensitive determination of dopamine using a Nafion/carbon nanotubes coated poly(3-methylthiophene) modified electrode, *Biosens. Bioelectron.*, **22** (2006) 664-669.

Wang, H. Y., Sun, Y., Tang, B., Study on fluorescence property of dopamine and determination of dopamine by fluorimetry, *Talanta*, **57** (2002) 899-907.

Wightman, R. M., May, L. J., Michael, A. C., Detection of dopamine dynamics in the brain. *Anal. Chem.*, **60** (1988) 769A-779A.

Wimley, W. C., White, S. H., Experimentally determined hydrophobicity scale for proteins at membrane interfaces, *Nat Struct Biol.*, **3** (1996) 842-848.

Yamamoto, I., Konto, A., Handa, T., Miyajima, K., Regulation of phospholipase D activity by neutral lipids in egg-yolk phosphatidylcholine small unilamellar vesicles and by calcium ion in aqueous medium, *Biochim. Biophys. Acta*, **1233** (1995) 21-26.

Yang, F., Lim, G. P., Begum, A. N., Ubeda, O. J., Simmons, M. R., Ambegaokar, S. S., Chen, P., Kayed, R., Glabe, C. G., Frautschy, S. A., Cole, G. M., Curcumin Inhibits Formation of Amyloid-β Oligomers and Fibrils, Binds Plaques, and Reduces Amyloid in Vivo, *J Biol. Biochem.*, **280** (2005) 5892–5901.

Yoshimoto M, Miyazaki Y, Umemoto A, Walde P, Kuboi R, Nakao K., Phosphatidylcholine vesicle-mediated decomposition of hydrogen peroxide, *Langmuir*, **23** (2007) 9416-9422.

Yoshimoto, M., Kuboi, R., Oxidative refolding of denatured/reduced lysozyme utilizing the chaperone-like function of liposomes and immobilized liposome chromatography, *Biotechnol. Prog.*, **15** (1999) 480-487.

Yoshimoto, M., Kuboi, R., Yang, Q., Miyake, J., Immobilized liposome chromatography for studies of protein-membrane interactions and refolding of denatured bovine carbonic anhydrase, *J. Chromatography B*, **712** (1998) 59-71.

Yoshimoto, N., Study on Interactively-induced fuction of Aβ and liposome under stress condition, PhD thesis (Osaka University) (2005).

Yoshimoto, N., Tasaki, M., Shimanouchi, T., Umakoshi, H., Kuboi, R., Oxidation of Cholesterol Catalyzed by Amyloid β-Peptide (Aβ)–Cu Complex on Lipid Membrane, *J.*

*Bioscience Bioeng.*, **100** (2005) 455–459.

Yoshimoto, N., Yoshimoto, M., Yasuhara, K., Shimanouchi, T., Umakoshi, H., Kuboi, R., Evaluation of temperature and guanidine hydrochloride-induced protein-liposome interactions by using immobilized liposome chromatography, *Biochem. Eng. J.*, **29** (2006) 174-181.

Zhang, L., Zhao, B., Yew, D. T., Kusiak, J. W., Roth, G. S., Processing of Alzheimer's amyloid precussor protein during $H_2O_2$-induced apoptosis in human neuronal cells, *Biochem. Biophys. Res. Com.*, **235** (1997) 845-848.

Zhang, Y., Cai, Y., Su, S., Determination of dopamine in the presence of ascorbic acid by poly(styrene sulfonic acid) sodium salt/single-wall carbon nanotube modified glassy carbon electrode, *Anal. Biochem.*, **350** (2006) 285-291.

Zhao, H., Zhang, Y., Yuan, Z., Electrochemical determination of dopamine using a poly(2-picolinic acid) modified glassy carbon electrode, *Analyst*, **126** (2001) 358-360.

Zheng, J., Zhou, X., Sodium dodecyl sulfate-modified carbon paste electrodes for selective determination of dopamine in the presence of ascorbic acid, *Bioelectrochemistry*, **71** (2006) 106-113.

Zou, K., Gong, J. S., Yanagisawa, K., Michikawa, M., A Novel Function of Monomeric Amyloid β-Protein Serving as an Antioxidant Molecule against Metal-Induced Oxidative Damage, *J. Neuroscience*, **15** (2002) 4833-4841.

Zucolotto, V., Ferreira, M., Cordeiro, M. R., Constantino, C. J. L., Moreira, W. C., Oliveira, O. N. J., Nanoscale processing of polyaniline and phthalocyanines for sensing applications, *Sensors Actuators B*, **113** (2006) 809-815.

# List of Publications

**[Original Papers]**

1. <u>Vu, H. T.</u>, Shimanouchi, T., Do, P. Q., Umakoshi, H., Pham, H. V., Kuboi, R., Polymethylthiophene / Nafion-Modified Glassy Carbon Electrode for Selective Detection of Dopamine in the Presence of Ascorbic Acid, *J. Appl. Electrochem.*, **39**, 2035-2042 (2009).

2. <u>Vu, H. T.</u>, Shimanouchi, T., Ishii, H., Umakoshi, H., Kuboi, R., Immobilization of Intact Liposomes on Solid Surfaces: a Quartz Crystal Microbalance study, *J. Colloid Interface Sci.*, **336**, 902-907 (2009).

3. Shimanouchi, T., Oyama, E., <u>Vu, H. T.</u>, Ishii, H., Umakoshi, H., Kuboi, R., Monitoring of Membrane Damages by Dialysis Treatment: Study with Membrane Chip Analysis, *Desalnation Water Treatment*, **13**, in press (2010).

4. <u>Vu, H. T.</u>, Shimanouchi, T., Shimauchi, N., Yagi, H., Umakoshi, H., Goto, Y., Kuboi, R., Catechol Derivatives Inhibit the Fibril Formation of Amyloid-β Peptides, *J. Biosci. Bioeng.*, **109**, in press (2010).

5. Shimanouchi, T., Tasaki, M., <u>Vu, H. T.</u>, Ishii, H., Yoshimoto, N., Umakoshi, H., Kuboi, R., Aβ/Cu Catalyzed-Oxidation of Cholesterol in 1,2-Dipalmitoyl Phosphatidylcholine Liposome Membrane, *J. Biosci. Bioeng.*, **109**, 145-148 (2010).

6. Shimanouchi, T., Shimauchi, N., Nishiyama, K, <u>Vu, H. T.</u>, Yagi, H., Goto, Y., Umakoshi, H., Kuboi, R., Characterization of Amyloid-β fibrils with Aqueous Two-Phase System: Implications of Fibrils Formation, *Solv. Extr. Res. Dev. Japan*, in press (2010).

**[Related Papers]**

1. <u>Vu, H. T.</u>, Quan, D. P., Tue, N. M., Nghi, T. V., Viet, P. H., Potentiometric Sensor for Hydrogen Ion Based on Neutral Carrier in A Poly(vinyl chloride) Membrane with Polyaniline Solid Contact, *J. Anal. Sci. Vietnam*, **10**, 72-79 (2005).

2. Quan, D. P., Tue, N. M., <u>Vu, H. T.</u>, Nghi, T. V., A Polypyrrole-Based Solid-Contact Lead Ion-Selective Electrode, *J. Anal. Sci. Vietnam*, **11**, 79-86 (2006).

**[Proceedings]**

1. Do, P. Q., <u>Vu, H. T.</u>, Cuong, P. B., Nghi, T. V., Viet, P. H., Potentiometric Sensor for Hydrogen Ion Based on Neutral Carrier in A Poly(vinyl chloride) Membrane with Polyaniline Solid Contact, *The 4th General Seminar of JSPS-VAST Core University Program*, Kumamoto, Japan, Sept. 21-23 (2004).

2. <u>Vu, H. T.</u>, Do, P. Q., Nguyen, M. T., Shimanouchi, T., Viet, P. H., Kuboi, R., Development of Electroactive Polymethylthiophene Based Dopamine Sensor, *The 6th General Seminar of JSPS-VAST Core University Program*, Kumamoto, Japan, Oct. 2-4 (2006).

3. Shimanouchi, T., Ishii, H., <u>Vu, H. T.</u>, Nishiyama, K., Umakoshi, H., Kuboi, R., Development of Separation and Analytic Method of Aβ Peptide Based on Biomembrane Abnormality ~ Membrane Chip Analysis Can Brighten a Potential Aspect of Alzheimer's Disease~, *The 1st Int'l Symp. on Process Chemistry 2008*, Kyoto, Japan, July 28-30 (2008).

4. Shimanouchi, T., Hiroiwa, A., <u>Vu, H. T.</u>, Nishiyama, K., Umakoshi, H., Kuboi, R., Analysis of Amyloid Fibrillization on Liposome Using Membrane Chip Analysis, *JSPS-*

*SNSF International Seminar on Membranomics (The 6th Symposium on Membrane Stress Biotechnology, MSB6)*, Osaka, Japan, Sept. 1-3 (2008).

5. Vu, H. T., Shimanouchi, T., Umakoshi, H., Kuboi, R., Immobilization of Intact Liposome on Solid Surface: A Quartz Crystal Microbalance Study, *JSPS-SNSF International Seminar on Membranomics (The 6th Symposium on Membrane Stress Biotechnology, MSB6)*, Osaka, Japan, Sept. 1-3 (2008).

6. Shimanouchi, T., Vu, H. T., Ishii, H., Oyama, E., Umakoshi, H., Kuboi, R., Amyloid Fibril Formation on Biomembrane: Analysis Using Membrane Chip System, *The 10th General Seminar of JSPS-VAST Core University Program*, Osaka, Japan, Nov. 26-28 (2008).

7. Shimanouchi, T., Vu, H. T., Umakoshi, H., Kuboi, R., Disaggregation of Catecholamine Derivative-Induced Amyloid Fibrils on Biomembranes, *The Asia-Pacific Biochemical Engineering Conference 2009 (APBioChEC'09)*, Kobe, Japan, Nov. 24-28 (2009) (*J. Biosci. Bioeng.*, Volume 108, Supplement 1, Pages S31-S32 (2009)).

# Acknowledgement